MAY 1962 MMPP 167-4
ORA 3710-2-T

MICHIGAN MEMORIAL PHOENIX PROJECT
PHOENIX MEMORIAL LABORATORY
THE UNIVERSITY OF MICHIGAN

A MATHEMATICAL STUDY OF GAS-PHASE HOT-ATOM REACTIONS

A THESIS BY CHI-HUA HSIUNG

THIS WORK WAS SUPPORTED BY:

THE DEPARTMENT OF CHEMISTRY

THE MICHIGAN MEMORIAL PHOENIX PROJECT

THE UNITED STATES ATOMIC ENERGY COMMISSION
CONTRACT NO. AT(11-1)—912

ANN ARBOR MICHIGAN

Errata and Addenda

In addition to obvious typographical errors please note the following.

Page No.	Line	Error	Correction
44	Figure Caption add		zero energy refers to the complete dissociation into nuclei and electrons[40].
69	3 up	g_s	q_s
73	Figure Caption add		Curve a: argon as additive; curve b: a totally effective scavenger is used as additive.
81	8	collision	collision cross-section
90	7	first "-"	+
98	10 11 16	$(1+\cos\theta_{ai})$	$(1-\cos\theta_{ai})$
113	5 up	He^4	CH_4
116	Figure Caption	CH_3T CD_3T	CH_3T/CD_3T
117	20	12.5-13.0%	13.6-14.1%
118	7 up	come is	comes in
125	Figure Caption add		●, unscavenged; ○, scavenged.
185	Ref. 26	(1960)	(1961)

A MATHEMATICAL STUDY OF GAS-PHASE HOT-ATOM REACTIONS

by

Chi-hua Hsiung

A dissertation submitted in partial fulfillment
of the requirements for the degree of
Doctor of Philosophy in The
University of Michigan
1962

Doctoral Committee:

Assistant Professor Adon A. Gordus, Co-chairman
Professor Joseph J. Martin, Co-chairman
Professor Richard B. Bernstein
Professor Giuseppe Parravano
Professor David V. Ragone
Professor G. Brymer Williams

ACKNOWLEDGMENTS

The author wishes to thank Professor Adon A. Gordus for his initiation of this research, his continued encouragement, and stimulating discussions throughout the course of the work, as well as his assistance in polishing the language used in this dissertation and correcting many technical errors.

Her sincere appreciation is also extended to all the members of the doctoral committee: Professors J. J. Martin, R. B. Bernstein, G. Parravano, D. V. Ragone, and especially to Professor G. B. Williams for his patient encouragement.

She would also like to express her deep gratitude to the American Institute of Chemical Engineers and to the Horace H. Rackham School of Graduate Studies for their fellowships, and to the United States Atomic Energy Commission and the Michigan Memorial-Phoenix Project for their financial assistance to this research.

Many thanks are due to Mrs. Jeanne Gordus for the long hours she spent typing this thesis.

And finally, she wishes to thank her husband, Hsien-Chih, without whose encouragement and constructive criticism over many problems, this thesis would not be possible.

TABLE OF CONTENTS

TABLE OF CONTENTS CONT' D

TABLE OF CONTENTS CONT'D

TABLE OF CONTENTS CONT'D

LIST OF TABLES

LIST OF FIGURES

LIST OF FIGURES CONT'D

Chapter I. INTRODUCTION

A. Hot-Atom Chemistry

Electromagnetic radiation or particles can transfer momentum to an atom in a molecule. If a sufficiently large momentum is acquired by the atom it will possess a high translational kinetic energy and will dissociate from its parent molecule. For example, it is calculated in Chapter II that the Br in CH_3Br will recoil and dissociate from the molecule if an energy greater than 20.7 ev is imparted to the bromine atom. For this energy, the dissociated atom will possess 14.7 ev. For bromine atoms to acquire an average of 14.7 ev of kinetic energy it would be necessary to heat the atoms to about 1.8 million degrees centigrade. Hence, such dissociating atoms are frequently called hot-atoms and the study of the reaction of these atoms with thermal energy molecules is called hot-atom chemistry.

The simplest way to transfer a large amount of momentum to an atom in a molecule is by a nuclear process. Thus, either nuclear activation such as (n,γ), (n,p), (γ,n) activation or nuclear decay can result in the production of hot atoms. The term, chemical effects of nuclear transformations, has become synonomous with hot-atom chemistry.

Atoms produced by photochemical activation have also been called hot-atoms. However, the photo-activated atoms invariably possess kinetic energies which are much less than that acquired in nuclear transformations. The chemical reactions involving the photo-activated atom are usually similar to those found at thermal energies. Hot atoms produced by nuclear transformation appear to undergo unique reactions which occur as a result of the very high kinetic energies of the atom.

For purposes of this dissertation we will be concerned primarily with hot atoms produced by nuclear transformations although certain of the chemical reaction mechanisms described here could also be of importance in photo-chemical reactions.

B. Review of Previous Work

In 1934 Szilard and Chalmers[1] observed that a large fraction of the radioactive I^{128} formed by neutron bombardment of liquid ethyl iodide could be extracted by an equeous solvent. Fermi and his co-workers[2] interpreted this observation in terms of the bond rupture caused by the recoil momenta of the emitted gamma rays.

Gluckauf and Fay[3] found that the hot atoms produced by the Szilard-Chalmers process re-entered into chemical combination and that the extent of reaction did not depend on the temperature of the system but did depend on the amount of chemically inert substance added to the system.

These two observations opened the field. Since then many experiments have been performed, both confirming the early discoveries and contributing new findings and theories. The two reviews by Willard[4,5] surveyed the advances in the field through 1955. A short review of the previous work in the field which is pertinent to this dissertation is given here.

1. Molecular Dissociation Following Nuclear Transformations

Conservation of momentum requires that an atom undergoing a nuclear transformation receive a recoil momentum equal to the momentum of the electromagnetic wave or particle emitted by the atom. The recoil energy thus imparted to an activated atom is of the order of 100 ev for (n,γ) activation reactions and of the order of 3 ev for beta-particle emission.[6]

For diatomic molecules, Suess[7] calculated that the internal energy increase is a function of both the total recoil energy received by the hot atom and the ratio of the mass of the non-activated atom to the mass of the hot atom. For (n,γ) activation, the diatomic molecule can remain intact following nuclear activation if (1) the hot atom is very heavy compared with the mass of the atom to which it is bonded, or (2) the neutron-binding energy is emitted, not as a single gamma ray, but as a gamma-ray cascade and, due to partial cancellation of gamma-ray momenta, the net momentum imparted to the atom is a small fraction of the maximum possible momentum[4,8].

Following $Br^{79}(n,\gamma)Br^{80m}$ activation, Wexler and Davies[9] found 1% of the Br^{80m} retained in the form of ethyl bromide. Cobble and Boyd[10] observed similar results in the $Br^{79}(n,\gamma)Br^{80}$ activation of $KBrO_3$ and suggested the use of the random-walk model to calculate the extent of partial cancellation of recoil momentum. For a series of alkyl halides, Gordus[11,12] measured the extent of failure to bond-rupture following (n,γ) activation and found that they were of the order of 0.1 to 1%.

Wexler and Davies[9] found that a portion of the activated iodine and bromine produced by the (n,γ) reaction are positively charged, presumably a result of the internal conversion of low-energy neutron capture-gamma rays.

2. Hot-Atom Reactions: Experimental Evidence and Proposed Mechanisms

Hamill and Williams[13] found that 13% of the Br^{80} formed by (n,γ) activation reacted with gaseous ethyl bromide to form HBr^{80} via a one-step hot-atom gaseous reaction:

$$Br^{80} + C_2H_5Br \rightarrow C_2H_4Br\cdot + HBr^{80}.$$

It was observed[14-16] that 54.4% of the I^{128} formed by the $I^{127}(n,\gamma)I^{128}$ process reacts with gaseous methane to form CH_3I^{128}; 13.3% of (n,γ) activated Br^{80} was found to react[17] with CH_4 to yield CH_3Br^{80}. The presence of hot reactions in these two systems was illustrated by the observations[14,17] that inert gases reduce the extent of reaction with CH_4.

A number of models have been proposed in an attempt to describe the mechanisms of the hot-atom reaction. Libby postulated[18,19] that the hot atom loses its excess energy by colliding elastically with its neighboring molecules (the "billiard ball model") until it reaches an energy low enough so that a collision will result in a displacement reaction (the "epithermal reaction" process). This oversimplified model is unable to account for the formation in the liquid phase of products which apparently are formed in two-step processes. Using this hypothesis, Miller, Grydon, and Dodson[20] and Capron and Oshima[21] formulated mathematical expressions to describe simple hot-atom reaction systems. Estrup and Wolfgang[22] further extended the formulation to describe systems which include non-reactive moderators. Their results have been used to describe the observed inert-gas moderation of the $T + CH_4$[22], $Br + CH_4$[17], and $I + CH_4$[14] systems.

To account for liquid-phase products which must be formed via two-step processes, Willard[4] proposed that some of the hot-atom collisions result in random fragmentation of the thermal molecules. Because of the complexity of the liquid phase, no mathematical formulation of this model has, as yet, been attempted and results are discussed qualitatively.

C. Purpose of this Study

The hot-atom reaction mechanism may be summarized as follows:

1. The hot atom (or ion) is formed with a high kinetic energy and dissociates from its parent molecule.
2. The excess kinetic energy of the hot atom is dissipated in collisions with atoms, molecules, or atoms in molecules.
3. When the energy of a hot atom reaches a certain value, the hot atom can, in a single collision,

> displace an atom or a radical in a molecule and enter into stable combination with the remainder of the molecule.

In this dissertation, attempts are made to formulate mathematical expressions to describe each step mentioned above. The validity of these expressions are tested using gas-phase experimental data appearing in the literature.

D. Published Data

Some of the mathematical formulations described in this thesis have appeared in published journal articles.

"A closed general solution of the probability distribution function for three-dimensional random-walk processes" was derived and appeared in The Journal of Chemical Physics, Volume 34, (1961), page 535. The use of this calculation is discussed in Appendix II.

"Momentum transfer to an atom in a molecule: internal excitation and bond-rupture" appeared in The Journal of Chemical Physics, Volume 36, (1962), page 947, and is discussed more fully in Chapter II and Appendix III.

"Failure to bond-rupture and nuclear recoil following (n,γ) activation" appeared in The Journal of Chemical Physics, Volume 36, (1962), page 954 and is discussed in Chapter III.

Chapter II. MOMENTUM TRANSFER IN A MOLECULE

A. General Considerations

Momentum transfer to an isolated atom is a simple problem in classical mechanics. However, if the atom which receives the impulse is bound chemically, it is not immediately obvious how the recoil energy becomes distributed among the various internal energy modes of the molecule.

For a diatomic molecule, Suess[7] calculated that the internal energy, E_i, will be increased by

$$\Delta E_i = E_T(\Sigma m_i - m_N)/\Sigma m_i, \quad (1)$$

where m_N is the atomic weight of the atom receiving the impulse, Σm_i is the molecular weight of the diatomic molecule, and E_T is the recoil energy acquired by the atom. In general, $E_T = Q^2/2m_N$, where Q is the momentum transferrred to the atom. For gamma-ray recoil[6], $E_T = (537\ E_\gamma{}^2)/m_N$ where E_T is in units of ev, m_N in amu, and the gamma ray energy, E_γ, in Mev.

Steinwedel and Jensen[23] calculated the fractional distribution of the internal energy between the vibrational and rotational modes of a diatomic molecule. In addition, they considered a quantum-mechanical approach to the problem.

Recently, Svoboda[24] discussed the relationship between rotational excitation and the bond dissociation energy. Wolfsberg[25] also included such an effect in his quantum-mechanical evaluation of the beta-decay recoil-excitation of C^{14} labeled ethane.

To calculate the recoil energy required for chemical bond rupture in a polyatomic molecule it is possible to utilize a quantum-mechanical approach. However, because of the uncertainties and assumptions associated with such derivations, the calculated value would be considered as only a very rough approximation.

The problem of recoil momentum activation of polyatomic molecules will be considered in terms of a mechanical model. The model which is proposed involves only a small number of well-defined assumptions, and these assumptions, at least for the simpler molecules, may not invalidate the results.

B. The Model

Consider a molecule as consisting of a group of point masses, the atoms linked together by springs. The molecule, therefore, is not rigid and the atoms in the molecule may undergo independent constrained motions in addition to the translational and rotational motions of the molecule. For a molecule composed of N atoms, 3N coordinates will be required to describe the molecule in detail. This can be achieved by first defining a set of coordinates $\vec{r}(x,y,z)$ with the center of gravity of the molecule, G, as the origin. The coordinates of the center of gravity of the molecule are $\vec{R}(X,Y,Z)$ and the translational motion of the center of gravity of the molecule is $\dot{\vec{R}}(\dot{X},\dot{Y},\dot{Z})$. The orientation of the molecule in space is usually represented by $\vec{\theta}(\theta,\varphi,\chi)$ and, thus, $\dot{\vec{\theta}}$ or $\vec{\omega}$ is the angular motion of the molecule about its center of gravity. In addition, the relative positions of the atoms in the molecule can be described as $\vec{r}_i(x_i, y_i, z_i)$ ($i = 1$ to N) thus resulting in 3N-6 independent coordinates. Although the positions, $\vec{r}_i$, describes 3N coordinates, not all are independent since (1) the choice of the origin as the center of gravity results in

$$\Sigma m_i \vec{r}_i = 0 \tag{2}$$

and (2) the translation and rotation of the molecule has been described by the translation and rotation of the (x,y,z) coordinates, i.e. $\dot{\vec{R}}$ and $\vec{\omega}$. Thus, there should be no net angular momentum with respect to the (x,y,z) coordinates. As a result,

$$\Sigma m_i \vec{a}_i \times \vec{v}_i = 0, \tag{3}$$

where $\vec{a}_i$ is the equilibrium position of the ith atom and $\vec{v}_i$ is the vibrational velocity of the _i_th atom with respect to the molecule.

When the framework (X,Y,Z) moves at a velocity, $\dot{\vec{R}}$, and rotates at an angular velocity, $\vec{\omega}$, and the atoms simultaneously vibrate around their equilibrium positions, $\vec{a}_i$, at velocities, $\vec{v}_i$, then, the space velocity of the _i_th atom, $\vec{S}_i$, is

$$\vec{S}_i = \dot{\vec{R}} + \vec{\omega} \times \vec{r}_i + \vec{v}_i .$$

Hence, the total energy of the molecule is

$$E_T = \tfrac{1}{2}\Sigma m_i \, (\dot{\vec{R}} + \vec{\omega} \times \vec{r}_i + \vec{v}_i)^2 + V(\vec{r}_i) . \tag{4}$$

Since $\dot{\vec{r}}_i = \vec{\omega} \times \vec{r}_i + \vec{v}_i$ and $\Sigma m_i \vec{r}_i = 0$, it can be shown that

$$\Sigma m_i \vec{v}_i = 0 .$$

Using Eqs. (2), (3), and (5), the total energy of the system is

$$E_T = \tfrac{1}{2}\Sigma m_i \dot{R}^2 + \tfrac{1}{2}\Sigma m_i (\vec{\omega}\times\vec{r}_i)\cdot(\vec{\omega}\times\vec{r}_i)$$
$$+ \tfrac{1}{2}\Sigma m_i v_i^2 + \vec{\omega}\cdot\Sigma m_i (\vec{\rho}_i\times\vec{v}_i) + V(\vec{r}_i), \qquad (6)$$

where $\vec{\rho}_i = \vec{r}_i - \vec{a}_i$ is the displacement of the ith atom and $V(\vec{r}_i)$ is the potential energy of the molecule.

The first term on the right-hand side of Eq. (6) is the translational energy of the molecule, the second term is the rotational energy, the third term is the vibrational energy, the fourth term is the rotational and vibrational coupling, and the last term is the potential energy of the molecule.

On averaging, it is found that $\vec{r}_i$ is approximately equal to $\vec{a}_i$ and that $\vec{\rho}_i$ approaches zero; hence, the internal energy may be approximated by

$$E_{int} = \tfrac{1}{2}\Sigma m_i (\vec{\omega}\times\vec{a}_i)\cdot(\vec{\omega}\times\vec{a}_i)$$
$$+ \tfrac{1}{2}\Sigma m_i v_i^2 + V(\vec{a}_i). \qquad (7)$$

If an atom in a molecule suddenly experiences a mechanical recoil and if the recoil energy is very large compared with the thermal motion of the molecule, then the total energy increase is

$$\Delta E_T = \tfrac{1}{2}\dot{R}^2\Sigma m_i + \tfrac{1}{2}\Sigma m_i (\vec{\omega}\times\vec{r}_i)\cdot(\vec{\omega}\times\vec{r}_i)$$
$$+ \tfrac{1}{2}\Sigma m_i v_i^2 + V(\vec{r}_i) - V(\vec{a}_i). \qquad (8)$$

The total internal-energy increase is

$$\Delta E_{int} = \tfrac{1}{2}\Sigma m_i (\vec{\omega}\times\vec{r}_i)\cdot(\vec{\omega}\times\vec{r}_i) + \tfrac{1}{2}\Sigma m_i v_i^2 + V(\vec{r}_i)$$
$$- V(\vec{a}_i). \qquad (9)$$

1. Vibrational and Rotational Energy Separation

Let us now examine the potential-energy change $[V(\vec{r}_i) - V(\vec{a}_i)]$. This change can result from both the vibrational and rotational motions. The vibrational effect on the potential energy is obvious. The rotational effect on the potential energy can be described as follows. When a molecule is rotating about its center of gravity, centrifugal forces develop stresses in the chemical bonds and, consequently, the bonds are stretched inelastically from their original equilibrium positions, $\vec{a}_i$, to new equilibrium positions, $\vec{b}_i$. This results in a rotational potential-energy change of $[V(\vec{b}_i) - V(\vec{a}_i)]$. The total potential energy change may be rewritten as $[V(\vec{r}_i) - V(\vec{b}_i)] + [V(\vec{b}_i) - V(\vec{a}_i)]$ where $[V(\vec{r}_i) - V(\vec{b}_i)]$, therefore, is the vibrational potential-energy change. Thus, the total internal-energy change, ΔE_{int}, can be divided into two parts: that resulting from the rotational-energy change, ΔE_r, and that resulting from the vibrational-energy change, ΔE_v, where

$$\Delta E_r = \frac{1}{2} \Sigma m_i \ (\vec{\omega} \times \vec{r}_i) \cdot (\vec{\omega} \times \vec{r}_i) + V(\vec{b}_i) - V(\vec{a}_i) \qquad (10)$$

and

$$\Delta E_v = \frac{1}{2} \Sigma m_i v_i^2 + V(\vec{r}_i) - V(\vec{b}_i) . \qquad (11)$$

Assuming that the atoms vibrate as simple harmonic oscillators around their equilibrium positions, $\vec{b}_i$, the vibrational-energy change becomes

$$\Delta E_v = \frac{1}{2} \Sigma m_i v_{oi}^2 \qquad (12)$$

where $\vec{v}_{oi}$ is the vibrational velocity of ith atom at its equilibrium location $\vec{b}_i$.

2. Momentum Excitation in Each Bond

Equations (10) and (12) represent the total vibrational and rotational-energy changes due to an impulse, $\vec{Q}$, received by an atom, N. Although this sudden impulse, $\vec{Q}$, will excite principally those bonds which link atom N to the remainder of the molecule, it will also cause some excitation in the other bonds in the molecule. In order to be able to calculate the impulse required to rupture a particular bond, it is necessary to express ΔE_r and ΔE_v as sums of the energy changes in each bond. The resulting expressions will depend upon the molecular configurations.

Let us consider a molecule which consists of a center atom, C, and (i-1) remaining atoms [1,2,....,j,....(i-1)] which are joined only to atom C. [Typical examples of such compounds are: CH_3Br where the Br receives the impulse, PCl_3 where the Cl receives the impulse, CH_3CH_2Br where the Br receives the impulse and the CH_3 is considered as a point mass. If the carbon in a compound such as CH_3Br receives the impulse, a slight modification of the final result is needed.] We define the bond which connects atoms C and j as j and define the vibrational and rotational-induced energy changes associated with this bond as ΔE_{vj} and ΔE_{rj}, respectively.

3. Vibrational-Energy Contribution

Using Eqs. (5) and (12), the vibrational-energy contribution is found to be

$$\Delta E_v = \sum_{j=1}^{i-1} \Delta E_{vj} = \frac{1}{2} \sum_{j=1}^{i-1} m_j \vec{v}_{oj} \cdot (\vec{v}_{oj} - \vec{v}_{oC}) \qquad (13)$$

Hence, the vibrational-energy change in bond j is

$$\Delta E_{vj} = \frac{1}{2} m_j \vec{v}_{oj} \cdot (\vec{v}_{oj} - \vec{v}_{oC}). \qquad (14)$$

4. Rotational-Energy Contribution

The rotational-energy change is separated on the basis that the rotational excitation of the chemical bonds is due to the centrifugal stresses developed in the bonds.

The centrifugal forces associated with atoms j and C are $\vec{F}_j = m_j\omega^2\vec{r}_j$ and $\vec{F}_C = m_C\omega^2\vec{r}_C$. However, $\vec{F}_C = -\sum_j \vec{F}_j$. Hence, the centrifugal force can be resolved into $-\vec{F}_j$ components (j=1 to j = i-1). The stress in bond j will be due to the centrifugal force, $\vec{F}_j$, on the jth atom and a portion of the centrifugal force of the atom C , $-\vec{F}_j$. Depicted in Fig. 1 are the forces acting on the bond, j, where G is the center of gravity and α_j is the angle between Gj and Cj.

The vector, $\vec{F}_j$, is next resolved into two components: F_{sj} is in the direction of bond j and will cause a stretching vibration of the bond; F_{bj} is perpendicular to the bond j and will cause a bending vibration in the bond. Using a simple valence-force approximation for the potential, we have

$$F_{sj} = 2F_j \cos \alpha_j = k_{sj}\, \delta_{sj} \qquad (15)$$

and

$$F_{bj} = 2F_j \sin \alpha_j = k_{bj}\, \delta_{bj}, \qquad (16)$$

where k_{sj} is the stretching-force constant, k_{bj}, the bending-force constant, δ_{sj} is the elongation of the bond j due to the stretching force F_{sj}, and $\delta_{bj} = \left|\vec{b}_j - \vec{b}_C\right| \theta_j$ where θ_j is the angle through which the bond is deflected due to F_{bj}.

The energy deposited in the bond due to stretching is

$$E_{sj} = 2m_j^2 r_j^2 \omega^4 (\cos^2 \alpha_j)/k_{sj} \qquad (17)$$

The energy deposited in the bond as a result of bending can be obtained in a similar manner. Thus, the total energy deposited in the bond due to rotation is

$$E_{rj} = 2m_j^2 r_j^2 \omega^4 \left[\frac{\sin^2\alpha_j}{k_{bj}} + \frac{\cos^2\alpha_j}{k_{sj}}\right]. \qquad (18)$$

The energies deposited in other bonds can be calculated in a similar manner. The fraction of the rotational energy, f_j, deposited in the bond j is

$$f_j = E_{rj} \Big/ \sum_{j=1}^{i-1} E_{rj}. \qquad (19)$$

The rotational energy change which is effective in the excitation of the bond j is

$$\Delta E_{rj} = f_j \, \Delta E_r = f_j \, \tfrac{1}{2}\Sigma m_i \, (\vec{\omega} \times \vec{r}_i) \cdot (\vec{\omega} \times \vec{r}_i) + V(\vec{b}_j) - V(\vec{a}_j) \qquad (20)$$

5. Potential-Energy Change Due to Inelastic Stretching

The potential-energy change of the bond j due to the rotation of the molecule can be approximated by $[V(d_{ej}) - V(d_{oj})]$ where d_{oj} and d_{ej} are the jth bond distances before and after inelastic stretching. Using a quadratic function,

$$V(d_j) = V(d_{oj}) - \tfrac{1}{2} k_{sj} (d_j - d_{oj})^2 - V_{rj}, \qquad (21)$$

where V_{rj} is the potential-energy change due to rotation of the molecule. As a result of conservation of angular momentum,

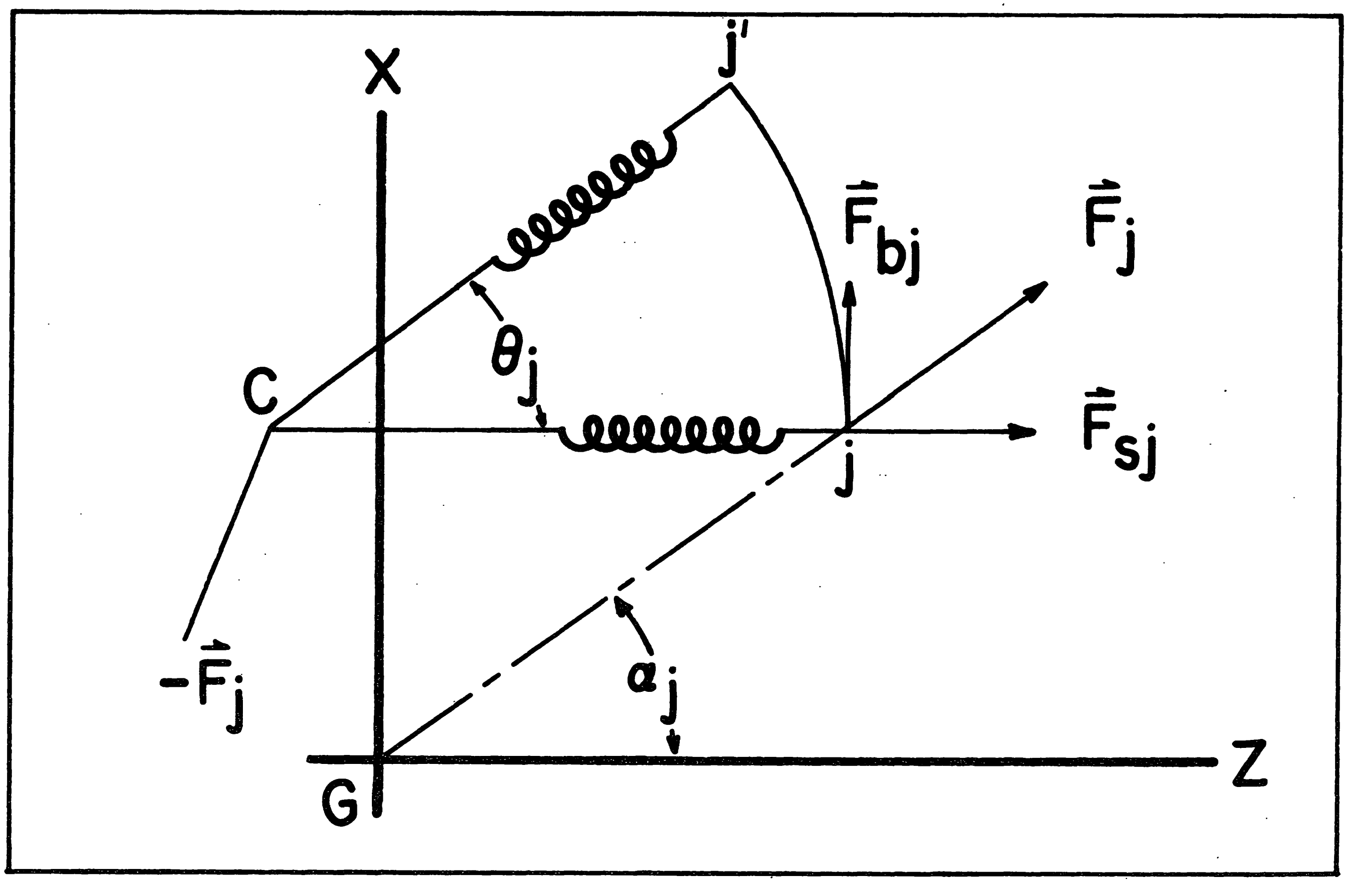

Figure 1. Centrifugal forces effecting the C-j bond.

$$V_{rj} = \tfrac{1}{2} m_j \, (\omega \, a_j)^2 \, (\cos^2\alpha_j) \, (a_j/r_j)^2. \tag{22}$$

For a small change, (r_j/a_j) may be approximated by (d_j/d_{oj}). Hence, from Eq. (21), the potential energy of the bond is

$$V(d_j) = V(d_{oj}) - \tfrac{1}{2} k_{sj}(d_j - d_{oj})^2 - \tfrac{1}{2} m_j(\omega a_j)^2(\cos^2\alpha_j)(d_{oj}/d_j)^2. \tag{23}$$

The new equilibrium distance, d_{ej}, is determined by $(\partial V(d_j)/\partial d_j)_{d_j = d_{ej}} = 0$ which results in

$$k_{sj}(d_{ej} - d_{oj}) - m_j(\omega a_j)^2(\cos^2\alpha_j)(d_{oj}^2/d_{ej}^3) = 0. \tag{24}$$

Combining Eqs. (20), (23), and (24),

$$\Delta E_{rj} = \tfrac{1}{2} f_j \Sigma m_i(\vec{\omega} \times \vec{r}_i) \cdot (\vec{\omega} \times \vec{r}_i) - \tfrac{1}{2} k_{sj} d_{oj}^2 \left[\frac{d_{ej}}{d_{oj}} - 1\right]\left[\frac{2d_{ej}}{d_{oj}} - 1\right], \tag{25}$$

and the total energy increase in bond j is $\Delta E_j = \Delta E_{vj} + \Delta E_{rj}$, which is obtained from Eqs. (14) and (25).

6. Rotational and Vibrational Excitations in a Molecule

If a momentum impulse, Q, were acquired by an atom, N, in a time-period so short that during that period it was not transmitted to the remainder of the molecule, then, $\vec{S}_N = (\vec{Q}/m_N) + {}_o\vec{S}_N$, where ${}_o\vec{S}_N$ is the velocity of the atom, N, before acquiring the impulse and $\vec{S}_N$ the velocity following the impulse. Thus, ${}_o\vec{S}_i \approx \vec{S}_i$ for $i \neq N$. If the impulse, $\vec{Q}$, is large compared to the momentum associated with the atoms of a thermal-energy molecule, then, $\vec{S}_N = \vec{Q}/m_N$ and $\vec{S}_i \approx 0$ for $i \neq N$. From conservation of momentum and the definition of space velocity,

$$\vec{\omega} \times \vec{r}_N + \vec{v}_N = \frac{\vec{Q}}{m_N} - \frac{\vec{Q}}{\Sigma m_i} = \frac{\Sigma m_i - m_N}{m_N \, \Sigma m_i} \vec{Q} \, . \tag{26}$$

The first term on the left-hand side of Eq. (26) describes the rotational effect and $\vec{v}_N$, the vibrational effect of $\vec{Q}$ on the Nth atom.

We may resolve $\vec{Q}$ into a component, $\vec{Q}_R$, which is perpendicular to $\vec{r}_N$ and results in a rotation of the molecule and into a component $\vec{Q}_V$, which will be in a random direction and will result in a vibration in the molecule which is dependent on the strength of the bonds and the moments of inertia.

Equation (26) can be separated into

$$\vec{\omega} \times \vec{r}_N = \frac{\Sigma \, m_i - m_N}{m_N \, \Sigma \, m_i} \vec{Q}_R \tag{27}$$

and

$$\vec{v}_N = \frac{\Sigma \, m_i - m_N}{m_N \, \Sigma \, m_i} \vec{Q}_V \, . \tag{28}$$

Realizing that there exists the relationships: $\vec{r}_N \perp \vec{\omega}$ and $\vec{r}_N \perp \vec{Q}_R$, it follows that

$$\vec{\omega} = \left[\frac{\Sigma \, m_i - m_N}{m_N \, \Sigma \, m_i}\right] \left[\frac{\vec{Q}_R \times \vec{r}_N}{r_N^{2}}\right] . \tag{29}$$

For k $\neq$ N,

$$\vec{v}_k = - \frac{\vec{Q}_V}{\Sigma \, m_i} - \frac{\vec{Q}_R}{\Sigma \, m_i} - \frac{\Sigma \, m_i - m_N}{m_N \, \Sigma \, m_i} \, \frac{(\vec{Q}_R \times \vec{r}_N) \times \vec{r}_k}{r_N^{2}} . \tag{30}$$

Consequently, the internal-energy increase in bond N is

$$\Delta E_{vN} = \frac{1}{2}\,\frac{\Sigma\, m_i - m_N}{m_N \Sigma\, m_i}\left[Q_V^2 + \frac{(\vec{Q}_V \cdot \vec{Q}_R)\left[m_N r_N^2 - (\Sigma\, m_i - m_N)(\vec{r}_C \cdot \vec{r}_N)\right]}{\Sigma\, m_i r_N^2} + \frac{\Sigma\, m_i - m_N}{\Sigma\, m_i}\,\frac{(\vec{r}_C \cdot \vec{Q}_R)(\vec{r}_N \cdot \vec{Q}_V)}{{r_N}^2}\right]. \tag{31}$$

In order to resolve $\vec{Q}$ into $\vec{Q}_R$ and $\vec{Q}_V$ we define the molecular coordinate system (x,y,z) choosing the center-of-mass, G, as the origin, and placing the bond N parallel to the z axis. The vector $\vec{Q}$ is resolved into Q_y, Q_t, and Q_r, where Q_y is parallel to the y axis, Q_t is on the plane xz and is perpendicular to $\vec{r}_N$ and Q_r is in the direction of $\vec{r}_N$. Since Q_r passes through the center of mass G, it will not affect the rotation of the molecule. Q_y will cause both a bending vibration of bond N and a rotation of the molecule, particularly in x- and z- directions, i.e. ω_x and ω_z. Q_t will also cause both a bending and a stretching vibration of bond N as well as a rotation in y-direction, ω_y. Let us write

$$Q_y = Q_{yv} + Q_{yr}$$

and

$$Q_t = Q_{tv} + Q_{tr},$$

where Q_{yv} and Q_{tv} are momenta effective in the vibration of the bond N, and Q_{yr} and Q_{tr} are momenta effective in the rotation of the molecule. We define the constants as given:

$$F_{yv} = \frac{{Q_{yv}}^2}{{Q_y}^2}, \qquad F_{yr} = \frac{{Q_{yr}}^2}{{Q_y}^2},$$

$$F_{tv} = \frac{Q_{tv}^2}{Q_t^2}, \qquad F_{tr} = \frac{Q_{tr}^2}{Q_t^2},$$

Upon averaging we obtain

$$\langle Q_V^2 \rangle_{Av} = \frac{1}{3}\left(1 + F_{yv} + F_{tv}\right) Q^2 \tag{32}$$

and

$$\langle \vec{Q}_V \cdot \vec{Q}_R \rangle_{Av} = \frac{1}{3}\left[(F_{yv}F_{yr})^{\frac{1}{2}} + (F_{tv}F_{tr})^{\frac{1}{2}}\right] Q^2 \tag{33}$$

based on the fact that $\langle Q_r^2 \rangle_{Av} = \langle Q_y^2 \rangle_{Av} = \langle Q_t^2 \rangle_{Av} = \frac{1}{3}Q^2$. Defining as γ the angle between $\vec{r}_C$ and $\vec{r}_N$, the vibrational-energy increase in bond N is

$$\langle \Delta E_{vN} \rangle_{Av} =$$

$$\frac{1}{6}\,\frac{Q^2}{m_N}\left[\frac{\Sigma m_i - m_N}{\Sigma m_i}\right]\left[1 + F_{yv} + F_{tv} + \left[(F_{yv}F_{yr})^{\frac{1}{2}} + (F_{tv}F_{tr})^{\frac{1}{2}}\right] \times \frac{m_N - (\Sigma m_i - m_N)\frac{r_C}{r_N}\cos\gamma}{\Sigma m_i}\right]. \tag{34}$$

It can be shown that when $r_N = a_N$,

$$\langle \omega_x^2 \rangle_{Av} = \left[\frac{\Sigma m_i - m_N}{\Sigma m_i}\right]^2 \left(\frac{Q^2}{3\, m_N}\right) \frac{F_{yr} \cos^2\alpha_N}{m_N\, a_N^2}, \tag{35}$$

$$\langle \omega_y^2 \rangle_{Av} = \left[\frac{\Sigma m_i - m_N}{\Sigma m_i}\right]^2 \left(\frac{Q^2}{3\, m_N}\right) \frac{F_{tr}}{m_N\, a_N^2}, \tag{36}$$

$$\langle \omega_z^2 \rangle_{Av} = \left[\frac{\Sigma m_i - m_N}{\Sigma m_i}\right]^2 \left(\frac{Q^2}{3\, m_N}\right) \frac{F_{yr}\sin^2\alpha_N}{m_N\, a_N^2}, \tag{37}$$

and

$$\langle \omega_x \omega_y \rangle_{Av} = \langle \omega_y \omega_z \rangle_{Av} = \langle \omega_z \omega_x \rangle_{Av} = 0. \tag{38}$$

Also,

$$\langle \omega^2 \rangle_{Av} = \frac{Q^2}{3\, m_N} \left[\frac{\Sigma\, m_i - m_N}{\Sigma\, m_i} \right]^2 \frac{F_{yr} + F_{tr}}{m_N\, a_N^{\;2}} \tag{39}$$

The total internal energy change in bond N will therefore be

$$\langle \Delta E_{\,iN} \rangle_{Av} = \mathfrak{F}\, \frac{Q^2}{2\, m_N} \left[\frac{\Sigma\, m_i - m_N}{\Sigma\, m_i} \right] \tag{40a}$$

where

$$\begin{aligned} \mathfrak{F} = \Bigg\{ & \frac{\Sigma m_i}{\Sigma m_i - m_N} \left[1 + F_{yv} + F_{tv} + \left[(F_{yv} F_{yr})^{\frac{1}{2}} + (F_{tv} F_{tr})^{\frac{1}{2}} \right] \frac{m_N - (\Sigma m_i - m_N) \frac{a_C}{a_N} \cos\gamma}{\Sigma m_i} \right] \\ & + f_N \, \frac{F_{yr} (I_{xx} \cos^2\alpha_N + I_{zz} \sin^2\alpha_N) + F_{tr} I_{yy}}{m_N a_N^{\;2}} \\ & - (F_{yr} + F_{tr}) \cos^2\alpha_N \left[\frac{d_{oN}}{d_{eN}} \right]^2 \left[2 - \frac{d_{oN}}{d_{eN}} \right] \Bigg\} \frac{\Sigma m_i - m_N}{3 \Sigma m_i} \end{aligned} \tag{40b}$$

7. Estimation of Constants

Consider Q_t acting on the atom as depicted in Fig. 2. As a result of Q_{tr}, the molecule will rotate; the inertia opposing rotation is I_{yy}. As a result of Q_{tv} the molecule will vibrate. The bond N will stretch and bend as a result of $Q_{tv} \sin\alpha_N$ and $Q_{tv} \cos\alpha_N$, respectively. If δ_{sN} is the maximum elongation of bond N due to $Q_{tv} \sin\alpha_N$, energy balance gives

$$\frac{Q_{tv}^{\;2} \sin^2\alpha_N}{m_N} = k_{sN}\, \delta_{bN}^{\;2} \,.$$

Similarly,

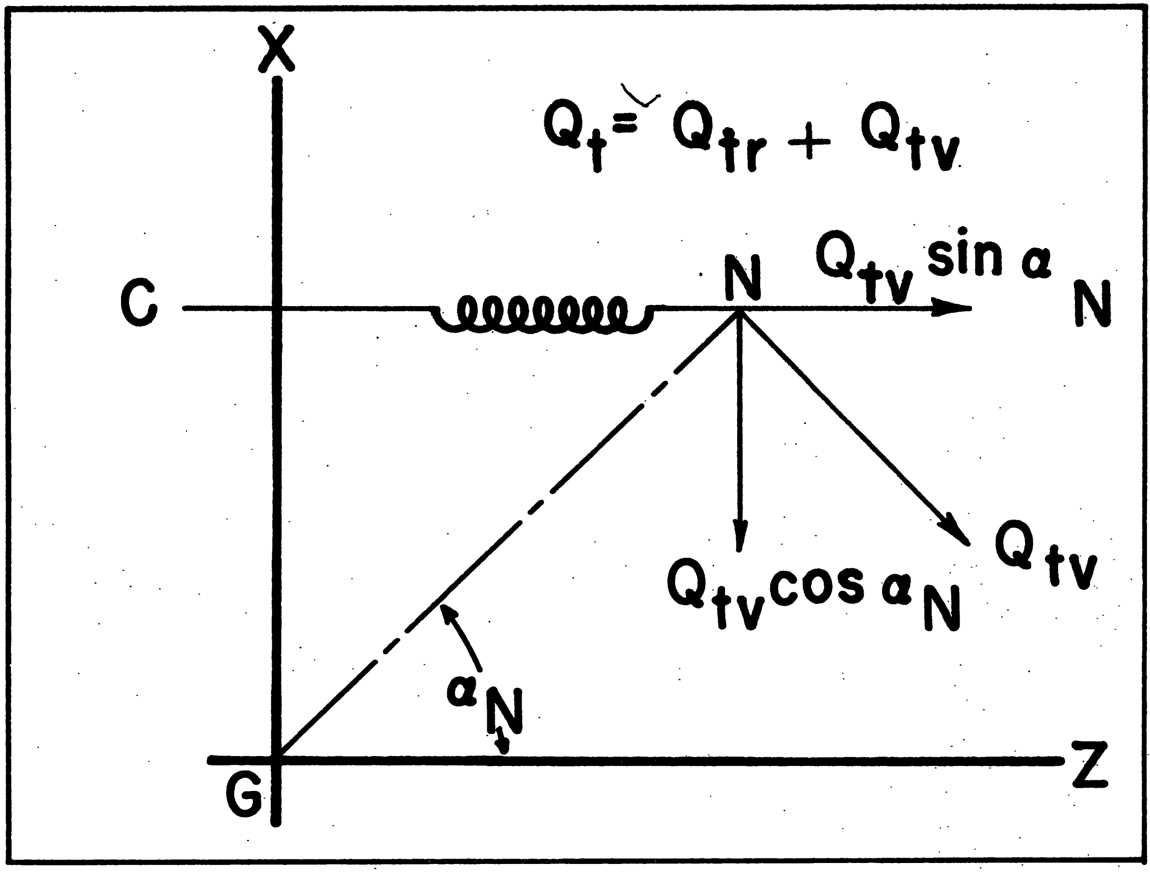

Figure 2. Resolution of the momentum·vector, Q_t.

$$\frac{Q_{tv}^2 \cos^2 \alpha_N}{m_N} = k_{bN}\, \delta_{bN}^2 .$$

The degree of difficulty in deforming a bond increases as m_N, δ_{sN}, and δ_{bN} increase. Let us assume that the deformation inertia opposing Q_{tv} is

$$m_N(\delta_{bN}^2 + \delta_{sN}^2) = Q_{tv}^2 \left[\frac{\cos^2\alpha_N}{k_{bN}} + \frac{\sin^2\alpha_N}{k_{sN}}\right] = \frac{Q_{tv}^2}{k_{tN}} ,$$

where

$$\frac{1}{k_{tN}} = \frac{\cos^2\alpha_N}{k_{bN}} + \frac{\sin^2\alpha_N}{k_{sN}} . \tag{41}$$

The total inertia that is opposing Q_t is therefore

$$I_{yy} + \frac{Q_{tv}^2}{k_{tN}} .$$

The fraction of inertia that is opposing Q_{tr} should also be the fraction of Q_t that is associated with Q_{tv}. Thus

$$\frac{I_{yy}}{I_{yy} + \dfrac{Q_{tv}^2}{k_{tN}}} = \frac{Q_{tv}}{Q_t} . \tag{42}$$

Solving Eq. (42) for Q_{tv}, it is found that

$$F_{tv}^{\frac{1}{2}} = \frac{Q_{tv}}{Q_t} = \frac{3}{2}(u_t)^{\frac{1}{3}} \left\{\left[1 + (1+u_t)^{\frac{1}{2}}\right]^{\frac{1}{3}} + \left[1 - (1+u_t)^{\frac{1}{2}}\right]^{\frac{1}{3}}\right\}, \tag{43}$$

where $u_t = \dfrac{4k_{tN}\, I_{yy}}{9Q^2}$. In a similar manner,

$$F_{yv}^{\frac{1}{2}} = \frac{Q_{yv}}{Q_y} = \frac{3}{2}(u_y)^{\frac{1}{3}} \left\{ \left[1 + (1+u_y)^{\frac{1}{2}}\right]^{\frac{1}{3}} + \left[1 - (1+u_y)^{\frac{1}{2}}\right]^{\frac{1}{3}} \right\}, \quad (44)$$

where $$u_y = \frac{4k_{bN}(I_{xx}\cos^2\alpha_N + I_{zz}\sin^2\alpha_N)}{9Q^2}.$$

C. Failure to Bond-Rupture

When $\langle\Delta E_{iN}\rangle_{Av}$ attains the value of the dissociation energy of bond N, E_{BN}, bond rupture results. Rearranging Eq. (40), the momentum required for bond rupture defined as $Q°$ will be

$$Q° = \left(\frac{6m_N E_{BN}}{(F_{yr} + F_{tr})\cos^2\alpha_N\,[B - d_N^{*2}(2 - d_N^*)]}\right)^{\frac{1}{2}} \frac{\Sigma m_i}{\Sigma m_i - m_N}, \quad (45)$$

where $$d_N^* = d_{oN}/d_{eN} \quad \text{and} \quad (46)$$

$$B = \frac{1}{(F_{yr}+F_{tr})\cos^2\alpha_N} \left\{ \frac{\Sigma m_i}{\Sigma m_i - m_N} \left[1 + F_{yv} + F_{tv} + \left[(F_{yv}F_{yr})^{\frac{1}{2}} + (F_{tv}F_{tr})^{\frac{1}{2}}\right] \frac{m_N - (\Sigma m_i - m_N)\frac{a_C}{a_N}\cos\gamma}{\Sigma m_i} \right] + f_N \frac{F_{yr}(I_{xx}\cos^2\alpha_N + I_{zz}\sin^2\alpha_N) + F_{tr}I_{yy}}{m_N a_N^2} \right\} \quad (47)$$

From Eqs. (24) and (45), B can also be evaluated in terms of the expression:

$$B = \frac{2E_{BN}(d_N^*)^4}{k_{sN}d_{oN}^2(1 - d_N^*)} + d_N^{*2}(2 - d_N^*). \quad (48)$$

In the particular case where the atom receives a gamma-ray momentum impulse, the energy of the gamma ray required for bond-rupture is $E^\circ_\gamma = Q^\circ c$, where c is the velocity of light.

D. Calculation of Q°

To calculate the recoil momentum required for bond-rupture, a method of successive approximations could be used. The steps are : (1) calculating I_{xx}, I_{yy}, I_{zz}, $\cos \alpha_N$, and $\cos \gamma$ for each molecule using bond-distance and bond-angle data, (2) assuming a value of Q°, (3) calculating u_y, u_t, and consequently, F_{yr}, F_{yv}, F_{tr}, F_{tv}, and B using the assumed value of Q° and Eqs. (43), (44), and (47), (4) solving for d^*_N in Eq. (48) using the value of B obtained in step (3), (5) calculating Q° by substituting the calculated values of F_{yr}, F_{tr}, B, and d^*_N into Eq. (45) and comparing with the assumed value of Q°.

To avoid these lengthy calculations generalized plots were prepared of some of the variables. These plots are discussed and sample calculations are given in Appendix III.

The minimum net recoil energies, $E^\circ_T = (Q^\circ)^2/2m_N$, required for bond-rupture were calculated for a series of halomethanes and are listed in Table I. It is noted that, in general, the heavier the mass of the radical attached to the activated atom, the smaller the net recoil energy required for bond rupture.

Also presented in Table I, as a percent of E°_T, are the rotational and the vibrational-excitation energies received by the bond ($E_{BN} = E_v^\circ + E_r^\circ$). For a diatomic molecule, Steinwedel and Jensen[23] have shown that $E_v/(E_v + E_r) = 2/3$. Typical values of this quantity for the compounds in Table I are: CH_3Br - 0.79, CD_3Br - 0.84, CF_3Br - 0.98, CCl_3Br - 1.00, CBr_4 - 1.00. It is seen that the heavier the radical attached to the activated atom, the more unlikely is rotational excitation. This is to be expected since (1) an increase in molecular weight is accompanied by an increase in the moments of inertia and (2) the bending-force constants for similar carbon-halogen bonds do not change appreciably. The net result is that, with increased molecular weight, rotation becomes more difficult compared with vibration of the molecule.

The fraction of the internal energy, $\mathfrak{F}^\circ$, received by the bond which joins the activated atom to the molecule is given in Table I for values of E_T° for each molecule. For these molecules, the average value of $\mathfrak{F}^\circ$ is 0.80. This value can serve as a means for predicting the energy E_T° required for bond-dissociation. Thus, on the average, $E_T^\circ = E_{BN}\,\Sigma m_i/[0.80 \times (\Sigma m_i - m_N)]$.

It is interesting to compare $\mathfrak{F}^\circ$ values for a series of structurally similar molecules. For the series: CH_3Br, CD_3Br, CF_3Br, CCl_3Br, CBr_4, the $\mathfrak{F}^\circ$ values are 0.895, 0.860, 0.819, 0.874, and 0.936, respectively. It may appear surprising that the $\mathfrak{F}^\circ$ values should first decrease and then increase. This is due to a combination of effects: (1) when the radical attached to the activated atom is of low molecular weight, it responds approximately as a point mass. As the molecular

Table I. Minimum Energy Required and Energy Distribution for Carbon-Halogen Bond Rupture[a].

Compound[b]	E°_T ev	$\frac{E^\circ_v}{E^\circ_T}$ %	$\frac{E^\circ_r}{E^\circ_T}$ %	$\mathfrak{F}^\circ$
CH_3I	27.29	6.63	1.94	0.818
CD_3I	23.86	8.00	1.80	0.795
CF_3I	8.34	23.61	1.57	0.719
CH_2I_2	5.52	36.79	0.02	0.700
C_2H_5I	20.41	9.47	1.60	0.599
i-C_3H_7I	12.97	13.92	2.81	0.665
n-C_3H_7I	12.76	13.39	2.28	0.623
CH_3Br	20.74	11.12	3.01	0.895
CD_3Br	18.54	13.19	2.61	0.860
CF_3Br	7.38	37.29	0.64	0.819
CCl_3Br	4.06	52.18	0.02	0.874
CH_2Br_2	6.14	41.83	0.02	0.775
CF_2Br_2	4.90[c]	53.06	0.02	0.858
CCl_2Br_2	3.64[c]	58.23	0.00	0.868
$CHClBr_2$	4.93[c]	51.70	0.02	0.839
$CHBr_3$	4.76	56.09	0.00	0.820
CBr_4	2.98	71.04	0.00	0.936
C_2H_5Br	15.14	16.00	2.63	0.700
1,1-$C_2H_4Br_2$	5.78[c]	46.69	0.02	0.813
CH_3Cl	14.68	20.72	3.06	0.840
CD_3Cl	13.26	23.93	2.38	0.819
CF_3Cl	6.14	56.05	0.17	0.872
CHF_2Cl	7.13[c]	45.76	0.26	0.803
CH_2Cl_2	7.45	42.80	0.00	0.757
CF_2Cl_2	5.63	59.66	0.00	0.862
$CHCl_3$	5.16	56.04	0.00	0.814
$CFCl_3$	5.21	62.99	0.00	0.864
CCl_4	4.46	66.11	0.00	0.873

Table I. (Con't.)

Compound[b]	E°_{T} ev	$\frac{E^{\circ}_{v}}{E^{\circ}_{T}}$ %	$\frac{E^{\circ}_{r}}{E^{\circ}_{T}}$ %	$\mathfrak{F}^{\circ}$
CH_4	6.78	64.06	1.13	0.696
CD_4	6.91	61.84	2.12	0.711
CFH_3	5.30	83.31	0.09	0.858
CF_2H_2	4.81	91.89	0.00	0.938
CF_3H	4.74	93.25	0.00	0.943
CF_4	9.33	65.38	1.07	0.847
CHF_3	9.15	54.17	1.02	0.757
CH_2F_2	9.90	47.60	1.29	0.771
CH_3F	13.50	28.94	5.43	0.779
CH_3T^+	2.18	67.41	1.40	0.837
$C_2H_5T^+$	1.79	83.71	0.09	0.925
n-$C_3H_7T^+$	1.66	90.36	0.00	0.966
i-$C_3H_7T^+$	1.69	88.76	0.00	0.950
$H_3C^{14}H_3N^+$	3.75	49.93	1.00	0.866

---

[a] The bond-dissociation energy, $E_{BN} = E^{\circ}_{r} + E^{\circ}_{v}$.

[b] The dissociating atom is the last element listed in the formula.

[c] Based on estimated E_{BN}.

weight of the radical increases (for constant E_T) it appears less like a point-mass radical and the energy absorbed as internal energy of the radical increases. Hence, $\mathfrak{F}$ decreases. (2) When the mass of the radical increases, E_T° decreases since the factor that principally affects the energy transferred into internal energy, $(\Sigma m_i - m_N)/ \Sigma m_i$, becomes larger. Due to the smaller recoil momentum acquired by the whole molecule, the internal energy received by the radical will be small. The radical again begins to approximate a point mass and $\mathfrak{F}^\circ$ increases.

E. Summary

A molecule is visualized as being composed of a group of point-mass atoms joined together by springs. When one of the atoms in the molecule receives a momentum impulse, Q, the atom will dissociate from the molecule if $Q \geqq Q^\circ$. An equation is derived relating Q° to the bond energy, bond angles and distances, and the masses of the atoms in the molecule.

In deriving this expression, two major assumptions are made. They are

1. The rotational and vibrational motions of the molecule are independent and can therefore be separated.
2. The momentum impulse is acquired by the atom in a time period which is short compared with the time required for the dissociation of the atom. This dissociation time is probably of the order of

10^{-14} sec., the time required for one vibration. This is, perhaps, the most crucial assumption, leading to the approximation that the atoms other than the reoiling atom do not experience an increase in space velocity. It is not obvious how to correct for this effect since the time sequence of momentum transfer through the molecule is not known. Since some intramolecular momentum transfer undoubtedly does occur, the calculated values of Q° must, of necessity, be low. The extent of correction needed to correct for this effect would probably depend upon the complexity of the molecule. Thus, for recoiling Br, Q° for CH_3Br could be closer to the correct value than would Q° for C_2H_5Br. Similarly, Q° for i-C_3H_7I could be more correct than Q° for n-C_3H_7I since, in the latter compound, the atoms, on the average, are separated from the recoiling iodine by a larger number of chemical bonds.

The various data used in calculating the values given in Table I are given in Appendix I. A simple calculation of E_T° is given in Appendix III where C_2H_5Br is used as the example.

Chapter III. THE APPLICATION OF THE MOMENTUM TRANSFER TO FAILURE TO BOND-RUPTURE

A. Molecular Dissociations following the (n,γ) Reactions

In the preceding chapter a method is proposed for calculating the increase in internal energy of a polyatomic molecule.

If a single gamma ray, of the order of 6 Mev energy, is emitted by an atom it would be expected that the activated atom would always rupture from its parent compound. The only exception would be, perhaps, the case where the activated atom was bonded to an atom of small atomic weight, as, for example, in the hydrogen halides. However, indirect experimental evidence[11] indicated that in the (n,γ) activation of gaseous C_2H_5I, of the order of 1% of the I^{128} did not rupture from the parent molecule.

Such failure to bond-rupture can be explained. In (n,γ) activation, and particularly in the activation of the halogens, the neutron-binding energy is released most frequently not as a single gamma quantum, but as a gamma-ray cascade. Because of partial cancellation of gamma-ray momenta, some of the atoms could receive a net-recoil momentum which is less than that required for bond rupture.

If the complete neutron capture - gamma ray cascade spectrum is known, and if there are no angular correlations between the gamma rays, then, using the method of random walks,[26,27] the net gamma-ray momentum probabilities can be calculated. (Such a calculation has been performed for the

$Cl^{35}(n,\gamma)Cl^{36}$ process.[26]) In addition, if the net gamma-ray momentum required for bond rupture can be calculated, then it is possible to predict the percent of the activated atoms which will fail to rupture from their parent compound.

1. Results

Let us assume that the I^{128} or Br^{80} splits from a molecule only if it receives a net gamma-ray momentum sufficient to cause carbon-halogen bond rupture. Then, for a series of molecules, a plot of the percent failure to bond-rupture vs. the calculated net gamma-ray energy required for bond rupture should be identical with a plot of the gamma-ray energy probability vs. the net gamma-ray energy.

Since, for these isotopes, the neutron capture-gamma ray data are inadequate to permit calculating the probabilities, the latter plot cannot be obtained. However, the general shape of the probability curve will, perhaps, be similar to that calculated for the $Cl^{35}(n,\gamma)Cl^{36}$ process.[26]

Listed in Table II are the literature values of the percent of halogen activity found in the organic phase,[12] and the net gamma-ray energy required for bond rupture, $E_\gamma^\circ = (E_T^\circ\, m_N/\, 537)^{\frac{1}{2}}$.

Presented in Figures 3 and 4 are the observed I^{128} and Br^{80} as organic as a function of the fractional gamma-ray energy, $E_\gamma^\circ\, /\, E_{max}$, where E_{max} is the neutron binding energy and equals 6.6 Mev for I^{128} and 7.3 Mev for Br^{80}. The dashed curve is the lower-energy portion of the probability vs. $E_\gamma\, /8.5$ Mev curve for the $Cl^{35}(n,\gamma)Cl^{36}$ process. This

TABLE II

Calculated Net Gamma-Ray Energy Required for Bond-Rupture and the Percent of Failure to Bond-Rupture.

Molecule[a]	E°_{γ}, Mev	Percent of Halogen Found as Organic[12]
CH_3Br	1.76	0.25
CD_3Br	1.66	0.20
CH_2Br_2	0.959	0.115
CF_3Br	1.05	0.105
CF_2Br_2	0.855	0.093
$CHClBr_2$	0.852	0.087
CCl_3Br	0.779	0.066
$CHBr_3$	0.843	0.048
CBr_4	0.667	0.031
C_2H_5Br	1.52	0.33
1,1-$C_2H_4Br_2$	0.941	0.173
CH_3I	2.39	1.09
CD_3I	2.24	0.68
CF_3I	1.33	0.12
CH_2I_2	1.08	0.068
C_2H_5I	2.12	0.82
n-C_3H_7I	1.73	0.66
i-C_3H_7I	1.61	0.30

[a] The atom receiving the gamma-ray impulse and dissociating is the last element listed in the formula.

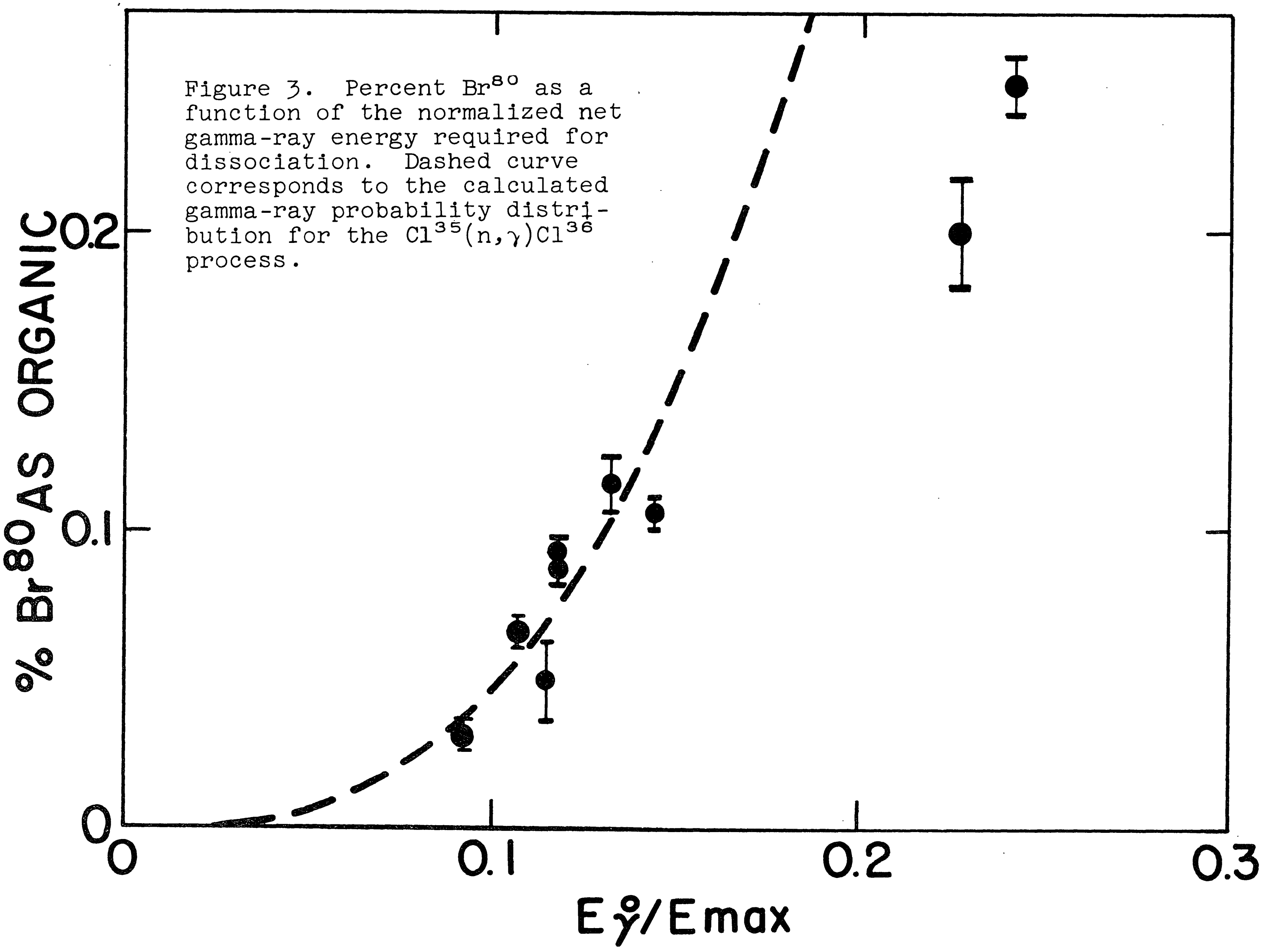

Figure 3. Percent Br^{80} as a function of the normalized net gamma-ray energy required for dissociation. Dashed curve corresponds to the calculated gamma-ray probability distribution for the $Cl^{35}(n,\gamma)Cl^{36}$ process.

curve differs slightly from that presented in Ref. 26 in that recent data [28] are included in the random-walk calculation.

2. Discussion

The data presented in Figs. 3 and 4 appear to describe a function characteristic of the energy distribution associated with (n,γ) activation. However, there is no assurance that the E_γ° energies ascribed to the compounds actually correspond to the net gamma-ray energies required for dissociation. It could be due to the fact that the formation of ionized or electronically excited halogen is not taken into account. It is known[9] that at least 18% of Br^{80} and 50% of I^{128} formed by (n,γ) activation is positively charged. Such positive charge probably results from the internal conversion of low-energy gamma-rays resulting from cascade-gamma emission.

If a positively charged alkyl-halide molecule is produced, two possible modes of dissociation are $RX^+ \rightarrow R + X^+$ and $RX^+ \rightarrow R^+ + X$. For most alkyl halides, the first process requires the larger amount of energy. If the energy imparted to the halogen is less than that required for the first process, but greater than that required for the second, then the molecule could remain intact until internal electronic rearrangement occurs. The value of E_γ° required for bond rupture of the positively charged molecule differs from that required for the neutral molecule. For example, $E_\gamma^\circ = 2.77$ Mev for $CH_3I^+ \rightarrow CH_3^+ + I$ and 2.55 Mev for neutral CH_3I. For $CH_3Br^+ \rightarrow CH_3^+ + Br$ and CH_3Br, $E_\gamma^\circ = 1.57$ and 1.76 Mev respectively.

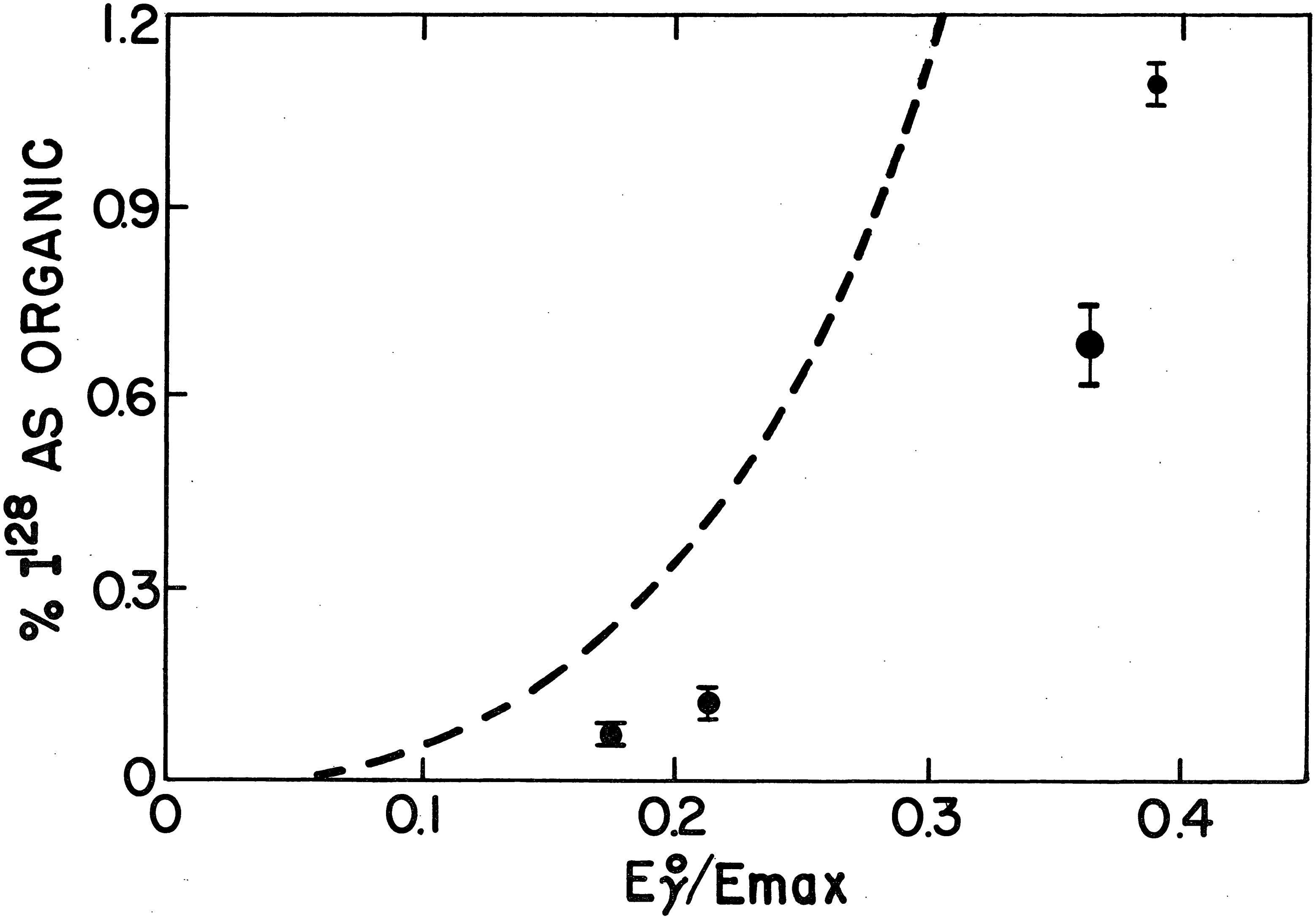

Figure 4. Refer to Fig. 3. Data are for C-I^{128} bond rupture.

Unfortunately, the ionization potential of many of the radicals are not available. Thus, it is not possible to determine whether the data would approximate a smoother curve if ionization effects were taken into account.

For gamma-cascade emission involving, perhaps, more than three or four gamma-ray quanta another problem arises. It is possible, in such cascade processes, that molecular dissociation occurs before all cascade-gamma rays are emitted. In order to determine the importance of this effect it is necessary to have knowledge of the lifetimes of intermediate nuclear states. Such information is not available, although it can be estimated[29,30] that the lifetimes may be of the order of 10^{-15} to 10^{-14} sec.

Since vibrational times are of the order of 10^{-14} sec., the number of gamma rays effecting dissociation may be less than the total number of gamma rays emitted by the nucleus. As a result, the gamma-ray energy-probability distribution which must be evaluated would differ from that calculated for the complete cascade processes, although this distribution would again represent a smooth rising curve. However, if, because of the differences in vibrational times, the number of gamma rays effecting dissociation vary from compound to compound, separate distribution curves would be required for each molecule and the experimental failure to bond-rupture data would not necessarily be expected to approximate a smooth rising curve.

From the above discussion it is apparent that it is not possible to calculate unambiguously either the gamma-ray recoil energy necessary for bond rupture or the recoil-energy distribution associated with the atoms prior to dissociation.

a. Higher Alkyl Halides Because of the assumption that the space velocities of the non-recoiling atoms are the same, it is not surprising that the data for alkyl halides containing more than one carbon atom if plotted in Figs. 3 and 4 would not approximate the same curve as that for the methyl halides. The greater the number of bonds separating an atom in a molecule from the atom receiving the recoil, the less effected will be the non-recoiling atom. Thus, a fraction of the energy could be deposited in the C-C bond. If it were possible to correct for this effect, the calculated E_{γ}° values would be numerically larger and the data for C_2H_5I, n-C_3H_7I, i-C_3H_7I, C_2H_5Br, and 1,1-$C_2H_4Br_2$ would probably be more in accord with the data for the methyl halides.

b. Cl^{36} Recoil Lacking any other means of comparison, the normalized, calculated $Cl^{35}(n,\gamma)Cl^{36}$ gamma-ray probability curve was also plotted in Figs. 3 and 4. There is no reason to expect the Br^{80} and I^{128} data to be in agreement with the Cl^{36} curve. This calculated curve serves only to indicate the general shape of the probability distribution curve associated with a gamma-recoil process which involves fairly complex gamma-ray cascades. However, the fact that the experimental data do approximate a smooth rising curve similar to that of Cl^{36} would suggest that the (n,γ) failure to bond-rupture is due to the partial cancellation of gamma-ray momenta.

3. Diatomic Molecules

The gamma-ray recoil energy, E_γ°, required for bond rupture of a diatomic molecule may be calculated exactly according to Eq. (2) since $\Delta E_i = E_{BN}$, the bond-dissociation energy. For Br^{80}-Br, $E_\gamma^\circ/E_{max} = 0.106$; for I^{128}-I, the value is 0.095. Referring to Figs. 1 and 2, it is seen that the expected extents of failure to bond-rupture would be approximately 0.05 and 0.02 percent respectively. For the hydrogen halides, E_γ°/E_{max} would be much greater than that included in the range of data given in Figs. 3 and 4.

B. Molecular Dissociation by Beta-Decay Recoil

In beta decay, if it is assumed that there is no angular correlation between the emitted beta particle and the neutrino, then the recoil energy, E_T, imparted to the product isotope is[31]:

$$E_T = 140\ [(W^2 - 1) + (W_m - W)^2]/m_N \qquad (49)$$

where E_T is in ev, W is the beta-ray energy in units of the beta-ray rest-mass energy equivalent: m_0c^2, W_m is the maximum beta-ray energy in this dimensionless form, and m_N is the mass in amu of the product isotope.

Using published carbon-14 and tritium beta-ray energy spectra[32,33], the energy, E_T imparted to the N^{14} or He^3 was calculated as a function of the probability, $P(E_T)$, that the imparted energy is $\leqq E_T$. These data are given in Figs. 5

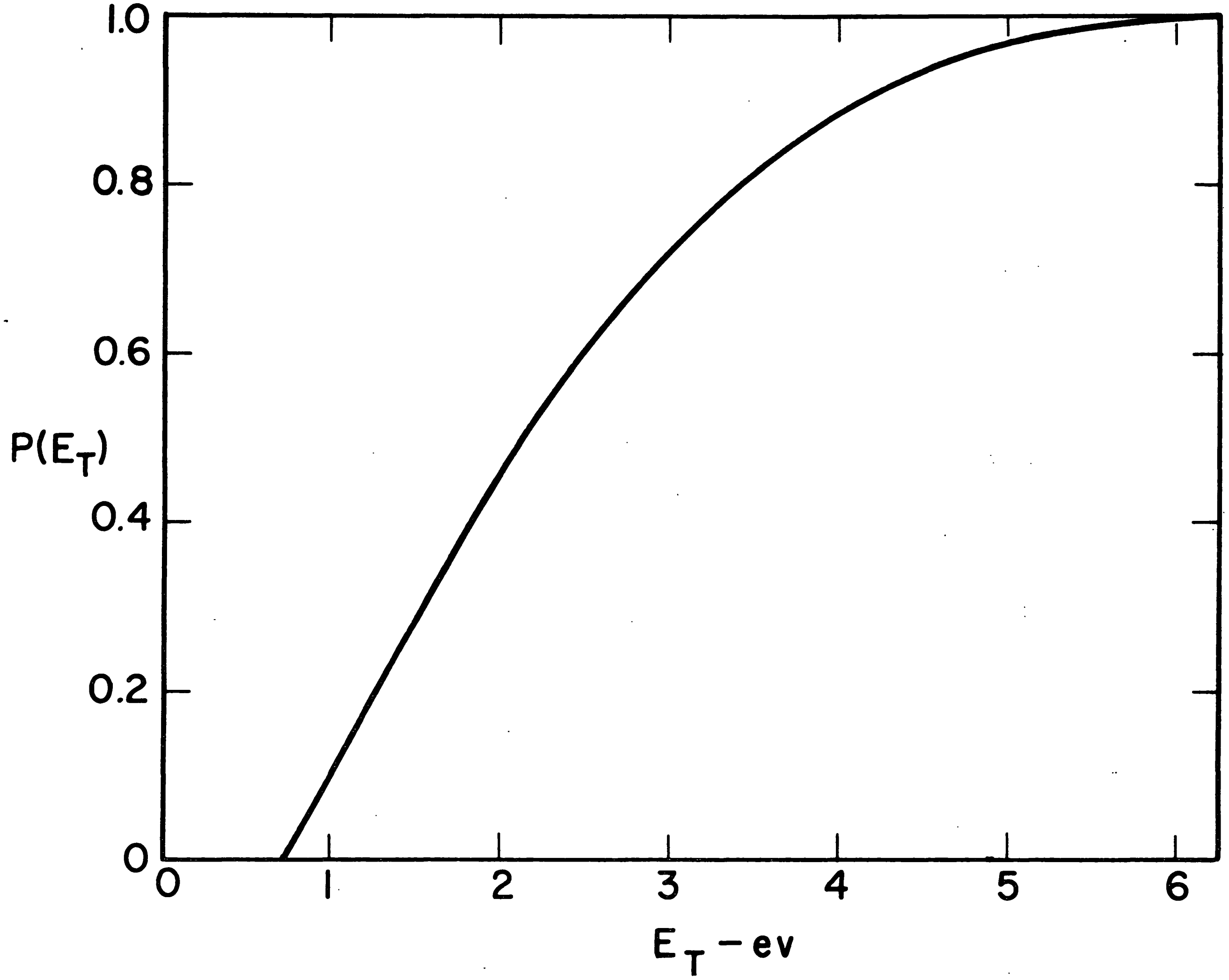

Figure 5. $P(E_T)$ vs E_T for C^{14} beta decay

and 6. For N^{14} and He^3, the maximum values of E_T are 6.08 and 3.35 ev respectively.

The expected C^{14} and H^3 beta-recoil failure to bond-rupture was calculated for a number of gaseous molecules for which experimental data were available. In performing the calculations, the influence of electronic excitation on the bond-dissociation energy was estimated using, as a guide, the Franck-Condon principle and the Morse potential function. The value of E_T^o was then calculated and the probability of acquiring less than this value was determined directly from the beta-ray recoil energy probability graph. In the case of the C^{14} decay of C_2H_6 to yield $CH_3NH_2^+$, insufficient data were available in the literature to predict the effect of electronic excitation on the bond-dissociation energy. For this molecule, E_T^o was calculated assuming that the $CH_3NH_2^+$ was not electronically excited. Using this E_T^o value, the corresponding probability value was obtained and this latter value multiplied by the probability that a $1s^2 2s2p^3$ carbon atom becomes a $1s^2 2s2p^3$ positive nitrogen[25]. This product is the expected C-N failure to bond-rupture.

These data are given in Table III and further discussions of these methods are presented below.

1. HT and T_2

Using a modified mass spectrometer, Wexler determined that 89.5% of the $(H\text{-}He^3)^+$ product of HT and 94.5 % of the $(T\text{-}He^3)^+$ product of T_2 remained bound during the 10^{-4} sec. transit time of the spectrometer[34]. He suggested that the

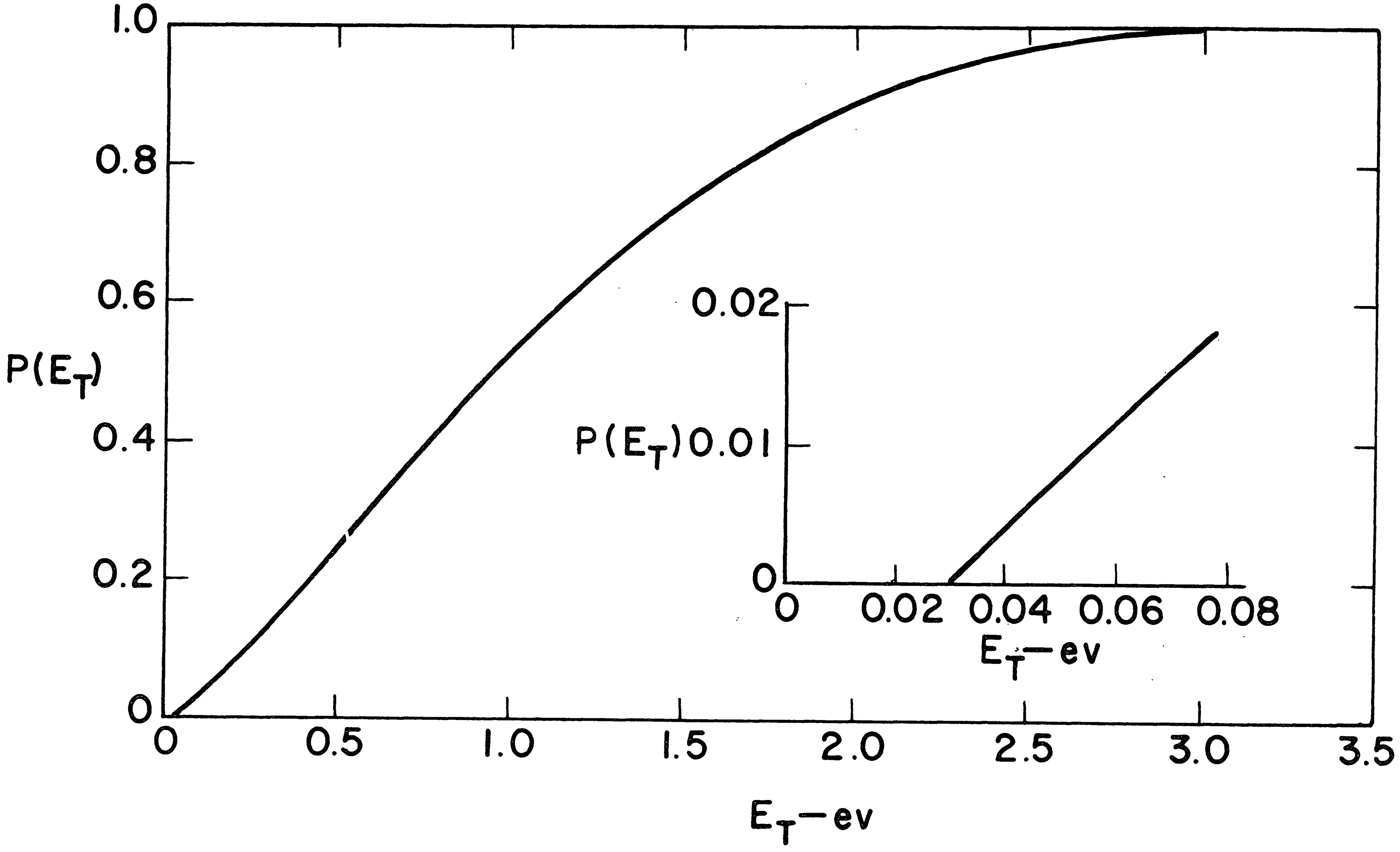

Figure 6. $P(E_T)$ vs E_T for H^3 beta decay

Table III. Minimum Energy Required for Bond Rupture

Parent Compound	E_T° ev	$\mathfrak{F}^\circ$	% non-rupture Calc.	Exp.
HT	a	1.0	a	89.5[34]
TT	a	1.0	a	94.5[34]
CH_3T	0.070	0.84	1.5	0.2[35]
C_2H_5T	0.059	0.93	1.1	0.2[36]
$CH_3CH_2CH_2T$	0.055	0.97	0.9	0.2[37]
CH_3CHTCH_3	0.056	0.95	1.0	0.2[37]
$C^{14}O_2$	3.06-3.82	0.85	73-87	81 [35]
$C_2{}^{14}H_6$	3.75	0.87	69	56 [38,39]

[a] Refer to text for calculated values.

greater stability of $(THe^3)^+$ was due principally to the slight difference in zero-point vibrational energies as well as the larger vibrational amplitude of $(THe^3)^+$. The following explanation appears to explain the observations more satisfactorily.

The potential curves for the ground state HT and T_2 molecules (curve A), the excited ionic state HHe^+ and THe^+ ions (curve B), and the ground ionic state HeH^+ and HeT^+ ions (curve C) are given in Fig. 7. Immediately following beta-particle emission, the positive charge should reside on the helium and a transition from A to B should result. If the molecule-ion remained in this state, vibrational dissociation would result and the failure to bond-rupture would be 0%. Since a large fraction of the ions are stable for periods much longer than a vibrational period of 10^{-14}sec., transitions from B to C must frequently occur. This implies that the charge-transfer rate exceeds the molecular-vibrational rate.

If the charge-transfer process is much faster than the vibrational rate, all ions would undergo a transition to curve C. Dissociation would then occur if the recoil energy exceeded that required for bond rupture. Since the amount of energy required for the dissociation of HeH^+ is twice[a] that required for HeT^+, the failure to bond-rupture of HeH^+ should be greater than that of HeT^+ in contradiction of the

---

[a] For a diatomic molecule, $E_T^\circ = E_{BN}\Sigma m_i/(\Sigma m_i - m_N)$. Thus, $E_T^\circ = 4\ E_{BN} = 7.28$ ev for ground-state HeH^+ dissociation and $E_T^\circ = 2\ E_{BN} = 3.46$ ev for ground state HeT^+ dissociation. A HeH^+ bond energy of 1.82 was assumed[40].

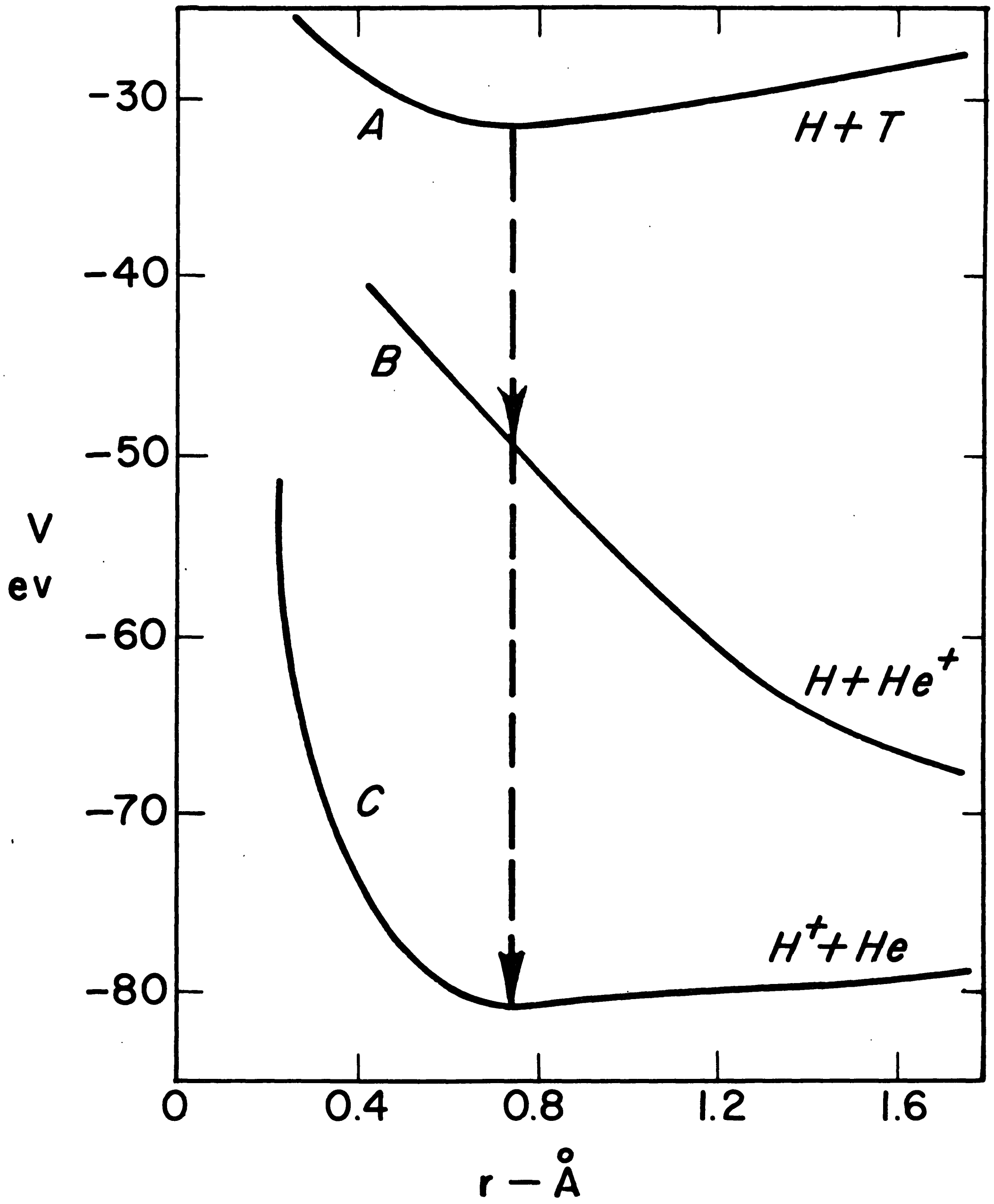

Figure 7. Electronic excitation of HT in tritium beta-decay.

experimental observations.

The data are explained if it is assumed that the charge-transfer rate is only slightly greater than the vibrational rate. Under these conditions most of the ions will undergo a transition from B to C. Since the vibrational frequency of HHe^+ is about $\sqrt{2}$ times as great as that of THe^+ it would be expected that a larger fraction of HHe^+ would be able to dissociate prior to charge-transfer. Some of those ions which succeed in reaching curve C can dissociate if they have sufficient energy. However, both molecules have received the same distribution of energy and for state C as stated above, a larger amount of HeT^+ should dissociate. In order that the combined dissociation from states B and C be such that the percent dissociated $HeT^+ < HeH^+$ it is necessary that a smaller number of dissociations occur in state C.

The potential function for the HeH^+ ion was calculated using the Morse equation and data of Evett[40]. It was assumed that curve C is identical for HeT^+ and HeH^+. The percent dissociation which would occur if all the ions were in the vibrational state $\underline{v}$ of curve C was then calculated using the tritium beta-recoil energy-probability curve. These results are given in Table IV. Since the observed amounts of HeH^+ and HeT^+ are 89.5 and 94.5%, respectively, the data of Table IV suggest that most of these ions would undergo a transition from curve B mainly to the $v = 0$ or $v = 1$ vibrational states of curve C.

Table IV. Tritium Beta-Recoil Dissociation

Vib. State, v	% Failure to Bond-Rupture[a] HeH^+	 HeT^+
0	100	100
1	100	96
2	100	80
3	92	56

[a] Assuming all ions are in the state _v_.

2. Tritiated Alkanes

Unfortunately, no data are available for use in predicting easily the extent of electronic excitation to be ascribed to such molecules as CH_3He^+ formed by tritium beta decay. In addition, the ground-state $C\text{-}He^+$ bond-dissociation energy is not known. This latter value was assumed to be approximately 0.05 ev and the calculated values of E_T° are given in Table III.

These low recoil energies are related on the probability graph, Fig. 6, to beta-ray energies of $<$ 580 ev. It is at these low energies that it is most difficult to perform reliable beta-ray energy measurement. Considering these many uncertainties it is surprising that the calculated and experimental data are in reasonable agreement.

3. $C^{14}O_2$

In this molecule, the atom receiving the impulse is bonded to two other radicals and the method of calculating the internal excitation following beta decay differs slightly from that given in Chapter II. The calculation for E_T° for the N-O bond rupture in the product molecule NO_2^+, is given in Appendix III where it is shown that $E_T^\circ = 1.92\ E_{BN}$. The bond-dissociation energy, E_{BN}, is 2.59 ev for ground-state NO_2^+. However, examination of the Morse potential curves for CO_2 and NO_2^+ indicates that, on the average, the NO_2^+ possesses about 0.6 to 1.0 ev of electronic excitation energy. This results in a calculated value of the failure to bond-rupture of 73-87%, in good agreement with the experimental data.

4. $C_2^{14}H_6$

For the ground electronic and vibrational state C^{14}-N^{14} dissociation, it was calculated that $E_T^{\circ} = 3.75$ ev is required. This corresponds to an 85% failure to bond-rupture. If it is assumed that those $CH_3NH_2^+$ molecules not in the ground electronic state will dissociate, then the above values can be multiplied by the probability that the C^{14} beta decay results in a ground state N^+. Wolfsberg[25] lists this latter value as 0.815. Thus, the minimum expected failure to bond-rupture is (0.85)(0.815)(100) = 69%. If vibrational excitation is considered, this value would be lower.

5. Summary

Considering the many assumptions involved in these calculations, the agreement with experimental data seems adequate. Of the various molecules discussed in this section, $C^{14}O_2$, because of its simplicity, is the one most worthwhile to consider further. However, a more precise calculation of the expected failure to bond-rupture of NO_2^+ would require an exact evaluation of the probabilities that the NO_2^+ molecule be formed in various vibrational excited states.

Chapter IV. THE NATURE OF HOT ATOMS AND THEIR INTERACTIONS WITH OTHER MOLECULES.

A. The Energy of the Radicals

1. Kinetic Energy of Radicals

Of the net recoil energy, E_T°, imparted to an atom, only a fraction of this energy is consumed in the bond rupture. Because the chemical reactivity of the radicals frequently depends upon their kinetic energy, it is of interest to determine the energies associated with the radicals.

If the net momentum, Q, exceeds that required for bond rupture, Q°, the total energy available to the newly-formed radicals following bond rupture is the difference between the net-recoil energy acquired by the molecule, $E_T = Q^2/2m_N$, and the bond dissociation energy, E_{BN}. The total kinetic energy acquired by the two radicals is equal to the kinetic energy of the parent molecule, $Q^2/2\Sigma m_i$, plus the bond-excitation energy which is in excess of the bond-dissociation energy, $\Delta E_{iN} - E_{BN}$.

The internal energy, E_{Ri}, associated with the radical, originally bonded to the activated atom, will therefore be equal to the total energy minus the bond-dissociation energy minus the kinetic energy of the radicals. Thus,

$$E_{Ri} = \frac{Q^2}{2m_N} - E_{BN} - \left[\frac{Q^2}{2\Sigma m_i} + \Delta E_{iN} - E_{BN}\right]$$

$$= \left[\frac{\Sigma m_i - m_N}{2m_N\Sigma m_i} - \frac{E_{BN}}{(Q^\circ)^2}\right] Q^2, \qquad (50)$$

where $\Delta E_{iN} = E_{BN}Q^2/(Q^\circ)^2$.

The velocity of the activated atom is $\vec{S}_N = \vec{\mathring{R}} + \vec{v}_N$ and that of the radical $\vec{S}_R = \vec{\mathring{R}} + \vec{v}_R$. Because of conservation of momentum, $\vec{v}_N = -(\Sigma m_i - m_N)\vec{v}_R/m_N$. As a result of the conservation of energy, the energy associated with the activated atom is

$$\langle E_N\rangle_{Av} = \frac{m_N}{\Sigma m_i}\left[\frac{Q^2}{2\Sigma m_i} + \frac{\Sigma m_i - m_N}{m_N}\left[\frac{Q^2}{(Q^\circ)^2} - 1\right] E_{BN}\right] \qquad (51)$$

and that of the radical originally bonded to the activated atom is

$$\langle E_R\rangle_{Av} = \frac{\Sigma m_i - m_N}{\Sigma m_i}\left[\frac{Q^2}{2\Sigma m_i} + \frac{m_N}{\Sigma m_i - m_N}\left[\frac{Q^2}{(Q^\circ)^2} - 1\right] E_{BN}\right]. \qquad (52)$$

The energy of the radicals as a function of the net recoil energy received by Br^{80} in CH_3Br is presented in Fig. 8. It is noted that the energies of the radicals are approximately a linear function of the net recoil energy, E_T. Thus, once the energy distribution between the radicals at the minimum recoil energy, E_T°, is known, the general trend of the energy distribution as a function of the net recoil energy, E_T, can be predicted. For a series of halomethanes, there are presented in Table V the energy distribution between the radicals

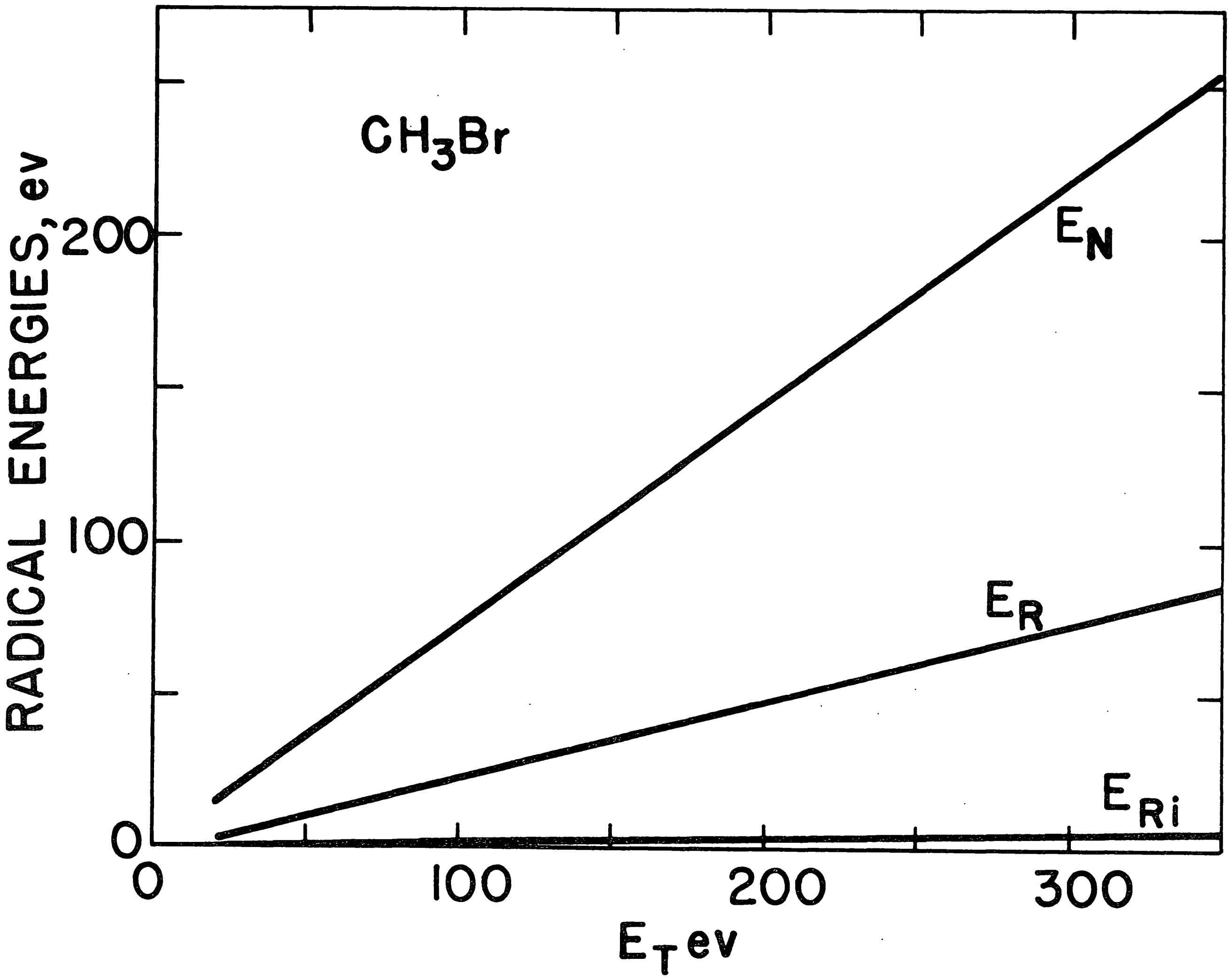

Figure 8. Energies of radicals as a function of the total energy imparted to the Br atom in CH$_3$Br.

Table V. Energy Distribution among the Radicals Evaluated at E°_T.

Compound[a]	E°_T ev	$\frac{E^\circ_N}{E^\circ_T}$, %	$\frac{E^\circ_R}{E^\circ_T}$, %	$\frac{E^\circ_{Ri}}{E^\circ_T}$, %
CH_3I	27.29	80.12	9.39	1.91
CD_3I	23.86	76.87	10.81	2.52
CF_3I	8.34	42.22	22.76	9.84
CH_2I_2	5.52	22.48	24.92	15.79
C_2H_5I	20.41	66.47	15.06	7.40
i-C_3H_7I	12.97	56.03	18.83	8.41
n-C_3H_7I	12.76	56.03	18.83	9.47
CH_3Br	20.74	70.91	13.30	1.66
CD_3Br	18.54	66.64	15.00	2.56
CF_3Br	7.38	28.83	24.86	8.38
CCl_3Br	4.06	16.25	24.06	7.49
CH_2Br_2	6.14	21.14	24.84	12.17
CF_2Br_2	4.90[b]	14.52	23.58	8.82
CCl_2Br_2	3.64[b]	10.84	22.09	8.84
$CHClBr_2$	4.93[b]	14.72	23.65	9.91
$CHBr_3$	4.76	9.99	21.63	12.29
CBr_4	2.98	5.82	18.28	4.86
C_2H_5Br	15.14	53.87	19.52	7.98
1,1-$C_2H_4Br_2$	5.78[b]	18.10	24.44	10.75
CH_3Cl	14.68	51.40	20.29	4.53
CD_3Cl	13.26	46.05	21.81	5.83
CF_3Cl	6.14	12.61	22.90	8.27
CHF_2Cl	7.13[b]	18.23	24.47	11.28
CH_2Cl_2	7.45	18.86	24.56	13.76
CF_2Cl_2	5.63	9.47	21.30	9.57
$CHCl_3$	5.16	9.71	21.44	12.81
$CFCl_3$	5.21	7.36	19.78	9.87
CCl_4	4.46	5.89	18.39	9.61

Table V. (Con't.)

Compound[a]	E_T° ev	$\frac{E_N^\circ}{E_T^\circ}$, %	$\frac{E_R^\circ}{E_T^\circ}$, %	$\frac{E_{Ri}^\circ}{E_T^\circ}$, %
CH_4	6.78	0.39	5.86	28.56
CD_4	6.91	1.00	9.00	26.04
CFH_3	5.30	0.09	2.85	13.66
CF_2H_2	4.81	0.04	1.88	6.19
CF_3H	4.74	0.02	1.41	5.32
CF_4	9.33	4.66	16.93	11.96
CHF_3	9.15	7.37	19.77	17.67
CH_2F_2	9.90	13.35	23.19	14.57
CH_3F	13.50	31.23	24.65	9.75
CH_3T^+	2.18	2.78	13.89	14.52
$C_2H_5T^+$	1.79	0.88	8.50	6.82
n-$C_3H_7T^+$	1.66	0.42	6.10	3.12
i-$C_3H_7T^+$	1.69	0.42	6.10	4.72
$CH_3H_3N^+$	3.75	16.96	24.22	7.89

[a] The dissociating atom is the last element listed in the formula.

[b] Based on estimated E_{BN}.

evaluated at E_T°; these values, therefore, represent the minimum kinetic energies (E°_N and E_R°) of the radicals.

Data of Figs. 3 and 4 were extrapolated to 100% so that the curve had the same shape as that for the $Cl^{35}(n,\gamma)Cl^{36}$ process[26]. To determine the probability distribution, $P(E_N)$, of the bromine atoms which rupture from their parent compound (99.75% of the Br^{80} for CH_3Br and 99.97% for CBr_4), it was necessary to correct the above extrapolated curve, $P(E_\gamma)$, for the failure to bond-rupture portion, $P(E_\gamma^\circ)$, of the same curve. Thus,

$$P(E_N) = [P(E_\gamma) - P(E_\gamma^\circ)]/[1 - P(E_\gamma^\circ)]. \qquad (53)$$

Presented in Fig. 9 is $P(E_N)$ plotted as a function of the translational recoil energy of the dissociated bromine atoms, the values of E_N having been calculated according to Eq. (51). Figure 10 is a plot similar to Fig. 9 for the energy distribution of dissociated iodine atoms originating from CH_3I^{128}.

2. Electronic Energy of the Radicals

In addition to kinetic energy, the hot atoms activated by nuclear processes may also receive an appreciable amount of electronic energy. For example, at least 50% of the I^{128} formed by the (n,γ) reaction is positively charged[9]. Thus, some of the hot reactions may involve electronically excited atoms or ions as was found in the reaction of I^{128} with CH_4[14].

3. Loss of Excitation Energy

The electronic excitation energy could be emitted as flourescent radiation if the transition was allowed. However, during the 10^{-8} sec. normally ascribed to the emission of flourescent radiation, the hot atom would undergo 10,000 or more collisions. The excitation energy could possibly be

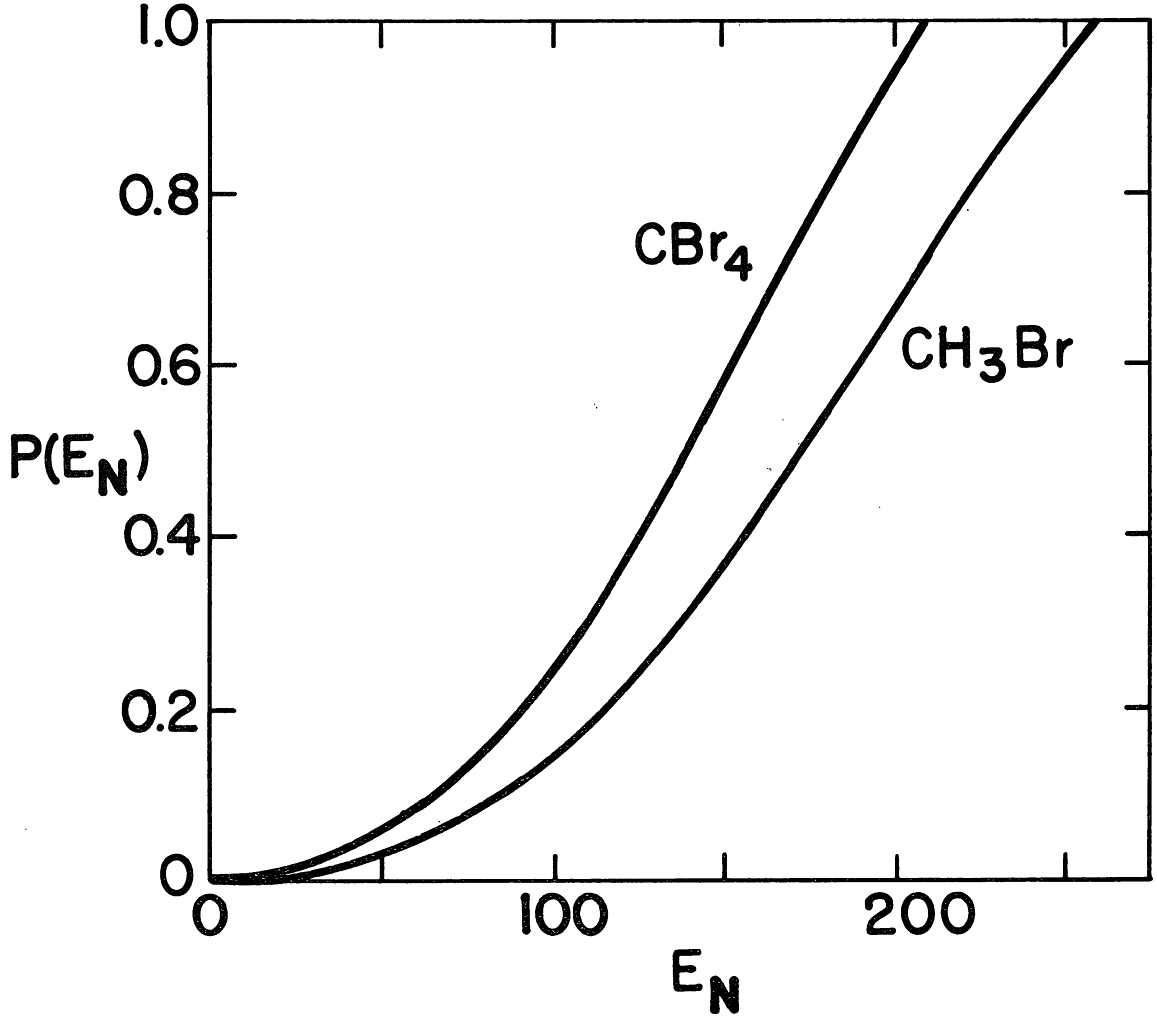

Figure 9. Probability distribution of recoil energies of Br^{80} dissociated from CH_3Br and CBr_4.

dissipated through inelastic collisions whereby the electronic energy is transformed into vibrational energy. The magnitude of electronic excitation energy far exceeds that of vibrational transition energies and such conversion would be ineffective. Hence, any electronic excitation energy associated with the hot atom or ion would normally be retained during a number of collisions. There would be exceptions, of course; the charge-transfer reaction: $I^+(^1D_2) + Xe \rightarrow I + Xe^+$ is one such process which was observed to occur[14]. In general, it would be expected that the collisional degradation of translational kinetic energy would be the main effect occurring, and this will be assumed to be the main result of a collision of a hot atom or ion with a thermal-energy gaseous molecule.

B. Chemical Interactions between Hot Atoms and Other Molecules

During a collision between a hot atom and a molecule, it is conceivable that part of the kinetic energy of the system could be transferred into the internal energy of the molecule. Such an encounter is known as an inelastic collision. Generally, this internal energy increase in the molecule is stored in the chemical bonds of the molecule; in other words, the chemical bonds in the molecule become excited during an inelastic collision. If the excitation is large enough, the excited bond could rupture. On the other hand, if the bond is only moderately excited the atom joined by the excited bond to its parent molecule can become reactive and the replacement of this atom would then be possible. Hence, two types of chemical reactions which might occur during an inelastic collision are dissociation and replacement reactions.

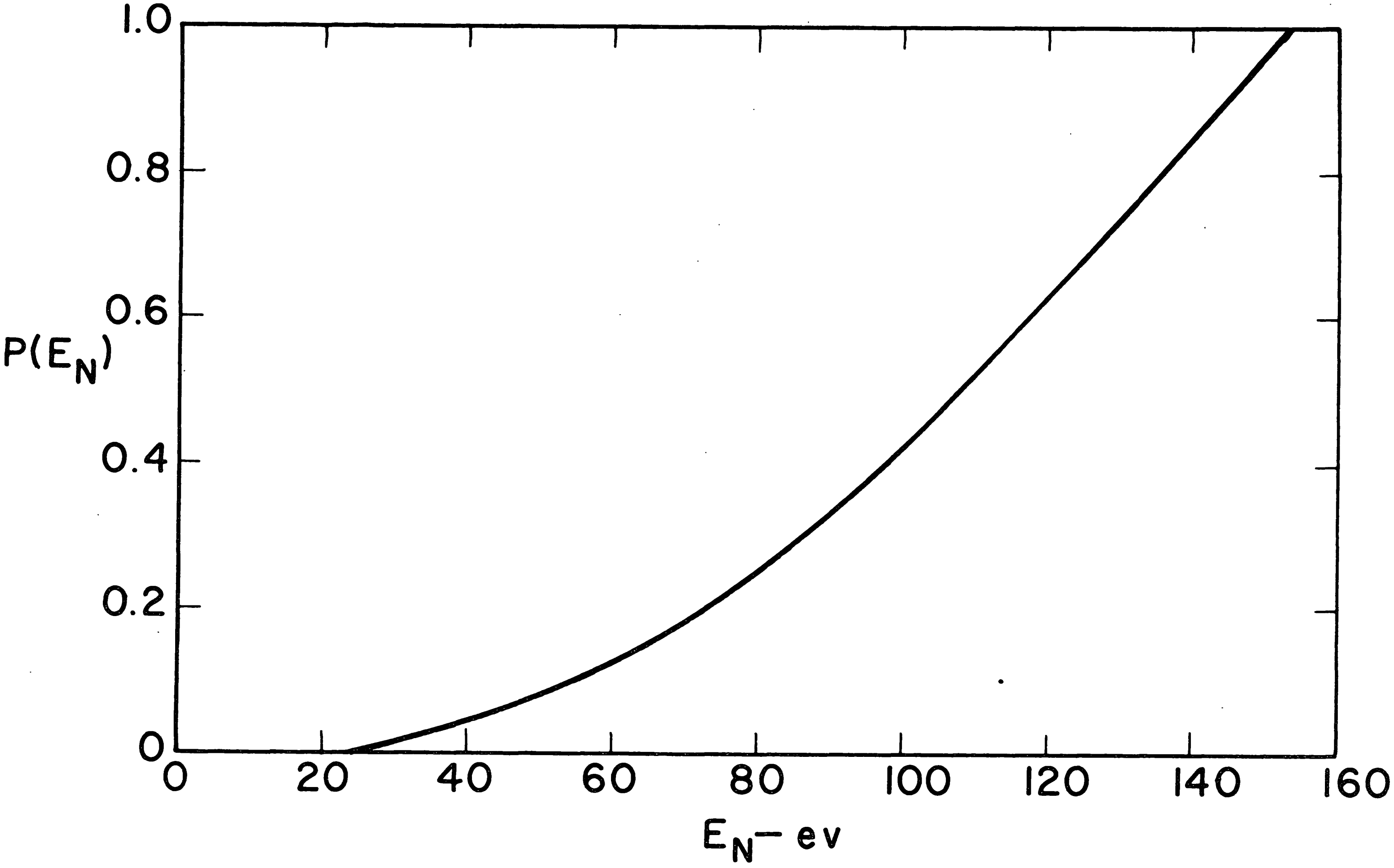

Figure 10. Probability distribution of recoil energies of I^{128} dissociated from CH_3I.

C. Mechanical Interactions

1. Energy Transfer in Elastic Collisions[41]

In elastic collisions, only the transfer of the translational energy is possible. The transfer of momentum is, however, restricted only to its head-on component, because, in elastic collisions, the particles are considered as frictionless and the transfer of the tangential component of the momentum is only possible through the friction between the particles. Thus, there will be no momentum transfer between their tangential components. On this basis, a set of equations could be derived when particles A and N collide in a manner as shown in Figure 11.

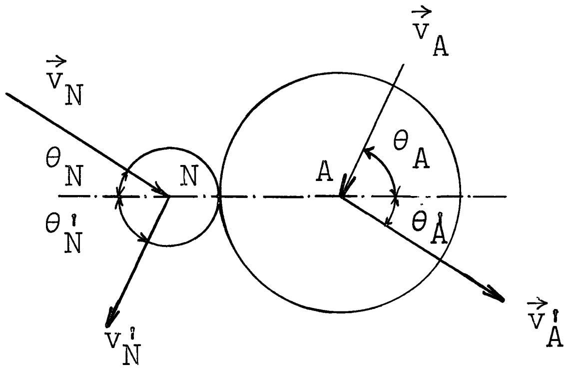

Figure 11

Collision between particles A and N

For the conservation of translational energy,

$$\tfrac{1}{2} m_A v_A^2 + \tfrac{1}{2} m_N v_N^2 = \tfrac{1}{2} m_A v_A'^2 + \tfrac{1}{2} m_N v_N'^2 , \qquad (54)$$

for the conservation of the head-on component of the momentum,

$$m_A v_A \cos\theta_A + m_N v_N \cos\theta_N = m_A v_A' \cos\theta_A' + m_N v_N' \cos\theta_N' \qquad (55)$$

and for the conservation of the tangential components of the momenta

$$m_A v_A \sin\theta_A = m_A v_A' \sin\theta_A' \qquad (56a)$$

and

$$m_N v_N \sin\theta_N = m_N v_N' \sin\theta_N' \qquad (56b)$$

where $\frac{1}{2} m\, v^2$ is the kinetic energy of the particle, m is its mass, v its velocity and θ its angle between its velocity vector and the collisional axis. Substituting Eqs. (54), (56a) and (56b) into the square of Eq. (55), one will arrive at the expression

$$\frac{1}{4} \frac{(m_A + m_N)^2}{m_A} (v_N^2 - v_N'^2) = (m_A v_A \cos\theta_A + m_N v_N \cos\theta_N)\ (v_N \cos\theta_N - v_A \cos\theta_A). \qquad (57)$$

The fractional change in the kinetic energy of particle N as a result of the collision is $\Delta E_N/E_N$, and according to Eq. (57), can be written as

$$\frac{\Delta E_N}{E_N} = \frac{\frac{1}{2} m_N (v_N^2 - v_N'^2)}{\frac{1}{2} m_N v_N^2} = \frac{4 m_A m_N}{(m_A + m_N)^2} \left(\frac{m_A v_A}{m_N v_N} \cos\theta_A + \cos\theta_N \right) \left(\cos\theta_N - \frac{v_A}{v_N} \cos\theta_A \right). \qquad (58)$$

If N is a hot atom which possesses a kinetic energy of more than 100 ev, and A is in the thermal region with a kinetic energy of approximately 0.025 ev., the velocity ratio of A and N before collision, v_A/v_N, became negligible. The energy degradation of the hot atom N is then

$$\left(\frac{\Delta E_N}{E_N} \right)_{max} = \frac{4 m_A m_N}{(m_A + m_N)^2} \cos^2\theta_N. \qquad (59)$$

The maximum energy is transferred in a head-on collision; i.e., $\theta_N = 0$, and

$$\left(\frac{\Delta E_N}{E_N}\right)_{max} = \frac{4m_A m_N}{(m_A+m_N)^2} \tag{60}$$

There will be no energy transfer when the two bodies, A and N, only glance each other; i.e., $\theta_N = \pi/2$.

2. Inelastic Collisions

In the collisions between hot atoms and molecules, inelastic collisions are more likely to occur than are elastic collisions. Benson[42] suggested a simple model to treat this rather complicated system. It was assumed that the molecule is made up of two elastic particles, A and B, linked together by a spring. The third particle, N, collides with the B part of the fictitious molecule A-B. It was also assumed that the two bodies, A and B, vibrated as an harmonic oscillator; that the duration of the collision is much longer than the time of a vibrational period; and that the kinetic energy of the hot atom, N, far exceeds the average vibrational energy of a simple harmonic oscillator. Using these assumptions, Benson found that for a head-on collision, the energy transferred into various forms were:

$$\frac{\Delta E_N}{E_N} = \frac{4m_B m_N}{(m_B+m_N)^2} \tag{61}$$

$$\frac{\Delta E_{AB}}{E_N} = -\frac{4m_B{}^2 m_N}{(m_A+m_B)(m_B+m_N)^2} \qquad (62)$$

$$\frac{\Delta E_v}{E_N} = -\frac{4m_A m_B m_N}{(m_A+m_B)(m_B+m_N)^2} \qquad (63)$$

where E_{AB} is the kinetic energy of the molecule A-B and E_v is the internal energy of the molecule A-B.

Following Benson's method and using his assumptions, expressions were derived for the interaction between A-B and N at any angle. Depicted in Fig. 12 is the encounter between A-B and N.

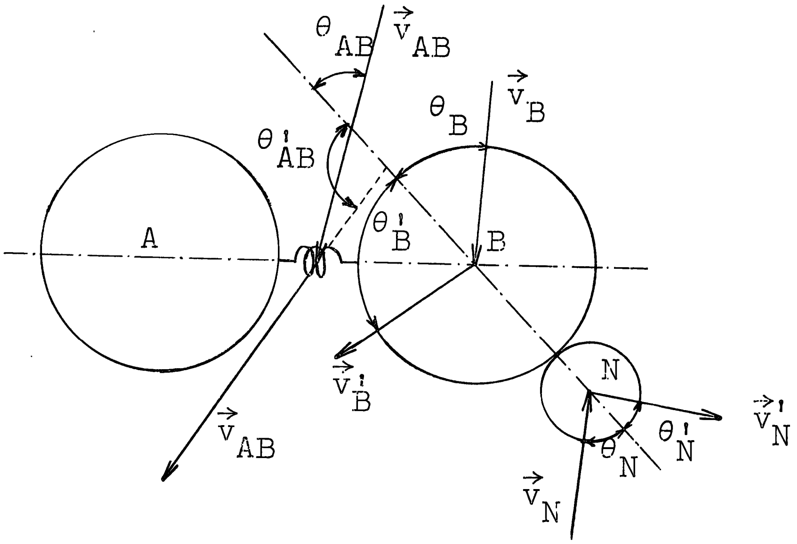

Figure 12. Inelastic collision between A-B and N.

During the elastic collision, the energy change of N should be determined exclusively by the nature of the contacting particles, B and N, as both are assumed to be elastic spheres. According to the energy transfer in elastic collisions, Eq. (58), the fractional change in the kinetic energy of N will be

$$\frac{\Delta E_N}{E_N} = \frac{4m_B m_N}{(m_B+m_N)^2}\left(\frac{m_B v_B}{m_N v_N}\cos\theta_B + \cos\theta_N\right)\left(\cos\theta_N - \frac{v_B}{v_N}\cos\theta_B\right) \tag{64}$$

This should also be the total energy transferred to the molecule A-B. However, only part of this energy is available for inelastic exchange and a considerable fraction of it must be consumed in the change of the translational energy of A-B in order to fulfill the law of conservation of momentum of the entire system.

Again the assumption that momentum transfer is only effective in the head-on direction has been used. The conservation of momentum of the system requires that

$$m_{AB}v_{AB}\cos\theta_{AB} + m_N v_N\cos\theta_N = m_{AB}v'_{AB}\cos\theta'_{AB} + m_N v'_N\cos\theta'_N \tag{65}$$

and

$$m_{AB}v_{AB}\sin\theta_{AB} = m_{AB}v'_{AB}\sin\theta'_{AB} \tag{66}$$

where v_{AB} is the center of mass velocity of A-B.

The energy balance and the momentum balance in the collision between B and N give

$$\tfrac{1}{2}m_Bv_B^2 + \tfrac{1}{2}m_Nv_N^2 = \tfrac{1}{2}m_Bv_B'^2 + \tfrac{1}{2}m_Nv_N'^2 \tag{67a}$$

and

$$v_N\sin\theta_N = v_N'\sin\theta_N'; \quad v_B\sin\theta_B = v_B'\sin\theta_B' \tag{67b}$$

and

$$m_Nv_N\cos\theta_N + m_Bv_B\cos\theta_B = m_Nv_N'\cos\theta_N' + m_Bv_B'\cos\theta_B' \tag{68}$$

and v_B is the velocity of the particle B and differs from the velocity of the center of the mass of A-B. From Eqs. (67a), (67b) and (68), it was found that

$$v_N'\cos\theta_N' = \frac{1}{m_B+m_N}\left[m_Nv_N\cos\theta_N + 2m_Bv_B\cos\theta_B - m_Bv_N\cos\theta_N\right]. \tag{69}$$

Consequently, Eqs. (65) and (69) yield the following

$$v_{AB}'\cos\theta_{AB}' = v_{AB}\cos\theta_{AB} + \frac{2m_Bm_N}{(m_A+m_B)(m_B+m_N)}(v_N\cos\theta_N - v_B\cos\theta_B) \tag{70}$$

Using Eqs. (66) and (70), the kinetic energy change of A-B was found to be

$$\frac{\Delta E_{AB}}{E_N} = \frac{\tfrac{1}{2}(m_A+m_B)(v_{AB}^2 - v_{AB}'^2)}{E_N} = \frac{4m_B^2\,m_N}{(m_A+m_B)(m_B+m_N)^2}$$

$$\times\left[\frac{v_B}{v_N}\cos\theta_B - \cos\theta_N\right]\left[\frac{(m_B+m_N)(m_A+m_B)v_{AB}}{m_Bm_Nv_N}\cos\theta_{AB} - \frac{v_B}{v_N}\cos\theta_B + \cos\theta_N\right]. \tag{71}$$

Conservation of energy requires that the total energy change of the system be zero, or $\Delta E_N + \Delta E_{AB} + \Delta E_v = 0$. This gives the change of internal energy of A-B

$$\frac{\Delta E_v}{E_N} = - \frac{\Delta E_N + \Delta E_{AB}}{E_N} = - \frac{4m_A m_B m_N}{(m_A+m_B)(m_B+m_N)^2}\left[\cos\theta_N - \frac{v_B}{v_N}\cos\theta_B\right]$$

$$\text{X}\left[\frac{(m_A+m_B+m_N)m_B v_B}{m_A m_N v_N}\cos\theta_B + \cos\theta_N - \frac{(m_A+m_B)(m_B+m_N)v_{AB}}{m_A m_N v_N}\cos\theta_{AB}\right]. \tag{72}$$

If N is a hot atom with an energy of more than 100 ev and the molecule A-B is in the thermal energy region with an energy of about 0.025 ev, then both v_{AB}/v_N and v_B/v_N approach zero. The energy changes in A-B and N, Eqs. (64), (71) and (72) become

$$\frac{\Delta E_N}{E_N} = \frac{4m_B m_N}{(m_B+m_N)^2}\cos^2\theta_N , \tag{73}$$

$$\frac{\Delta E_{AB}}{E_N} = - \frac{4m_B{}^2 m_N}{(m_A+m_B)(m_B+m_N)^2}\cos^2\theta_N \tag{74}$$

and

$$\frac{\Delta E_v}{E_N} = - \frac{4m_A m_B m_N}{(m_A+m_B)(m_B+m_N)^2}\cos^2\theta_N . \tag{75}$$

The angle, θ_N, is random, and upon averaging over the entire range of θ_N, it was found that the average energies transferred in an inelastic collision are:

$$\frac{\langle\Delta E_N\rangle_{Av}}{E_N} = \frac{1}{2}\int_0^{\pi} \frac{\Delta E_N}{E_N} \sin\theta_N d\theta_N = \frac{4m_Bm_N}{3(m_B+m_N)^2} , \qquad (76)$$

$$\frac{\langle\Delta E_{AB}\rangle_{Av}}{E_N} = - \frac{4m_B^2m_N}{3(m_A+m_B)(m_B+m_N)^2} , \qquad (77)$$

and

$$\frac{\langle\Delta E_v\rangle_{Av}}{E_N} = - \frac{4m_Am_Bm_N}{3(m_A+m_B)(m_B+m_N)^2} . \qquad (78)$$

These equations differ from that for head-on collision only by a factor of one-third. This is to be expected since only about one-third of all collisions have velocity components along the molecular axis, A-B, and about two-thirds of all collisions take place laterally and are ineffective in energy transfer. In this treatment, the classical concept of an oscillator has been used. However, in the quantum-mechanical sense, the oscillator has a discrete set of allowable energy levels which further limits the inelastic energy transfer. Hence, Eq. (78) represents the maximum possible energy transfer in a collision.

Chapter V. DISSOCIATION AND RECOMBINATION REACTIONS

In reactions activated by nuclear processes the total mole-fraction of activated atoms is usually less than 10^{-12}. Since the atoms will remain hot for less than about 10^{-10} seconds, during a molecular bombardment not more than a few hot atoms would be present in the system. Hence, it is highly unlikely that a thermal molecule which has collided with a hot atom would again meet the same or another hot atom. Any dissociation of a thermal molecule by a hot atom must, therefore, be a one-step process and the minimum hot-atom energy required for a dissociative inelastic collision, E_{N_o}, can be calculated on the basis of a one-step mechanism.

For hot atoms possessing an initial energy, E_N°, Eq. (76) becomes

$$\frac{\langle \Delta E_N \rangle_{Av}}{E_N^\circ} = \frac{E_N^\circ - \langle E_N \rangle_{Av}}{E_N^\circ} = 1 - q \qquad (79)$$

where

$$q = \frac{4 m_B m_N}{3(m_B + m_N)^2} - 1 \qquad (80)$$

After one collision, $\langle E_N \rangle_{Av} = q\, E_N^\circ$. After k collisions, $\langle E_N \rangle_{Av} = q^k\, E_N^\circ$. If E_{N_o} is the minimum average hot-atom energy required for dissociation of a thermal molecule, then $q\, E_{N_o}$ is the minimum hot-atom energy following this last dissociative collision. Hence,

$$q\, E_{N_o} = q^k\, E_N^\circ \qquad (81)$$

and

$$k = \frac{\log E_{N_o} - \log E_N^\circ}{\log q} + 1 \qquad (82)$$

The quantity, k, is therefore the average number of thermal A-B molecules dissociated by a hot atom, N, of initial energy, E_N°.

If the reaction system contains molecules other than the A-B species, Eq. (82) must be modified. Consider first a system consisting of A-B and G where G is a non-reactive molecule or atom such as an inert gas. Defining q_A and q_G as the energy degradation factors for collisions of the hot-atom with the molecule and with the inert substance, then, for a series of collisions, of which k_A are between A-B and N and k_G are between G and N, the energy of the hot atom is $E_N^\circ\ q_A^{k_A}\ q_G^{k_G}$. If E_{N_o} again refers to the lower energy limit of a dissociative collision between N and A-B then

$$q_A E_{N_o} = E_N^\circ\ q_A^{k_A}\ q_G^{k_G} \qquad (83)$$

Equation (83) can be rewritten in the form

$$k_G = K - L\ k_A \qquad (84)$$

where the constants are

$$K = (\log E_{N_o} - \log E_N^\circ + \log q_A)/\log q_G \qquad (85a)$$

and

$$L = \log q_A/\log q_G \qquad (85b)$$

The probability that N collides with A-B is g_A; the probability that N collides with G is $1 - g_A$. This probability factor is a function of the mole-fraction of A-B, X_{AB}, and the collision cross-sections of N with A-B, σ_{AB}, and N with G, σ_G. Thus,

$$g_A = \frac{X_{AB}\,\sigma_{AB}}{X_{AB}\,\sigma_{AB} + X_G\,\sigma_G} \tag{86}$$

Although the collision cross-sections are energy dependent, it is shown in Appendix I-F that the cross-section ratio, and, therefore, g_A remain constant.

The probability, ξ, that k_A collisions occur as N is reduced in energy from E_N° to $q_A\,E_{N^\circ}$ is

$$\xi(E_N^\circ,\, k_A,\, k_G,\, g_A) = \binom{k_A + k_G}{k_A}\, g_A^{\;k_A}\,(1 - g_A)^{k_G} \tag{87}$$

where the first term on the right-hand side of Eq. (87) is the binomial coefficient.

Combining Eqs. (84) and (87),

$$\xi(E_N^\circ,\, k_A,\, g_A) = \binom{K-(L-1)k_A}{k_A}\, g_A^{\;k_A}\,(1-g_A)^{K-Lk_A} \tag{88}$$

The average value of k_A as a function of E_N° and g_A is

$$<k_A(E_N^\circ,\, g_A)>_{Av} = \frac{\int_o^{K/L} k_A \binom{K-(L-1)k_A}{k_A}\, g_A^{\;k_A}\,(1-g_A)^{K-Lk_A}\,dk_A}{\int_o^{K/L} \binom{K-(L-1)k_A}{k_A}\, g_A^{\;k_A}\,(1-g_A)^{K-Lk_A}\,dk_A} \tag{89}$$

The averaging was performed by integration rather than summation since an average energy-degradation factor, q, was used. The final numerical result differs only slightly from that found by the summation process.

It has been pointed out that the probability distribution of initial hot-atom energies could be calculated in certain cases from the spectrum of emitted gamma rays or approximated using failure to bond-rupture data. The integration of $<k_A(E_N^\circ, g_A)>_{Av}$ over the entire energy range of E_N° would give the average number of dissociative collisions as a function of g_A.

$$<k_A(g_A)>_{Av} = \int_0^{(E_N^\circ)_{max}} \frac{dP(E_N^\circ)}{dE_N^\circ} <k_A(E_N^\circ, g_A)>_{Av} \, dE_N^\circ \tag{90}$$

From Eq. (90) the extent of collisional dissociation reactions could be estimated. As an example, for the system G + CH_3I, using Eq. (78) the minimum dissociative energy, E_{N_o}, for the C-I bond is 60.3 ev. For C-H dissociation, E_{N_o} = 426 ev. If hot iodine atoms are produced by the (n,γ) reaction, $(E_N^\circ)_{max}$ is 154 ev and only C-I dissociation in CH_3I is possible. The average number of C-I bonds which would be broken per hot atom as a function of E_N° and the mole-fraction of argon was calculated using Eq. (89) and is presented in Fig. 13.

For a system consisting of CH_3I and a scavenger, S, of cross-section $\sigma_S = \sigma_{CH_3I}$, which will completely deactivate the I, at any energy, in a single collision, the equations must be modified. For this system, $g_S = 0$ and the maximum number of bonds which would be broken, $(k_A)_m$, will be given in terms of the relationship for a single substance, Eq. (81),

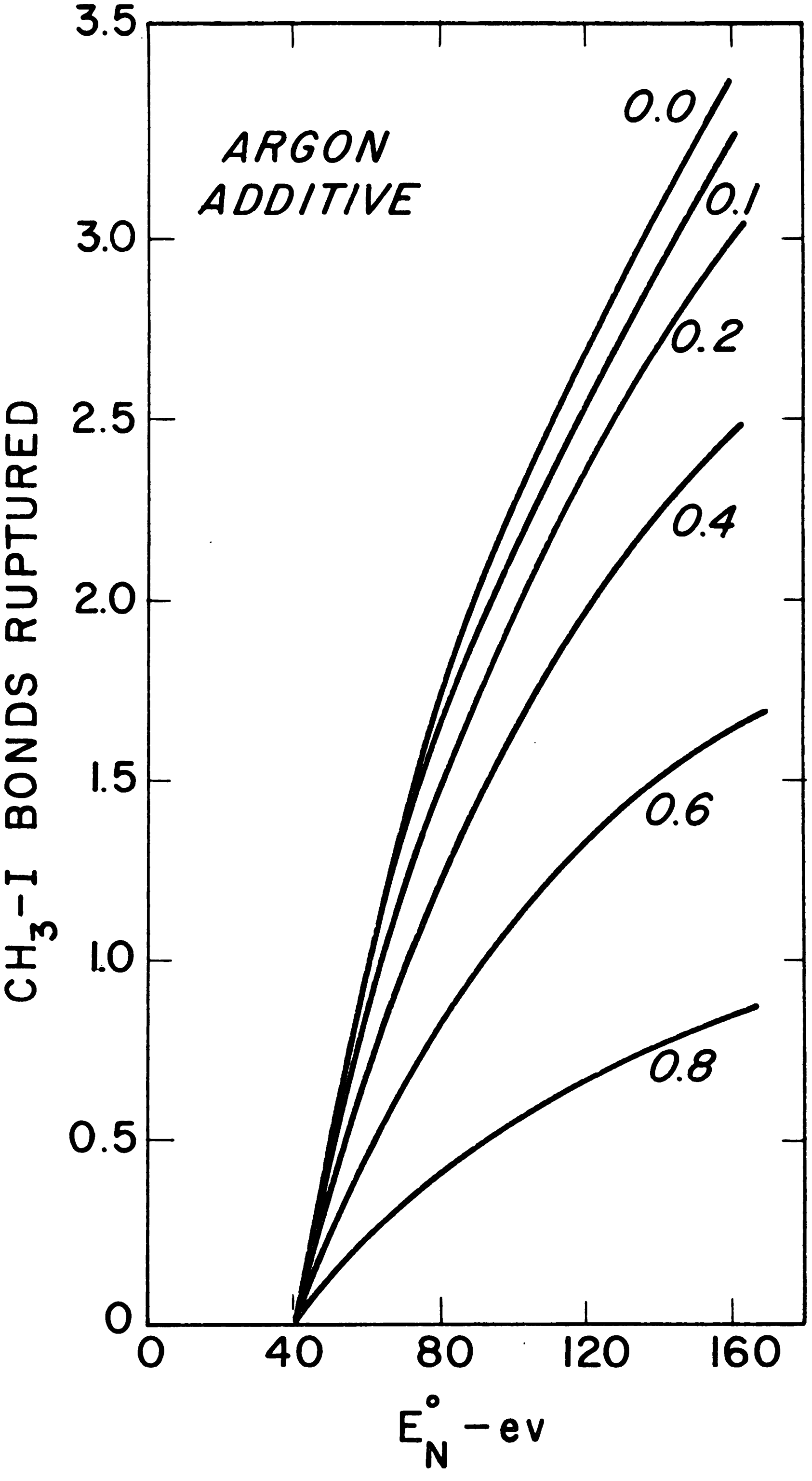

Figure 13. Average number of C-I bonds in CH_3I dissociated by hot iodine as a function of the initial energy of the hot iodine atom and the mole fraction of argon additive.

$$q_A E_{N_o} = q_A^{(k_A)_m} E_N^\circ . \tag{91}$$

Thus,

$$(k_A)_m = \frac{\log E_{N_o} - \log E_N^\circ}{\log q_A} + 1 \tag{92}$$

and

$$\langle k_A \rangle_{Av} = \frac{\sum_{o}^{(k_A)_m} k_A (1-g_S)^{k_A} g_S}{\sum_{o}^{(k_A)_m} (1-g_S)^{k_A} g_S} \tag{93}$$

Figure 14 is a plot in terms of Eq. (93).

Using the I^{128} distribution of initial energies, E_N°, Fig. 10, k_A was calculated as a function of the mole-fraction of the additive using Eqs. (90) and (93). These results are given in Fig. 15. It is seen in Fig. 15 that an effective scavenger would easily reduce the radical concentration. However, even without a scavenger, the concentration of radicals produced by the hot atoms is so low that gas-phase recombination reactions are improbable. On the other hand, the low diffusion rates in liquids would result in a high local concentration of radicals and some extent of reaction between radicals could be possible.

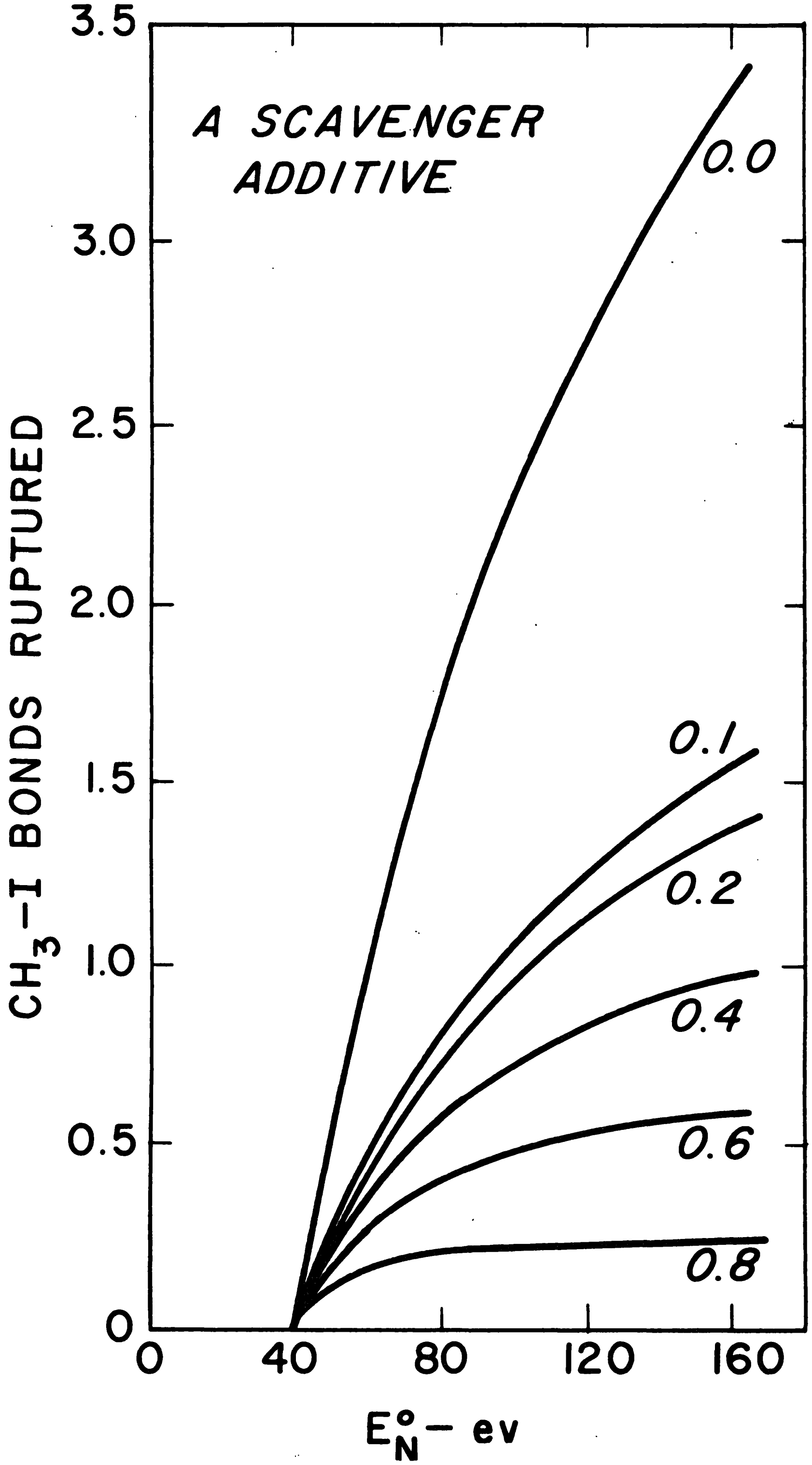

Figure 14. Refer to Fig. 13. An effective scavenger is used.

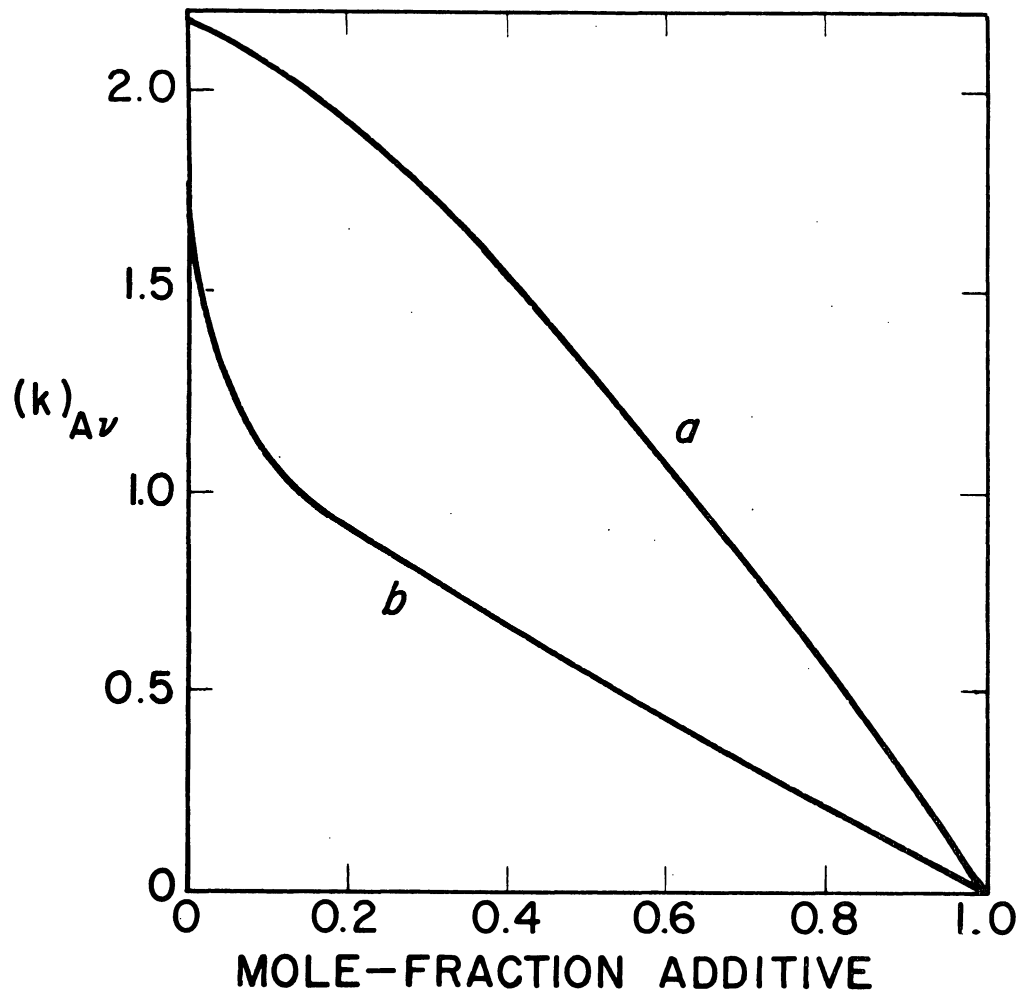

Figure 15. Average number of C-I bonds in CH_3I dissociated as a function of the mole fraction of additive.

Chapter VI. HOT-ATOM REACTIONS

A. Introduction

Hot atoms are usually highly excited both kinetically and electronically, immediately after breaking away from their parent molecules following a nuclear transformation. Often the electronic excitation is so great that positively-charged species are formed[9]. These hot atoms are chemically very reactive and will undergo many unique chemical reactions with some otherwise relatively inert molecules[14-16]. The unusual reactiveness of hot atoms is attributed to the high kinetic and electronic energies of these atoms.

Experimental data indicate that the addition of inert-gas moderators to the hot reaction system exhibit an effect similar to that of neutrons cooling down in an inert media[14,17,22]. Attempts have been made to explain the hot chemical reactions theoretically by means of the 'neutron cooling down' model. Miller, Gryder, and Dodson[20], early in 1950, successfully used this model to describe some hot-atom reactions in binary liquid systems. Capron and Oshima[21] later, using a different method, obtained similar results for the hot atom reaction in certain single-component systems. Estrup and Wolfgang[22] developed an equation that described the effect of inert-gas moderation. The disadvantage of the above mentioned equation is that it is semi-empirical and experimental data are needed in order to obtain the required constants for it. There was no restriction in the method of Miller, et. al.

In this part of the research, Miller's method has been used as a basis for correlating the experimental results using only the thermodynamic data and the transport properties of the substances in the reaction system.

B. Assumptions

Many assumptions have been made in formulating mathematically the expressions to be used in calculating the expected yields of products of hot-atom reactions. Whereas the minor assumptions are introduced when they occur in the derivation, the major assumptions are given here. They are:

1. The energy associated with a newly-formed atom is greater than the maximum energy which will permit stable formation of a chemical product. This assumption is valid for many hot-atom reactions. For example, it will be shown that for the reaction, $Br + CH_4 \rightarrow CH_3Br + H$ to occur, the Br atom must possess between 13.6 and 15.1 ev of kinetic energy. According to Fig. 9, more than 99 percent of the bromine atoms which rupture from either CH_3Br or CBr_4 as a result of the $Br^{79}(n,\gamma)Br^{80}$ process will possess more than 15.1 ev of kinetic energy. As a result, hot bromine atoms from either source

would be able to react with CH_4 with equal probability[12]. Hence, the molecule which provided the hot atom is generally of no concern and only the kinetic energy associated with the recoiling atom is of interest. There, of course, are exceptions to the above statement. Only a small fraction of the bromine in HBr^{80} would dissociate; the failure to bond-rupture is estimated[12] to be about 85 percent. In this case it would be mainly hot HBr molecules which would collide and react with CH_4. This type of hot-molecule reaction is not considered here although it could be handled easily by slightly modifying the equations. Similarly, low-energy hot atoms produced by beta decay or produced photochemically cannot be handled directly in terms of the equations to be presented since the kinetic energy possessed by these atoms is generally less than the maximum energy which will result in chemical stabilization. A slight modification in the equations, however, would permit calculating the expected product yields.

2. The number of hot atoms in a system is so small that the probability is infinitely small that a given thermal molecule will collide more than once with a hot atom. Thus, any reactions can be assumed to occur between a thermal molecule

and a hot atom and must take place in a one-step process.

3. The hot atoms lose their energy through elastic and inelastic collisions. All collision-contact angles are considered equally possible and, as a result, per collision, the hot-atom energies will be distributed between the initial pre-collision energy, E, and the minimum energy, expressed as $E - E(4m_A m_N)/(m_A+m_N)^2$.

   If the collision of the hot atom with the molecule is considered to be elastic, m_A is the total mass of the molecule, Eq. (60). If the collision is inelastic, m_A is the mass of the portion of the molecule which makes contact with the hot atom, Eq. (61)

4. The reaction takes place through the formation of a collision complex:

   $$N^* + A\text{-}B \rightarrow (A\text{-}B\text{-}N)^* \rightarrow A + (B\text{-}N)^* \xrightarrow[\text{de-excitation}]{}$$

   where N* is the hot atom and A-B the thermal molecule. Differing from the collision complexes in thermal reactions, this complex (a) has a very short lifetime, (b) merely denotes that, during the collision, the hot atom and molecule are in close proximity in a configuration indicated by the complex, and (c) the product of the reaction is determined by the configuration of the collision complex. This is a critical assumption since the possible reaction products will depend on the possible collisional configurations. The exact hot-atom reaction mechanism is still uncertain; however, experimental data lend support to this postulate of a collisional complex.

5. There exists a definite energy range in which reaction is possible. From the energy standpoint, this is a natural consequence of the preceding assumption. If the energy of the hot atom exceeds a calculated value, the energy associated with the collision complex is too great to allow a stable compound to be formed. On the other hand, the minimum energy required for reaction will be determined in terms of the endothermicity in endothermic reactions.

6. According to assumption 5, there is a definite energy range in which the reactions can occur. In order to make this model mathematically expressible, it is necessary, further, to assume that the reaction will definitely occur once the hot atom in the favorable reaction energy zone meets a reactive molecule. This does not say that the reaction probability in that energy zone is unity. It merely states that, for a hot atom of energy, E, if, in one collision with a reacting

molecule its energy falls into the reaction-energy zone, then a reaction will result. However, in one collision, the energy of the hot atom does not necessarily fall into the reaction-energy zone. Hence, the reaction probability of a hot atom with energy, E, is also the fraction of hot atoms that will be in the reaction energy zone. This fraction is defined as F(E).

If more than one reaction is possible in a particular reaction-energy zone, then the probability of occurrence of a given reaction, s, in that reaction zone must be considered. Hence the ith reaction probability of a hot atom with energy E will be $s_iF_i(E)$. This probability of occurrence of a given reaction, s, has been referred to as a steric factor[43-45]. It can be calculated from the configuration of the molecule and will be discussed in detail in a later section.

C. Nomenclature

The most frequently used terms employed in the derivation are defined as follows:

E°	the initial kinetic energy of the hot atom.
E^a	the maximum energy the hot atom may have and be able to react to form any of the possible products.

E^b	the maximum energy the hot atom may have in forming a particular product.
E^y	the minimum energy the hot atom must have to form a particular product.
E^z	the minimum energy the hot atom must have to form any of the possible products.

Thus, the maximum reactive energy range is from E^a to E^z and the energy range for producing a particular product is from E^b to E^y. If the product under consideration is formed in the maximum reactive energy range, then $E^b = E^a$ and $E^y = E^z$. For example, in the reaction of Br with CH_4, it will be shown that HBr is formed in the range 4.3 to 22.5 ev and CH_3Br is formed in the range 13.6 to 15.1 ev. According to the definitions, $E^a = 22.5$ and $E^z = 4.3$ ev. For the product, CH_3Br, $E^b = 15.1$ and $E^y = 13.6$ ev; for the product, HBr, $E^b = 22.5$ and $E^y = 4.3$ ev.

In a binary mixture of A and B, A is always capable of reacting with the hot atom whereas the molecule or atom, B, may be reactive or virtually inert except for possible charge-transfer reactions.

Further definitions are:

r_i the minimum fraction of its energy which the hot atom can retain following a collision with molecule i. Thus:

$$r_i = \left[\frac{M_i - m_N}{M_i + m_N}\right]^2$$

M_i	the mass of the molecule i
m_N	the mass of the hot atom
g_i	the probability that the hot atom will collide with the molecule i in the mixture, where $g_i = \dfrac{X_i \sigma_i}{\sum_i X_i \sigma_i}$
X_i	the mole fraction of species i in the mixture
σ_i	the collision between the hot atom and molecule i where $\sigma_i = \pi(r_i + r_N)^2$
r_i	the collision radius of molecule i
r_N	the collision radius of the hot atom
s_j	the fractional probability of forming a given product in a reaction zone where more than one product can be formed. In this zone, $\sum_j s_j = 1.0$.
R_j	the yield of a product, j, assuming $s_j = 1.0$ throughout its energy range
Y_j	the yield of a product j taking into account s_j factors. Y_j, then, is the fraction of the total hot atoms which have been stabilized in the form of compound j. Using, again, the example of Br + CH_4 where CH_3Br and HBr are the two products, and the HBr energy range encloses

that of CH_3Br,

$$Y_{CH_3Br} = s_{CH_3Br}R_{CH_3Br}$$

$$Y_{HBr} = R_{HBr} - Y_{CH_3Br}$$

$n(E°, E)dE$ the number of hot atoms of initial energy, E°, which have an energy between E and E + dE.

In addition, two dimensionless quantities, a and b, are defined as

$$a = \frac{g_A}{1-r_A} \qquad b = \frac{g_B}{1-r_B}$$

D. Theoretical Considerations

A mixture of A and B in which both molecules can react with the hot atom but are inert to each other constitutes a system with competing reactions. The characteristic energies for A and B are:

E_A^a, E_A^z, E_{Aj}^b, E_{Aj}^y and E_B^a, E_B^z, E_{Bj}^b, E_{Bj}^y, where j refers to the product. Let us arbitrarily set $E_A^a > E_B^a$.

1. Energy Distribution of Hot Atoms

If the energy of a hot atom is greater than E^a no reaction is possible. Collisions with both A and B will only result in the energy degradation of the hot atom. Under steady-state conditions, the number of hot atoms which will undergo collisions with an energy E + dE equals the number of hot atoms entering this energy interval[20]. Mathematically,

$$n(E^\circ,E)dE = \ell\delta(E-E^\circ)dE + g_A\int_E^{E^\circ} \frac{n(E^\circ,E_1)dE}{E_1(1-r_A)}\, dE_1$$

$$+ (1-g_A)\int_E^{E^\circ} \frac{n(E^\circ,E_1)dE}{E_1(1-r_B)}\, dE_1 \qquad (94a)$$

or

$$n(E^\circ,E)dE = \ell\, \delta(E-E^\circ)dE + (a+b)\int_E^{E^\circ} \frac{n(E^\circ,E_1)dE}{E_1}\, dE_1 \qquad (94b)$$

where ℓ is the number of newly-formed hot atoms of energy E° and $\delta(E-E^\circ)$ is the Dirac delta-function and has the following properties:

$$\delta(E-E^\circ) = \infty \qquad \text{if} \qquad E = E^\circ$$

$$\delta(E-E^\circ) = 0 \qquad \text{if} \qquad E \neq E^\circ$$

$$\int_{E_1}^{E_2} \delta(E-E^\circ)\, dE = 1 \qquad \text{if} \qquad E_2 > E^\circ > E_1$$

$$\int_{E_1}^{E_2} \delta(E-E^\circ)dE = 0 \qquad \text{if} \qquad E^\circ > E_2 > E_1$$

or

$$E_2 > E_1 > E^\circ.$$

In the energy range between E_A^a and E_B^a, only those hot atoms which collide with B will survive since a collision with A leads to the formation of a stable product. For steady-state conditions in this energy range there results:

$$n(E°,E)dE = (1-g_A)\ \ell\delta(E-E°) + b \int_E^{E°} \frac{n(E°,E_1)dE}{E_1}\, dE_1. \qquad (95)$$

Since both A and B can react with hot atoms between E_B^a and E_B^z or E_A^z, whichever is greater, the energy distribution of hot atoms is zero in this range. If the maximum degradation of energy of a hot atom of energy E_B^a results in an energy > E_B^z or E_A^z, whichever is greater, then $n(E°,E)dE = 0$ for $E <$ E_B^z or E_A^z, whichever is greater.

Using the Leibnitz rule, the solution of Eq. (94b) for $E° > E_A^a$ and $E > E_A^a$ is

$$n(E°,E)dE = \ell\ \delta(E-E°)dE + (a + b)\ \frac{\ell}{E°}\left(\frac{E°}{E}\right)^{a+b} dE. \qquad (96)$$

Similarly, the solution of Eq. (95) for $E° > E_B^a$ and $E_A^a > E > E_B^a$ is

$$n(E°,E)dE = (1-g_A)\left[\ell\ \delta(E-E°)dE + b\ \frac{\ell}{E°}\left(\frac{E°}{E}\right)^{b} dE\right]. \qquad (97)$$

If only A is reactive Eqs. (96) and (97) still apply. The distribution remains unchanged for $E > E_A^a$ but the applicability of the distribution function for $E_A^a > E > E_B^a$ is now extended to $E_A^a > E > E_A^z$ since $E_B^a = 0$.

For a system consisting of a single component, A, g_A = 1.0. The distribution for $E < E_A^a$ will equal zero if the maximum energy degradation of atoms of E_A^a is to an energy $E > E_A^z$.

2. The Fraction of Hot Atoms Entering the Reaction Zone

Following collisions between hot atoms of energy E and thermal energy molecules, i, the energies of the hot atoms will be distributed evenly between E and r_iE. The probability of a hot atom having an energy between E_1 and $E_1 + dE_1$ is $dE_1/E(1-r_i)$ for $E > E_1 > r_iE$. The fraction, $F_i(E)$, of hot atoms which enter a reaction zone as a result of a single collision can be obtained by integrating the above probability expression over the energy of the reaction zone of interest,

$$F_i\ (E) = \int_{E'}^{E''} \frac{dE_1}{E(1-r_i)} = \frac{E'' - E'}{E(1-r_i)} \qquad (98)$$

This fraction will depend on the energy region as indicated in Table VI.

3. Calculation of the Yield

The yield, $R_j(E°)$, is the ratio of the number of hot atoms stabilized as compound j to the total amount of hot atoms. The number of atoms of initial energy E° which enter the reaction zone of molecule i to form product j is

$$g_i \int_{E_i^y}^{E_i^b/r_i} n(E°,\ E)\ F_i(E)\ dE \qquad (99)$$

The total number of atoms of initial energy E° is ℓ. Thus,

Table VI.

The Reaction Probability for Different Energy Ranges.

Energy Range	$F_i(E)$
$E > E_i^b > E_i^y > r_iE$	$\dfrac{E_i^b - E_i^y}{E(1-r_i)}$
$E > E_i^b > r_iE > E_i^y$	$\dfrac{E_i^b - r_iE}{E(1-r_i)}$
$E_i^b > E > E_i^y > r_iE$	$\dfrac{E - E_i^y}{E(1-r_i)}$
$E_i^b > E > r_iE > E_i^y$	1
$E > r_iE > E_i^b > E_i^y$	0
$E_i^b > E_i^y > E > r_iE$	0

$$R_j(E^\circ) = \frac{g_i}{\ell} \int_{E_i^y}^{E_i^b/r_i} n(E^\circ,E)\ F_i(E)\ dE \qquad (100)$$

Since both $n(E^\circ,E)dE$ and $F_i(E)$ depend on the energy range examined, Eq. (100) must be evaluated in segments.

Frequently, as in (n,γ) activation, the hot atoms are formed with a spectrum of initial energies, E°. If such is the case, the average yield can be calculated in terms of Eq. (101).

$$\langle R_j \rangle_{Av} = g_i \frac{\int_{E_i^y}^{E_i^a/r_i} \frac{dP(E^\circ)}{d\ E^\circ}\ \frac{1}{\ell} \int_{E_i^y}^{E_i^b/r_i} n(E^\circ,E)F_i(E)dEdE^\circ}{\int_{E_i^y}^{E_i^a/r_i} \frac{dP(E^\circ)}{d\ E^\circ}\ dE^\circ} \qquad (101)$$

where $dP(E^\circ)/dE^\circ$ is the initial energy distribution of the hot atoms.

Theoretically, $dP(E^\circ)/dE^\circ$ can be determined in a manner suggested in Chapter IV. If most of the hot atoms have an initial energy which is much greater than E_i^a/r_i, on the average, a number of collisions will be needed before the atoms reach the reaction zone. By then, the distribution will be fairly uniform and, to a first approximation, $dP(E^\circ)/dE^\circ$ can be assumed to be a constant.

The hot reaction begins at $E = E^a$ and a sudden decrease in $dP(E^\circ) / dE^\circ$ occurs at that energy. Shown in Fig. 16 is the energy distribution of hot atoms of energy E' after one collision.

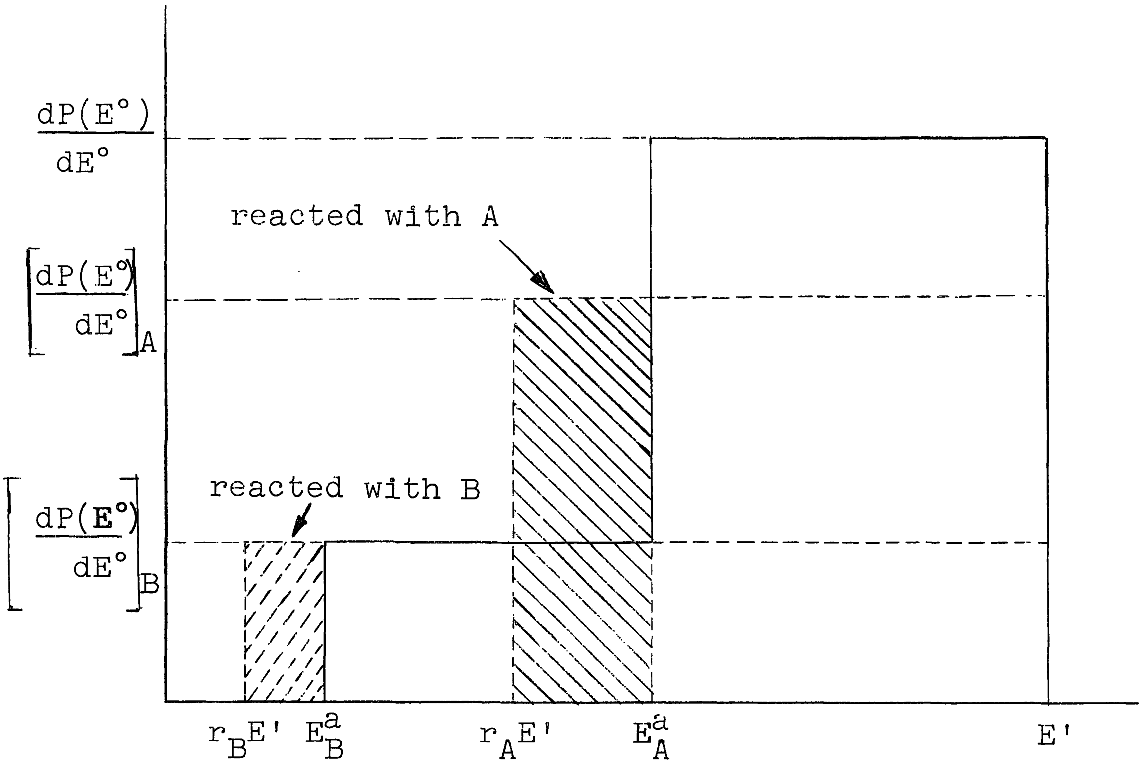

Figure 16. Energy distribution of a hot atom after one collision.

From Fig. 16 it is seen that

$$g_A = E'(1 - r_A)\left[\frac{dP(E^\circ)}{d\ E^\circ}\right]_A$$

$$1 - g_A = E'(1 - r_B)\left[\frac{dP(E^\circ)}{d\ E^\circ}\right]_B$$

and therefore,

$$\frac{dP(E^\circ)}{dE^\circ} = (a+b)E' \quad \text{for} \quad E^\circ > E_A^a \tag{102}$$

$$\frac{dP(E^\circ)}{dE^\circ} = bE' \quad \text{for} \quad E_A^a > E^\circ > E_B^a \tag{103}$$

$$\frac{dP(E^\circ)}{dE^\circ} = 0 \quad \text{for } E^\circ < E_B^a \tag{104}$$

Substituting Eqs. (102) and (103) into Eq. (101),

$$\langle R_i \rangle_{Av} = \frac{1}{\left[\frac{E_A^a}{r_A} - E_A^a\right] + \frac{b}{a+b}\left[E_A^a - E_A^y\right]} \left\{ \int_{E_A^a}^{E_A^a/r_A} R_i(E^\circ)dE^\circ + \frac{b}{a+b} \int_{E_A^y}^{E_A^a} R_i\,(E^\circ)\,dE^\circ \right\}. \tag{105}$$

Equation (105) may now be used to calculate $\langle R_i \rangle_{Av}$ values for systems of competing reactions, inert-gas moderation, etc.

E. Evaluation of Various Systems

A large number of reaction systems could exist, each with different relative reaction energy zones. Given here are solutions for a few systems which will be of interest.

1. Competing Reactions.

(a) $E_A^a \geqslant E_A^b > r_A E_A^a > E_A^y = E_A^z \gg 0$

$$\langle R_A\rangle_{Av} = \frac{a}{\left[\frac{E_A^a}{r_A} - E_A^a\right] + \frac{b}{a+b}\left[E_A^a - E_B^a\right]} \left\{ \frac{E_A^b}{(a+b)(a+b-1)}\left(\frac{E_A^a}{E_A^b}\right)^{a+b} \right.$$

$$+ \left(\frac{E_A^b}{a+b} - \frac{r_A\ E_A^a}{a+b-1}\right)\left(\frac{1}{r_A}\right)^{a+b}$$

$$+ \ (1 - g_A)\left[\left(\frac{E_A^b}{b} - \frac{r_A E_B^a}{b-1}\right)\left(\frac{E_A^a}{E_B^a}\right)^b\right.$$

$$\left.\left. - \left(\frac{E_A^b}{b} - \frac{r_A E_A^a}{b-1}\right)\right]\left[\left(\frac{1}{r_A}\right)^b - \frac{a}{a+b}\right] \right\} \qquad (106)$$

(b) $E_B^a \geqslant E_B^b > r_B E_B^a > E_B^y = E_B^z \geqslant 0$

$$\langle R_B\rangle_{Av} = \frac{b}{\left[\frac{E_B^a}{r_B} - E_A^a\right] + \frac{b}{a+b}\left[E_A^a - E_B^a\right]} \left\{ \frac{E_B^b}{(a+b)(a+b-1)}\left(\frac{E_B^a}{E_B^b}\right)^{a+b} \right.$$

$$- \left(\frac{E_B^b}{a+b} - \frac{r_B E_A^a}{a+b-1}\right)\left(\frac{E_B^a}{E_A^a r_B}\right)^{a+b}$$

$$+ \ (1-g_A)\left[\left(\frac{E_B^b}{b} - \frac{r_B E_B^a}{b-1}\right)\left(\frac{E_A^a}{E_B^a}\right)^b - \left(\frac{E_B^b}{b} - \frac{r_B E_A^a}{b-1}\right)\right]$$

$$\left. \times \left[\left(\frac{E_B^a}{E_A^a r_B}\right)^b - \frac{a}{a+b}\right] \right\} \qquad (107)$$

(c) $E_A^a \geqslant E_A^b > E_A^y > r_A E_A^a \neq 0$

$$\langle R_A \rangle_{Av} = \frac{a}{\left[\frac{E_A^a}{r_A} - E_A^a\right] + \frac{b}{a+b}\left[E_A^a - E_B^a\right]} \left\{ \frac{E_A^b}{(a+b)(a+b-1)} \left(\frac{E_A^a}{E_A^b}\right)^{a+b} - \frac{E_A^y}{(a+b)(a+b-1)} \left(\frac{E_A^a}{E_A^y}\right)^{a+b} + \frac{E_A^b - E_A^y}{a+b} \left(\frac{1}{r_A}\right)^{a+b} + \frac{(1-g_A)(E_A^b - E_A^y)}{b(a+b)} \left[\left(\frac{E_A^a}{E_B^a}\right)^b - 1\right] \left[(a+b)\left(\frac{1}{r_A}\right)^b - a\right] \right\} \qquad (108)$$

(d) $E_B^a \geqslant E_B^b > E_B^y > r_B E_B^a \neq 0$

$$\langle R_B \rangle_{Av} = \frac{b}{\left[\frac{E_B^a}{r_B} - E_A^a\right] + \frac{b}{a+b}\left[E_A^a - E_B^a\right]} \left\{ \frac{E_B^b}{(a+b)(a+b-1)} \left(\frac{E_B^a}{E_B^b}\right)^{a+b} - \frac{E_B^y}{(a+b)(a+b-1)} \left(\frac{E_B^a}{E_B^y}\right)^{a+b} + \frac{E_B^b - E_B^y}{a+b} \left(\frac{E_B^a}{E_A^a r_B}\right)^{a+b} + \frac{(1-g_A)(E_B^b - E_B^y)}{b(a+b)} \left[\left(\frac{E_A^a}{E_B^a}\right)^b - 1\right] \left[(a+b)\left(\frac{E_B^a}{r_B E_A^a}\right)^b - a\right] \right\} \qquad (109)$$

2. Inert-Gas Moderation

Consider A as the reactive component and B as an unreactive component.

(a) $E^a \geqslant E^b > E^y > r_A E^a \geqslant r_A E^b > r_A E^y$

$$\begin{aligned}\langle R\rangle_{Av} = \frac{a}{E^a\left[\frac{a+b}{r_A} - a\right] - bE^y} \Bigg\{ & \frac{1}{a+b-1}\left[E^b\left(\frac{E^a}{E^b}\right)^{a+b} - E^y\left(\frac{E^a}{E^y}\right)^{a+b}\right] + (E^b - E^y)\left(\frac{1}{r_A}\right)^{a+b} + \frac{(1-g_A)}{b(b-1)} \\ & \times \left[(a+b)\left(\frac{1}{r_A}\right)^b - a\right]\left[-(b-1)(E^b - E^y) - E^b\left(\frac{E^a}{E^b}\right)^b + E^y\left(\frac{E^a}{E^y}\right)^b\right]\Bigg\} \end{aligned} \qquad (110)$$

(b) $E^a \geqslant E^b > r_A E^a \geqslant E^y \geqslant r_A E^b > r_A E^y$

$$\begin{aligned}\langle R\rangle_{Av} = \frac{a}{E^a\left(\frac{a+b}{r_A} - a\right) - bE^y} \Bigg\{ & \frac{E^b}{a+b-1}\left(\frac{E^a}{E^b}\right)^{a+b} \\ & + \left[E^b - r_A\, E^a \,\frac{a+b}{a+b-1}\right]\left[\frac{1}{r_A}\right]^{a+b} \\ & + \frac{(1-g_A)}{b(b-1)}\left[(a+b)\left(\frac{1}{r_A}\right)^b - a\right]\Bigg[-(b-1)E^b + br_A E^a - E^b\left(\frac{E^a}{E^b}\right)^b \\ & + E^y\left(\frac{E^a}{E^y}\right)^b - E^y\left(\frac{r_A E^a}{E^y}\right)^b\Bigg]\Bigg\} \end{aligned} \qquad (111)$$

(c) $E^a \geqslant E^b > r_A E^a \geqslant r_A E^b > E^y > r_A E^y$

The equation for $\langle R\rangle_{Av}$ is the same as that for case (b), Eq. (111).

(d) $E^a \geqslant E^b > r_A E^a \geqslant r_A E^b > E^y = E^z = 0$

$$\langle R\rangle_{Av} = \frac{ar_A}{E^a\left[a(1-r_A)+b\right]}\left\{\frac{E^b}{a+b-1}\left(\frac{E^a}{E^b}\right)^{a+b} - \left[E^b - r_A E^a\frac{a+b}{a+b-1}\right]\left[\frac{1}{r_A}\right]^{a+b}\right.$$
$$\left. + \frac{1-g_A}{b(b-1)}\left[(a+b)\left(\frac{1}{r_A}\right)^b - a\right]\left[-(b-1)E^b + br_A E^a - E^b\left(\frac{E^a}{E^b}\right)^b\right]\right\} \quad (112)$$

3. Single Component Systems

The solutions may be found by setting $g_A = 1.0$.

(a) $E^a > rE^a > E^b > E^y$

$$\langle R\rangle_{Av} = 0 \quad (113)$$

(b) $E^a \geqslant E^b > rE^a > E^y > rE^b$

or $E^a \geqslant E^b > rE^a \geqslant rE^b > E^y$ (E^y can = 0.)

$$\langle R\rangle_{Av} = \left[\frac{E^a}{E^b}\right]^{\frac{r}{1-r}} - \frac{E^a - E^b}{E^a(1-r)}\left[\frac{1}{r}\right]^{\frac{r}{1-r}} \quad (114)$$

(c) $E^a \geqslant E^b > E^y > rE^a$

$$\langle R\rangle_{Av} = \frac{E^b - E^y}{E^a(1-r)}\left[\frac{1}{r}\right]^{\frac{r}{1-r}} + \left[\frac{E^a}{E^b}\right]^{\frac{r}{1-r}} - \left[\frac{E^a}{E^y}\right]^{\frac{r}{1-r}} \quad (115)$$

Equations (113), (114), and (115) can be obtained by integrating the equations given by Capron and Oshima[21]. The agreement indicates that the methods used by Miller, et.al.,[20] and Capron and Oshima[21] are identical. Since Miller's method was simpler, it was adopted in this derivation.

F. Estimation of the Reactive Energy Range

It is postulated that the hot-atom reaction takes place via a collision complex:

$$h^* + a\text{-}b \rightarrow a\text{-}b\text{-}h^* \rightarrow a + bh^* \rightarrow \text{de-excitation.}$$

As was stated earlier, the complex, a-b-h*, differs from the collision complex in thermal reactions and simply denotes the configuration of the molecule + hot-atom pair when these two particles are closest to each other.

According to a momentum balance, the internal energy, ΔE_i, acquired by the complex is

$$\Delta E_i = \frac{m_{ab}\, E_h + m_h\, E_{ab}}{m_{abh}} \tag{116}$$

Since $E_h \gg E_{ab}$,

$$\Delta E_i = \frac{m_{ab}}{m_{abh}} E_h \tag{117}$$

Only a fraction, $\mathfrak{F}$, [Eq. (40), Table I], of the internal energy will be acquired by a-b in the collision and will be associated with the a-b bond. Thus,

$$\mathfrak{F}\Delta E_i = \mathfrak{F} \frac{m_{ab}}{m_{abh}} E_h . \tag{118}$$

The maximum energy released in the dissociation of a-b-h* is the dissociation energy of bond b-h*, $D_{b\text{-}h}$. If the energy, $D_{b\text{-}h}$, is transferred completely to the bond, a-b, then the maximum energy received by the bond a-b is $D_{b\text{-}h} + \mathfrak{F}\Delta E_i$. Dissociation of bond a-b will result if its bond-dissociation energy, $D_{a\text{-}b}$, is exceeded. Mathematically,

$$D_{b-h} + \mathfrak{F} \frac{m_{ab}}{m_{abh}} E_h \geqslant D_{a-b} \tag{119}$$

or

$$E_h \geqslant \frac{m_{abh}(D_{a-b} - D_{bh})}{m_{ab}\,\mathfrak{F}} \tag{120}$$

If the energy received by the complex exceeds D_{b-h}, the reaction will not lead to a stable product. The upper limit of E_h is

$$E_h \leqslant \frac{m_{abh}}{m_{ab}} D_{b-h} \tag{121}$$

G. Estimation of the Steric Factor

The steric factor, s, is defined as the relative probability that the hot atom reacts with a certain atom in a molecule. Intuitively, one would think that the geometry of the interacting pair alone determines the value of s. However, Odum and Wolfgang[45] have pointed out that although the path of the reaction is controlled mainly by the geometry of the colliding particles, it is also influenced by the intertia of the atom or group which is to be replaced by the hot atom. This inertial effect depends on the mass of the group being replaced, the kinetic energy of the hot atom, and the interaction potential. Clearly, the analysis of this effect is complicated and it can only be discussed qualitatively.

The geometrical steric factor, s_g, can be calculated easily from the geometry of the interacting pair. For the interaction between the hot atom and the ith atom in a molecule, s_{gi} will be the ratio of the surface area of the ith atom exposed to the hot atom, A_i, to the total surface of all atoms in the molecule exposed to the hot atom, ΣA_i.

$$s_{gi} = A_i / \Sigma A_i. \tag{122}$$

In the collision of a hot atom with a diatomic molecule, a-b,

$$s_{ga} = A_a / (A_a + A_b) \tag{123}$$

If r_a and r_b are the covalent radii of atoms a and b, respectively, r_h is the atomic radius of the hot atom, and ab is the interatomic distance in molecule a-b, then conditions indicated in Fig. 17 will exist. The arc u v w is described by a circle of radius $r_a + r_h$ with its center at a. This semicircle describes the various possible positions of the center of the hot atom for a + h collisions. Similarly, the semicircle, u t w, of radius, $r_b + r_h$, describes the various possible positions of the center of the hot atom for b + h collisions. The portion of the spherical surface described by the revolution of arc u v w along the axis a-b is A_a and the surface described by arc u t w is A_b. From spherical trigonometry, these areas are

$$A_a = 2\pi\ (r_a + r_h)^2(1 + \cos\theta_a) \tag{124}$$

$$A_b = 2\pi\ (r_b + r_h)^2(1 + \cos\theta_b) \tag{125}$$

where θ_a and θ_b are defined in Fig. 17.

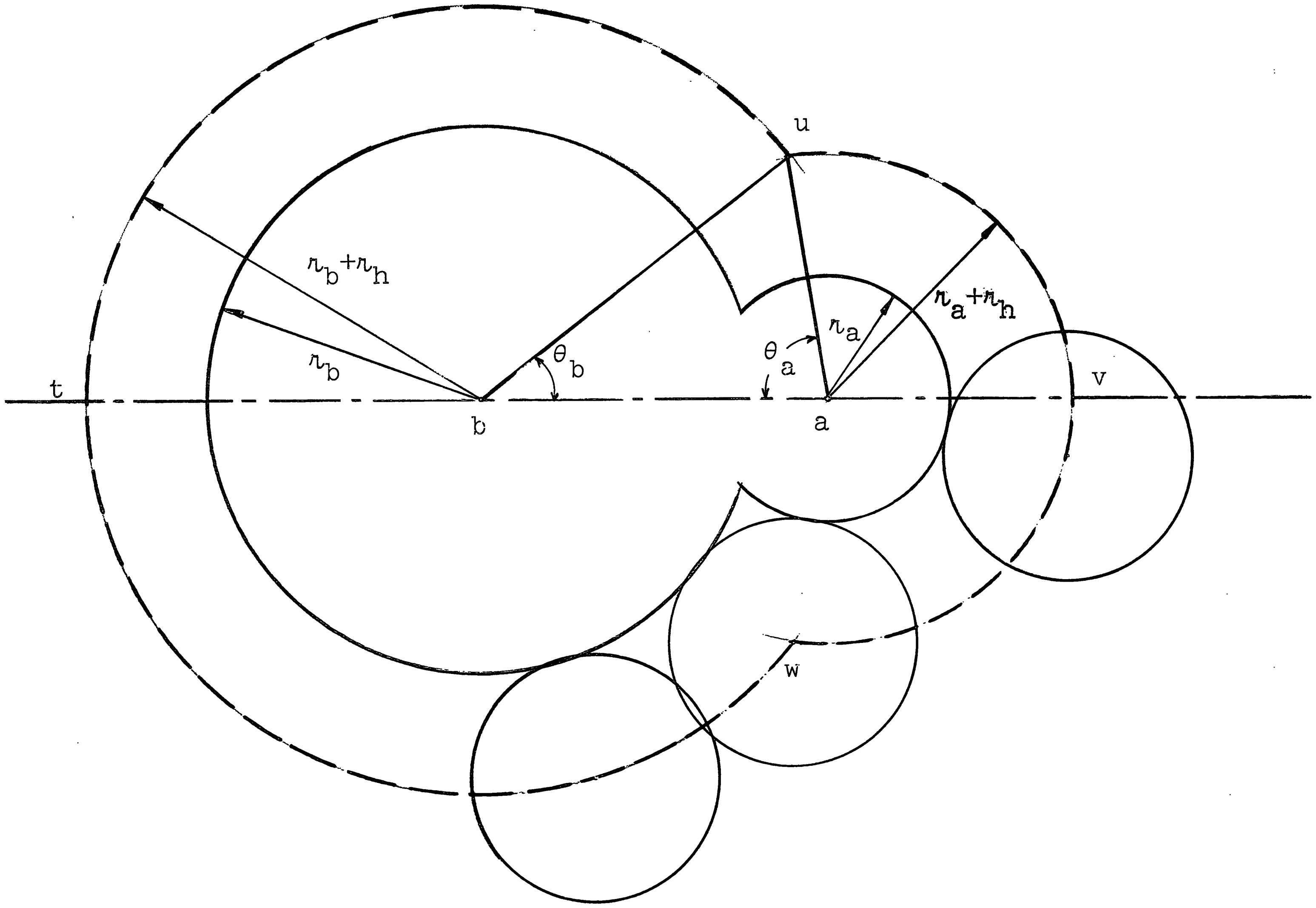

Figure 17. Geometry of collisions between h and ab.

The other common reaction process involves the interaction between a hot atom and a tetrahedral molecule such as methane or substituted methanes. This can be analysed by a spherical triangle, a_1a_2d, which covers one-eighth of the surface of the tetrahedral molecule as shown in Fig. 18. This triangle encompasses one-sixth of the exposed area of a_1, one-third of that of a_2, and approximately one-eighth of that of c. Following the treatment used for a diatomic molecule, the exposed surface areas are

for a_1, $\frac{1}{3}\pi(r_{a_1} + r_h)^2(1 + \cos\theta_{a_1})$,

for a_2, $\frac{2}{3}\pi(r_{a_2} + r_h)^2(1 + \cos\theta_{a_2})$,

and for c , $\Big[\frac{1}{8}$ total area of c - $\frac{1}{6}$ the area covered by a_1 - $\frac{1}{3}$ the area covered by $a_2\Big]$, thus, for c,

$\pi(r_c + r_h)^2(\frac{1}{3}\cos\theta_{c_1} + \frac{2}{3}\cos\theta_{c_2} - \frac{1}{2})$

For all triangles in the molecule

$$A_{ai} = 2\pi(r_{a_i} + r_h)^2(1 + \cos\theta_{a_i}) \quad \text{for } i = 1, 2, 3, 4 \tag{126}$$

$$A_c = 2\pi(r_c + r_h)^2\left[\sum_{i=1}^{i=4}\cos\theta_{c_i} - 2\right]. \tag{127}$$

where θ_{a_i} and θ_{c_i} are defined in Fig. 19.

Given in Table VII are geometric steric factors calculated for some common interacting pairs.

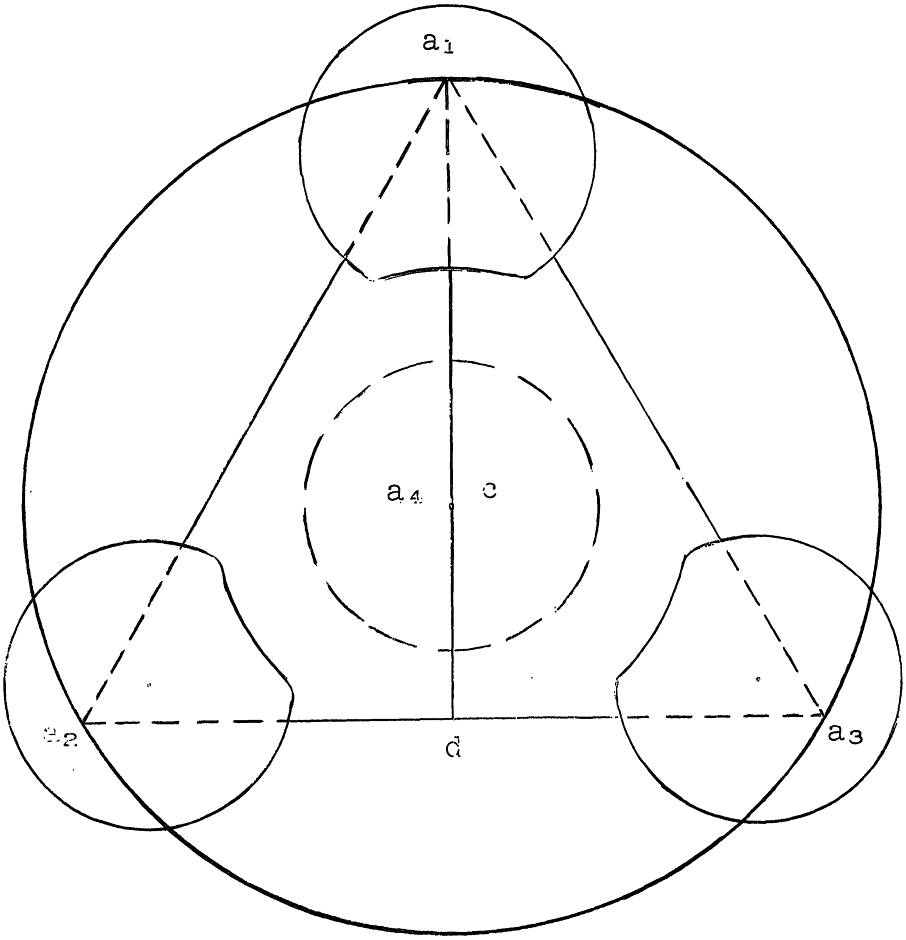

Figure 18. Pictorial representation of a tetrahedral molecule of center atom C and four atoms: a_1, a_2, a_3, and a_4.

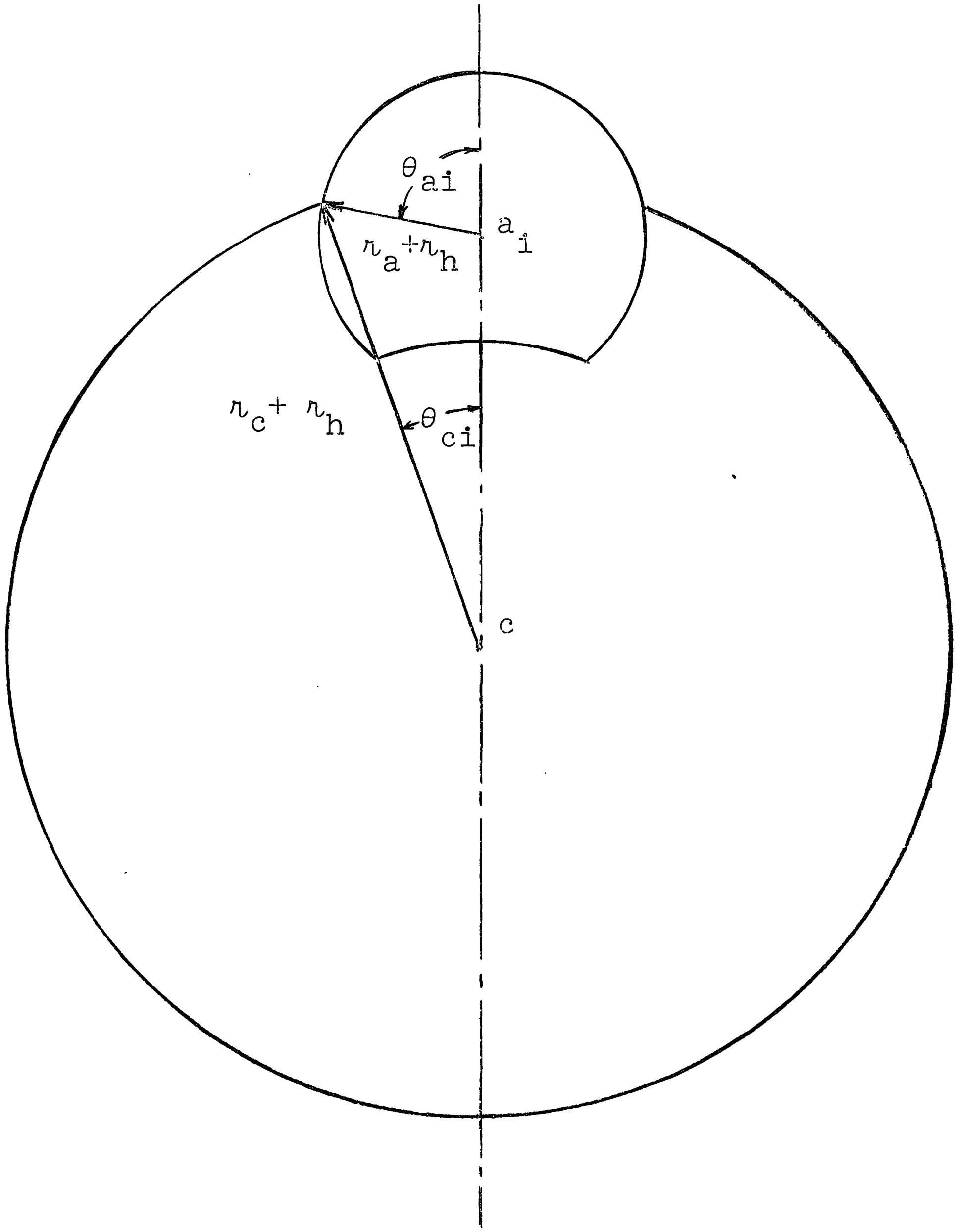

Figure 19. Definition of the angles θ_{ai} and θ_{ci}.

Table VII. Calculated Geometric Steric Factors

Interacting Pair	Product	s_g
CH_4 or CD_4 + T	CH_3T or CD_3T	0.37
	HT or DT	0.63
CH_4 + Br	CH_3Br	0.32
	HBr	0.68
CF_4 + T	CF_3T	0.03
	TF	0.97
CHF_3 + T	CHF_2T	0.07
	CF_3T	0.05
	HT	0.11
	TF	0.77
CH_2F_2 + T	CH_2FT	0.08
	CHF_2T	0.09
	HT	0.25
	TF	0.58
CH_3F + T	CH_3T	0.06
	CH_2FT	0.19
	HT	0.39
	TF	0.36

If it is assumed that all other assumptions in the derivation are correct then, using experimental data, it is possible to calculate the steric factors, s_{exp}, for a given reaction. When this is done, it is usually found that $s_{exp} \neq s_g$. In the calculation of the product yield, s_g was used in some cases, and in others, data of Urch and Wolfgang[43] were used. They determined the relative probability that a hot tritium atom attacks C-C and C-H bonds in alkanes and also determined the relative probability of abstraction and replacement reactions in an attack on a C-H bond. The particular steric factor used in a calculation is given in Table VIII.

The steric factors should be identical for a reaction with isotopic molecules. In this case the steric factor will not appear in certain calculations of the yield ratio and this ratio will serve as a better indication of the validity of the various assumptions. Such calculations are given in Chapter VII.

H. The Energy-Degradation Factor

The energy-degradation factor, r, will depend on the mass of the atom, molecule, or portion of the molecule with which the hot atom collides. This factor is of importance in calculating the hot-atom energy-distribution function following a series of collisions. For T + CH_4 collisions, for example, it seems reasonable, because of the relative sizes of the two particles, that some of the collisions could be between T and H in CH_4 and others between T and C in CH_4. If this be the case, the factor, r, can be replaced by an effective energy-degradation factor, r_e.

Consider a molecule consisting of two types of atoms. When hot atoms encounter this molecule there are c collisions with one of the types of atoms and d collisions with the other type of atoms. The energy-degradation factors are r_c and r_d, respectively, The effective energy-degradation factor is

$$r_e = (r_c^{\,c}\, r_d^{\,d})^{\frac{1}{c+d}} = r^{\frac{c}{c+d}}\, r^{\frac{d}{c+d}} \qquad (128)$$

But $c/(c+d) = s_c$, the steric factor for interactions of the hot atom with the first type of atom. Similarly, for the other types of atom, $d/(c+d) = s_d$. Hence,

$$r_e = r_c^{\,s_c}\, r_d^{\,s_d} \qquad (129)$$

Chapter VII. CALCULATED YIELDS

A. Quantities Used in the Calculations

Using the methods outlined in the previous chapter, various quantities needed in the calculation of the expected reaction yield are given in Table VIII.

B. Isotope Effects

The isotope effect in a chemical reaction is attributed to the difference in isotopic masses. In hot-atom reactions an isotopic change in mass will effect the value of the energy-degradation factor, r, the upper and lower reaction-energy limits, E^b and E^y, and the reaction probability, F(E). The steric factor, however, should remain unchanged. If the yield for a product, j, is given by the equation $Y_j = R_j \, s_i$, then, in calculating the yield ratio for a pair of isotopic molecules, the steric factor does not appear; the yield ratio $Y_j/Y'_j = R_j/R'_j$. The isotopic yield ratio should provide a more reliable indication of the validity of the model than would the calculation of the individual yields.

1. $T - H_2 + D_2$

Lee, Musgrave, and Rowland[46] determined experimentally the ratio of Y_{HT}/Y_{DT} as a function of the mole fraction of H_2 for the reaction of tritium atoms with an $H_2 + D_2$ mixture. These experimental data are indicated by the open circles in Fig. 20.

Using an internally consistent set of data (refer to App. I-E) the radius of tritium (0.53Å) can be compared with the dimensions of an H_2 or D_2 molecule (covalent radius: 0.37Å, interatomic distance: 0.74Å). Because the sizes of T and H_2 or D_2 are comparable it might be expected that both T + H and T + D as well as T + H_2 and T + D_2 collisions are possible. Expected yields and yield ratios could be calculated for both types of collisions. The actual expected yields should then be somewhere between these two extremes.

This system involves two competing reactions, where $A = H_2$ and $B = D_2$. For this case $E_A^a = E_A^b = 11.3$ ev, $E_A^y = E_A^z = 0.88$ ev, $E_B^a = E_B^b = 8.0$ ev, $E_B^y = E_B^z = 0.61$ ev. If the collisions are assumed to be between T and H or T and D, then $r_A = 1/4$, $r_B = 1/25$. If the collisions are between T and H_2 or T and D_2, then $r_A = 1/25$, $r_B = 1/49$.

If the mole fraction of $H_2 = 1.0$, then $g_A = 1.0$. For T + H collisions, Eq. (114) is used and $Y_{HT} = 1.00$. For T + H_2 collisions, Eq. (115) is used and $Y_{HT} = 0.98$.

If the mole fraction of $H_2 = 0.0$, then $g_A = 0.0$. For T + D collisions, Eq. (115) is used and $Y_{DT} = 0.98$. For T + D_2 collisions, Eq. (115) is used and $Y_{DT} = 0.97$.

For the mixtures, if the collisions are between T and H or T and D, Y_{HT} and Y_{DT} are obtained using Eqs. (106) and (109), respectively. If the collisions are between T and H_2 or T and D_2, Y_{HT} and Y_{DT} are obtained used Eqs. (108) and (109), respectively. In using these equations, g_A is

Table VIII. Important Quantities Used in the Calculations

Hot Atom or Ion	Molecules A	B	r_A	r_B	Product	E^b ev	E^y ev	s
T	H_2	D_2	0.040	0.020	HT	11.3	0.88	1.0
			0.250	0.040	DT	8.0	0.61	1.0
T	CH_4	He^4	0.342	0.020	CH_3T	5.25	2.73	0.50
					HT	5.37	0.91	0.50
T	CD_4	He^4	0.148	0.020	CD_3T	5.08	2.58	0.50
					DT	5.20	0.91	0.50
T	CH_3F		0.424		CH_2FT	4.81	2.03	0.192
					HT	4.92	0.58	0.389
					CH_3T	4.81	3.53	0.059
					TF	6.33	0.13	0.360
T	CH_2F_2		0.468		CHF_2T	4.68	1.80	0.088
					HT	4.78	0.51	0.254
					CH_2FT	4.68	3.85	0.081
					TF	6.16	0.51	0.577
T	CHF_3		0.514		CF_3T	4.61	1.77	0.048
					HT	4.72	0.50	0.112
					CHF_2T	4.61	4.27	0.072
					TF	6.07	0.91	0.768
T	CF_4		0.536		CF_3T	4.57	4.13	0.027
					TF	6.02	1.15	0.973
Br	CH_4	Xe	0.445	0.059	CH_3Br	15.2	13.5	0.50
		Kr		0.000	HBr	22.5	4.77	0.50
		Ar		0.111				
		Ne		0.360				
$Br^+(^3P_2)$	CH_4		0.445		CH_3Br^+	22.9	4.28	0.50
					HBr^+	23.8	4.21	0.50
Br	C_2H_6		0.468		C_2H_5Br	10.3	4.85	0.332
					CH_3Br	10.7	1.91	0.043
					HBr	13.8	1.56	0.625

Table VIII. (Con't.)

Hot Atom or Ion	Molecules A	Molecules B	r_A	r_B	Product	E^b ev	E^y ev	s
I($^2P^\circ_{3/2}$)	CH_4	Xe	0.605	0.000	CH_3I	21.1	15.0	0.50
		Kr		0.053	HI	27.5	11.1	0.50
I($^2S_{1/2}$)	CH_4		0.605		CH_3I^+	29.5	8.52	0.50
I^+($^3P_2$)					HI^+	27.5	9.75	0.50
I($^4P_{5/2}$, $^4P_{3/2}$, $^4P_{1/2}$)	CH_4		0.605		CH_3I	26.8	10.5	0.50
					HI	27.5	9.75	0.50
I^+($^3P_1$, $^3P_0$)	CH_4		0.605		CH_3I^+	21.7	2.40	0.50
					HI^+	20.0	4.31	0.50
I^+($^1D_2$)	CH_4		0.605		CH_3I^+	14.0	0.0	0.50
					HI^+	12.2	0.0	0.50
I($^2P^\circ_{3/2}$)	CH_4^+		0.605		CH_3I^+	24.8	0.0	0.50
					HI	27.5	0.0	0.50
I($^2P^\circ_{3/2}$)	CD_4		0.531		CD_3I	14.2	7.32	0.50
					DI	22.6	8.00	0.50
I^+($^3P_2$)	CD_4		0.531		CD_3I^+	24.1	8.02	0.50
					DI^+	22.6	8.00	0.50
I($^2P^\circ_{3/2}$)	C_2H_6		0.624		C_2H_5I	11.9	9.90	0.332
					CH_3I	12.3	5.03	0.043
					HI	16.1	5.70	0.625
I^+($^3P_2$)	C_2H_6		0.624		$C_2H_5I^+$	8.54	0.00	0.332
					CH_3I^+	13.3	0.00	0.043
					HI^+	16.1	0.00	0.625
I($^2P^\circ_{3/2}$)	C_3H_8		0.624		n-C_3H_7I	8.16	8.07	0.238
			0.398		i-C_3H_7I	7.82	7.83	0.080
			0.398		C_2H_5I	8.84	3.86	0.024
			0.624		CH_3I	9.07	3.36	0.024
					HI	16.5	4.74	0.634

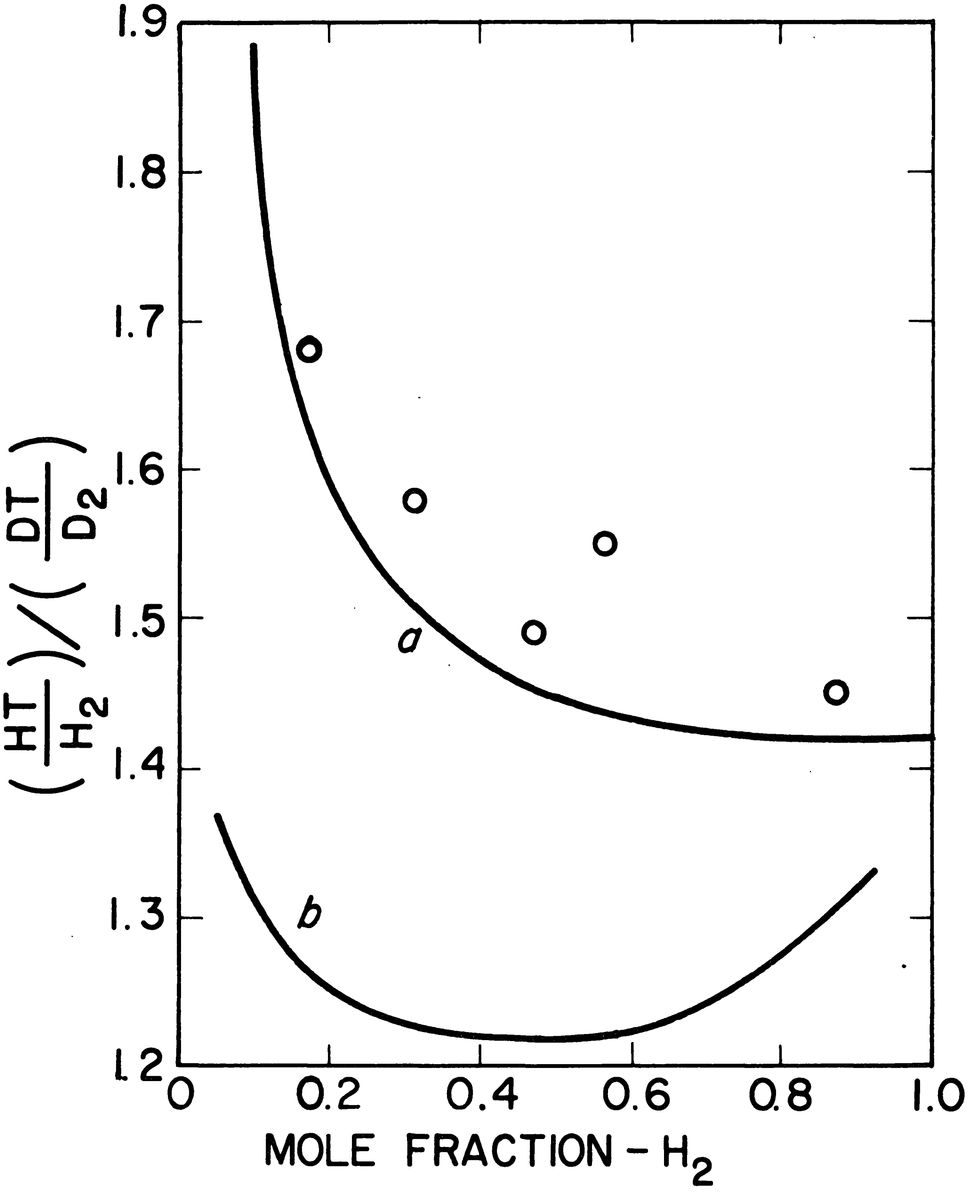

Figure 20. Isotopic specific activity ratio as a function of the mole fraction of H_2 in H_2-D_2 mixtures. Data are of Lee, Musgrave, and Rowland[46]. Curve a was calculated assuming T + H_2 and T + D_2 collisions, curve b, assuming T + H and T + D collisions. Neither curves were corrected for thermal exchange.

Table IX. HT and DT Yields in the System $T + H_2 + D_2$

Mole Fraction H_2	T + H or D Collisions				$T + H_2$ or D_2 Collisions			
	Y_{HT}	Y_{DT}	Specific Activity[a]	Corrected Specific Activity[b]	Y_{HT}	Y_{DT}	Specific Activity[a]	Corrected Specific Activity[b]
0.0	0.00	0.99	—	—	0.00	0.97	—	—
0.1	0.08	0.53	1.31	1.50	0.12	0.59	1.87	1.87
0.2	0.16	0.51	1.25	1.44	0.23	0.57	1.58	1.64
0.3	0.24	0.46	1.23	1.40	0.32	0.49	1.52	1.59
0.4	0.34	0.41	1.22	1.35	0.41	0.42	1.47	1.53
0.5	0.43	0.35	1.22	1.34	0.50	0.35	1.45	1.51
0.6	0.53	0.29	1.22	1.32	0.60	0.28	1.43	1.49
0.7	0.65	0.23	1.22	1.30	0.70	0.21	1.42	1.46
0.8	0.76	0.15	1.23	1.29	0.80	0.14	1.42	1.44
0.9	0.87	0.07	1.24	1.27	0.90	0.07	1.42	1.43
1.0	1.00	0.00	—	—	0.98	0.00	—	—

[a] The specific activity = $(Y_{HT}/Y_{DT})/[X_{H_2}/(1-X_{H_2})]$

[b] Corrected for thermal exchange reactions: $T + H_2$ and $T + D_2$.

equal to the mole fraction of H_2 since the cross-sections are equal for the two types of collisions. The steric factors equal 1.0.

These various data are listed in Table IX and the specific activities $(Y_{HT}/Y_{DT})/[X_{H_2}/(1 - X_{H_2})]$ are plotted in Fig. 20 for T + H_2 or D_2 collisions (curve a) and T + H or D collisions (curve b).

One additional effect should be considered. Those tritium atoms which bypass the reactive-energy range (11.3 - 0.61 ev) can react further with H_2 or D_2 in a thermal exchange reaction. At 1000°K, the ratio[47,48] of the rate constants for the reactions $(H + H_2 \rightarrow H_2 + H)/(H + D_2 \rightarrow HD + D)$ and for the reactions $(D + H_2 \rightarrow DH + H)/(D + D_2 \rightarrow D_2 + D)$ are about 1.7 - 2.2. No data are available for the T + H_2 and T + D_2 exchange reactions.

The calculated specific activities were therefore corrected for the thermal-exchange reaction assuming the $T + H_2/T + D_2$ rate-constant ratio was 1.9. As an example, for T + H_2 or D_2 collisions, when $X_{H_2} = 0.2$, the fraction of tritium atoms available for the thermal-exchange reaction is 1.00 - 0.23 - 0.57 = 0.20. Of these, $(0.20)(1.9)(0.2)/[(1.9)(0.2) + (1.0)(0.8)] = 0.06$ form HT and 0.20 - 0.06 = 0.14 form DT. The corrected specific activity is $(0.29/0.71)/(0.20/0.80) = 1.64$.

Rowland[49] considers the experimental data accurate to about ± 3%. For the T + H_2 or D_2 collisions, the corrected data are in agreement with the experimental within ± 1.4 %.

For the T + H or D collisions, the corrected data are 12.5% lower than the experimental data.

The irradiated samples contained[46] 15-17 mm He^3 and about 630 mm total $H_2 + D_2$. Thus, the mole fraction of He^3 is only 0.025. The presence of He^3 will affect the specific activity ratio in two ways but the two effects are in opposite directions. Since the energy range for production of HT is greater than that for production of DT, collisions of T with the small amount of He^3 will cause a small decrease in the HT yield but an even smaller decrease in the DT yield. Thus, the specific activity ratio will be slightly smaller. However, these additional tritium atoms which have not formed HT or DT in the hot reaction energy zones can then react thermally to form HT or DT and, for this reaction, the HT product will predominate. The corrected specific activity will be approximately the same as if the presence of He^3 was neglected.

The above calculations do not necessarily indicate that the colliding partner must be H_2 or D_2 rather than H or D. If the thermal-exchange rate-constant ratio was 2.2, for example, rather than 1.9, the corrected curve for T + H or D collisions would be more in agreement with the experimental data and the T + H_2 or D_2 corrected curve would lie above the experimental points.

The excellent agreement between theory and experiment suggests that the mathematical model serves properly to describe hot-atom reactions in these simple systems.

2. T - CH_2D_2 and T - CH_4 + CD_4

Lee, Musgrave, and Rowland[50] determined the (HT/DT)/(CH_4/CD_4) and (HT + DT)/(CH_3T + CD_3T) ratios in the reaction systems: T - CH_2D_2 and T - CH_4 + CD_4. Although they were able to separate HT and DT, the CH_3T and CD_3T products appeared as a single gas chromatography peak.

These systems constitute a reaction mixture involving competing reactions. The T - CH_2D_2 system can be handled as though it were an equimolar mixture of CH_4 and CD_4. Using effective energy-degradation factors, 0.342 for T-CH_4 and 0.148 for T - CD_4, calculation of the values of R is made using Eq. (108) for CH_3T, Eq. (106) for HT, and Eq. (109) for CD_3T and DT.

Lee, Musgrave, and Rowland[50] observe (HT + DT)/(CH_3T+CD_3T) ratios of about 0.82 to 0.90. As is discussed on page 124 and depicted in Fig. 26, the calculated ratio of HT/CH_3T for non-moderated systems will depend on the choice of s_{CH_3T} and varies from 1.0 for s = 0.6 to 2.0 for s = 0.4. For s = 0.5, a ratio (HT + DT)/(CH_3T + CD_3T) of 1.12 is calculated. Although this value is certainly greater than the observed value of 0.82 to 0.90, the calculated value is more in agreement with Wolfgang's observations that the HT/CH_3T ratio is > 1.0

The isotopic methane yield ratios and specific activities can be calculated unambiguously since the steric factor cancels. However, $Y_{HT} = R_{HT} - R_{CH_3T}\, s_{CH_3T}$ and Y_{DT} =

R_{DT} - R_{CD_3T} s_{CD_3T}. A calculation of the specific activity ratio, $(Y_{HT}/Y_{DT})/(CH_4/CD_4)$ will therefore require knowledge of s_{CH_3T} and s_{CD_3T}. If these steric factors are assumed equal to 0.5, then the calculated specific activity ratio involving HT and DT is 1.24 for 0.50 mole-fraction CH_4, in good agreement with the experimental value of 1.29.

3. T - CH_4 + He and T - CD_4 + He

Estrup and Wolfgang[22] and Cross and Wolfgang[51] have performed a number of experiments to determine the effect of He^4 on the yields of the T + CH_4 and T + CD_4 reactions. These experimental data are given in Figs. 21 and 22. The discussion here will be limited to the isotope effect in the production of CH_3T and CD_3T. Detailed calculations for these systems are given in Appendix III. The calculated yields of CH_3T and CD_3T are given by the solid lines in Figs. 21 and 22. In performing these calculations, an effective energy degradation, r_e, was used although the yield ratio is not effected appreciably by this choice. For any mole fraction of He^4, $Y_{CH_3T}/Y_{CD_3T} = R_{CH_3T}/R_{CD_3T}$ since the steric factors, s_{CH_3T} and s_{CD_3T}, are assumed equal and therefore cancel.

The calculated yield ratio, Y_{CH_3T}/Y_{CD_3T}, as a function of the mole fraction of He^4, is plotted as a solid line in Fig. 23. The best visually drawn upper and lower-limit curves which encompass about 90% of the experimental data of Figs. 21 and 22 were used to calculate the experimental yield ratio. These experimental ratios are indicated by

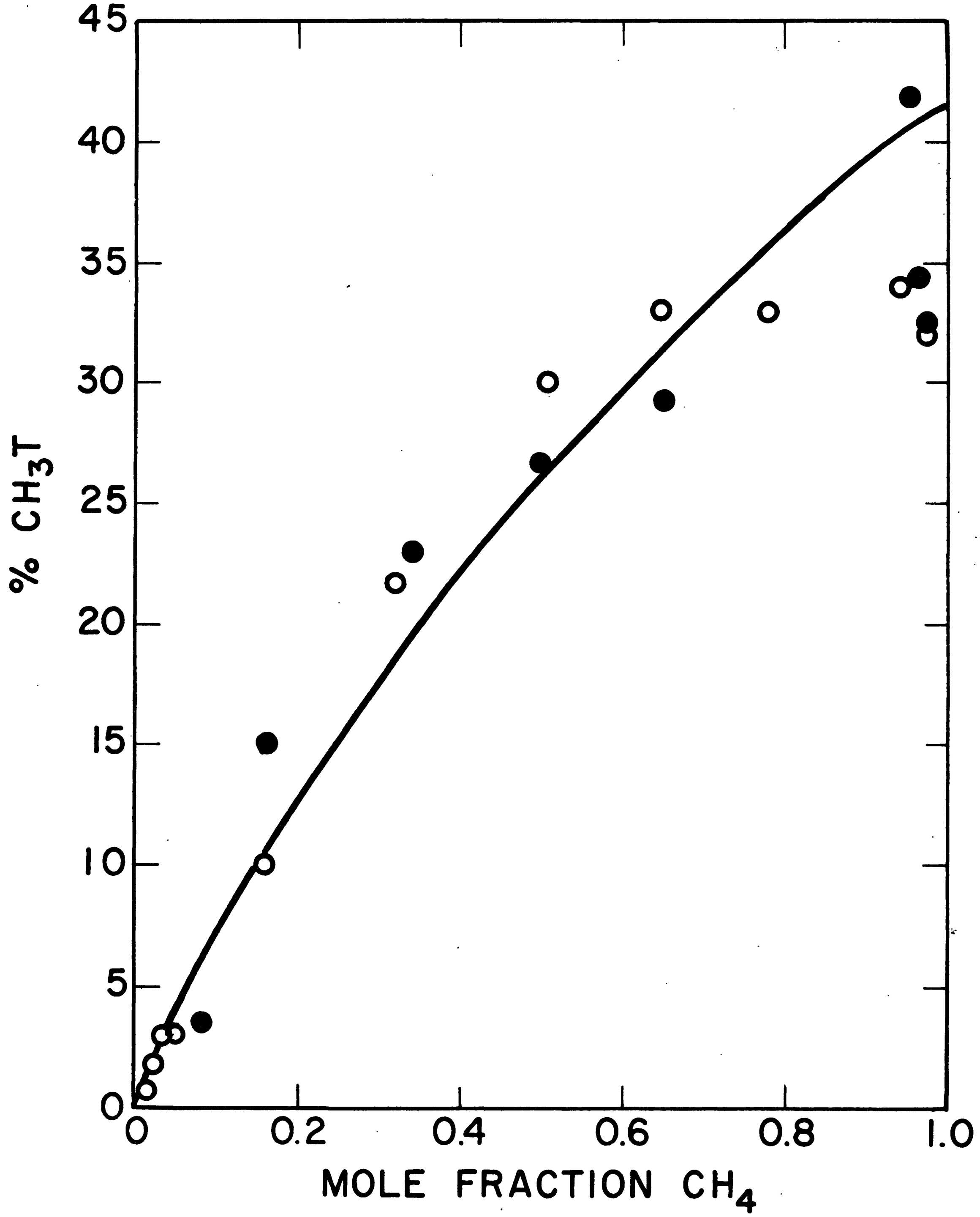

Figure 21. Percent CH_3T in T - CH_4 + He systems as a function of the mole fraction of CH_4. Data: ○ , Estrup and Wolfgang[22]; ●, Cross and Wolfgang[51]; solid curve is calculated.

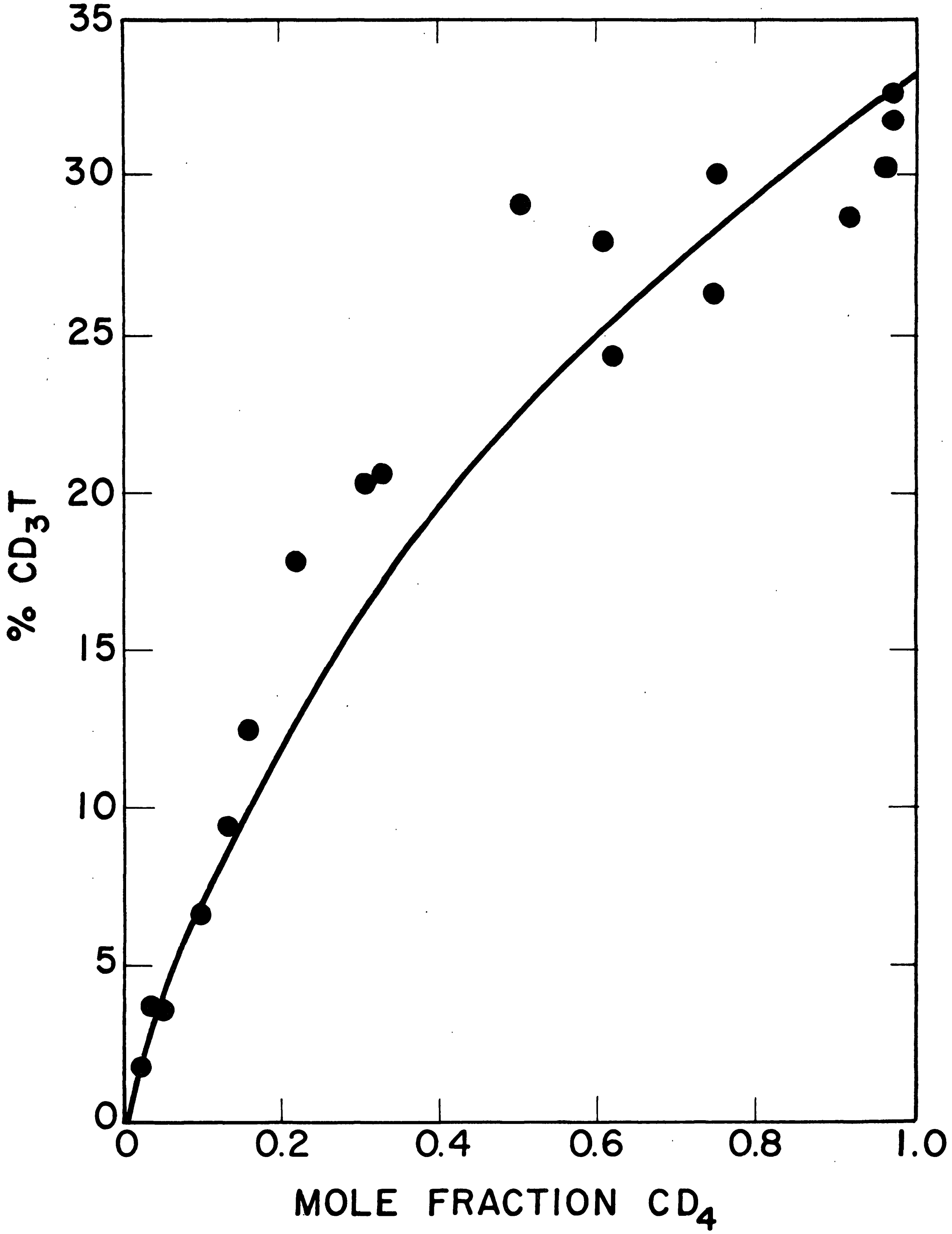

Figure 22. Percent CD_3T in T - CD_4 + He systems as a function of the mole fraction of CD_4. Data: Cross and Wolfgang[51]; solid curve, calculated.

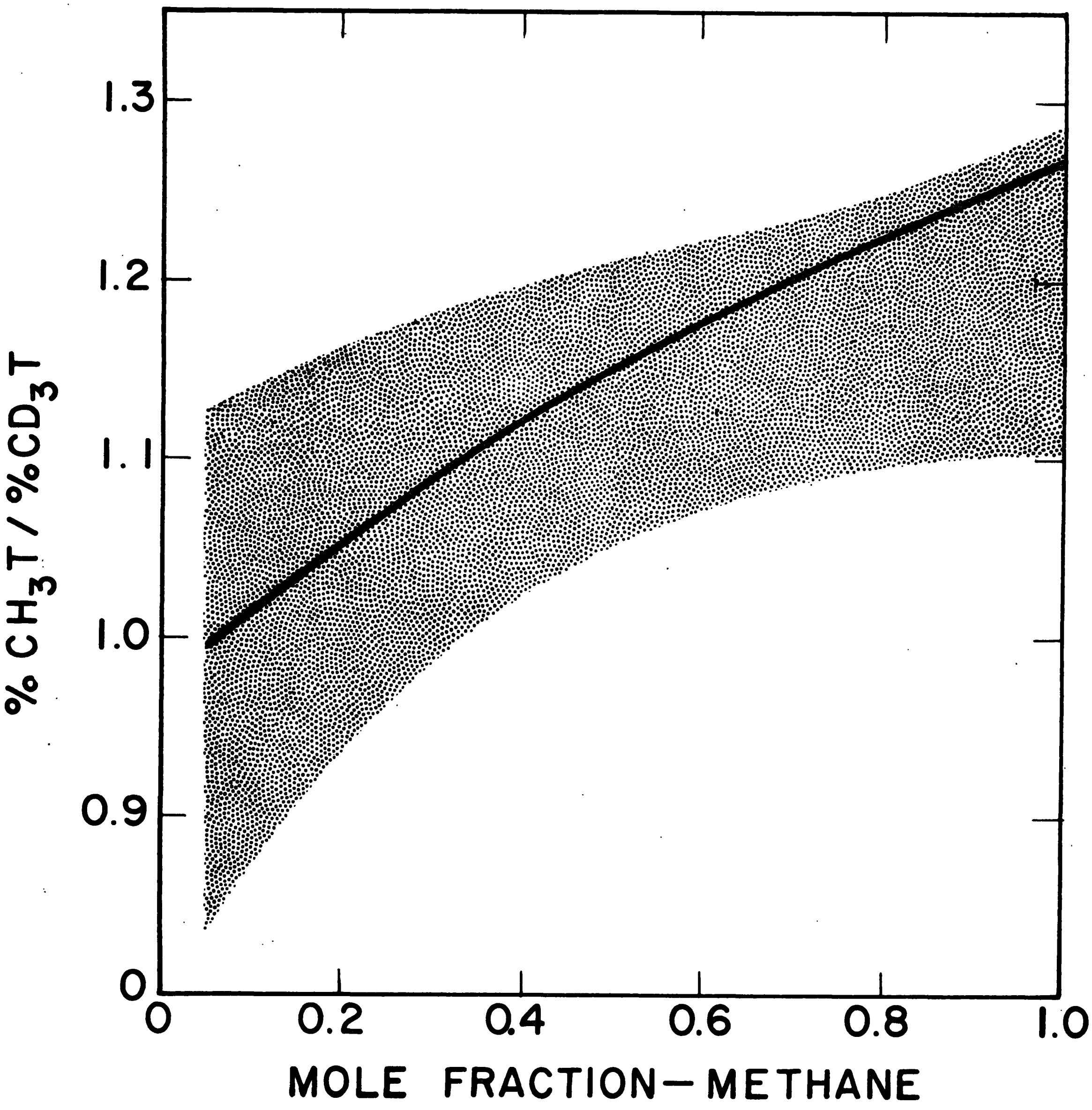

Figure 23. CH_3T CD_3T ratio vs. the mole fraction of methane in T - CH_4 + He and T - CD_4 + He systems. Ratio of experimental data is indicated by the shaded band; calculated ratio is the solid curve.

the speckled band of Fig. 23. The agreement seems excellent.

4. I^{128}- CH_4 and I^{128}- CD_4

At least 50% of the I^{128} produced by the $I^{127}(n,\gamma)I^{128}$ process is positively charged[9]. In non-moderated CH_4 or CD_4 systems, the ratio: CH_3I/CD_3I was calculated to be 0.92 if the I^{128} is a ground-state neutral iodine ($^2P_{3/2}$) and 1.01 if the iodine is I^+ ($^3P_2$). Similar values are to be expected for other iodine species.

Rack and Gordus[14] determined that the non-moderated CH_3I^{128} yield is 54.4 ± 0.5% and that the non-moderated CD_3I^{128} yield is[52] 52.3 ± 1.0%. The yield ratio is therefore 1.04 ± 0.02%, in agreement with theory.

5. Br^{80}- CH_4 and Br^{80}- CD_4

The CH_3Br^{80} yield in non-moderated Br^{80} + CH_4 systems is 13.3 ± 0.5% when the Br^{80} is produced by (n,γ) activation[17]. No data are availble for the analogous Br^{80} + CD_4 reaction. A calculation of the expected yield ratio; CH_3Br/CD_3Br, indicates a value of 0.98 if the Br^{80} is ionic and 0.94 if ground-state neutral Br^{80} is involved. Thus, the expected yield is about 12.5 - 13.0%.

6. Conclusions

The excellent agreement between the theoretical and experimental values of the isotope yield-ratio suggests that the proposed model is a reasonably valid representation of the reaction mechanism. It should be noted, however, that this agreement does not suggest that the proposed steric factors are valid since the steric factors do not enter into the calculation of the organic yield ratio. The particular choice of the energy-degradation factor, r, does not strongly effect the calculated yield-ratio except in the case of the $T + H_2$ and $T + D_2$ reactions. Hence, the agreement between theory and experiment does not completely validate the choice of r.

C. Inert-Gas Moderated Systems

1. $T - CH_4 + He^4$

One of the most extensive studies of the effects of inert gases on a hot-atom reaction is that of Estrup and Wolfgang[22]. and Cross and Wolfgang[51] who examined the $T + CH_4$ system. The vast majority of their data are concerned with the He^4 moderation of this reaction and the discussion here will be limited to these data.

a. The Steric Factor - Unlike the calculation of the isotope yield ratio: CH_3T/CD_3T, the determination of the individual yields requires knowledge of the steric facotr. It was stated earlier that the relative sizes of the tritium atom and the methane molecule are such that, in a collision with CH_4, the tritium come is contact with only a portion of the molecule. The geometry of the colliding particles indicates that $s_g = 0.37$ for CH_3T formation and therefore $s_g = 0.63$ for HT formation.

If it is assumed that all other aspects of this mathematical model are valid, then, using the experimental data of Wolfgang and co-workers, it is possible to calculate the experimental steric factor, s_{exp}. Since $Y_{CH_3T} = R_{CH_3T}\ s_{CH_3T}$, the value of s_{CH_3T} can be calculated using the calculated value of R_{CH_3T} and the experimental value of Y_{CH_3T}. In a similar manner, experimental values of Y_{HT} can be used to calculate s_{CH_3T} according to the equation: $Y_{HT} = R_{HT} - R_{CH_3T}\ s_{CH_3T}$.

Using experimental CH_3T data for scavenged systems, s_{CH_3T} was found to equal 0.58. For corresponding experimental HT data in scavenged systems, s_{CH_3T} was found to equal 0.74.

The value of s_{CH_3T} can also be found from a combination of these two yields: $s_{CH_3T} = (R_{HT}/R_{CH_3T}) \Big/ [1 + (Y_{HT}/Y_{CH_3T})]$. This representation has the advantage that it is necessary to know only the relative HT and CH_3T yields rather than the absolute yields. Using this equation, s_{CH_3T} is found to be 0.66 for scavenged systems. This latter value is the average of the two values above calculated from the individual yields. This correspondence is not a general rule and occurs here only because Y_{HT} is approximately equal to Y_{CH_3T} in the scavenged systems.

It is not at all obvious why the experimentally-derived steric factor should differ so from the geometric steric factor. An effect described by Odum and Wolfgang[45] as an inertial effect, has, in a sense been accounted for in the calculation of $\mathfrak{F}$, the fraction of the internal energy associated with the C-H bond, and has also been partially accounted for in the calculation of the effective energy-degradation factor, r_e. It may be, however, that this inertial effect is indeed so important a factor in the hot-atom reaction that this mathematical model does not take full cognizance of it. However, upon examining the various data for a variety of systems, it is seen that the calculated values are always in reasonable agreement with experiment. When the calculated yield is high, the experimental yield is high. When the calculated yield indicates only a few percent yield, invariably the experimentally observed yield is only a few percent. It is therefore difficult to assess accurately and judge, with any high degree of conviction, the various possible choices of the steric factor.

It is of interest to note that the value of s_{CH_3T} derived from the Y_{HT}/Y_{CH_3T} experimental data[22,51] for unscavenged systems is 0.41, in very good agreement with the geometric factor.

Lacking any other means of determining this steric factor the decision was made to use, simply, $s_{CH_3T} = 0.50$. The solid curves of Figs. 21, 22, and 25 were calculated using this value.

b. <u>The Energy-Degradation Factor</u> - The total tritium stabilized as HT and CH_3T is independent of the steric factor since $Y_{HT} + Y_{CH_3T} = (R_{HT} - Y_{CH_3T}) + Y_{CH_3T} = R_{HT}$. The effect of different choices of the energy-degradation factor can then be evaluated in terms of its effect on R_{HT}. Presented in Fig. 24 are two curves. Curve a was calculated assuming the collisions were between T and the methane molecule.

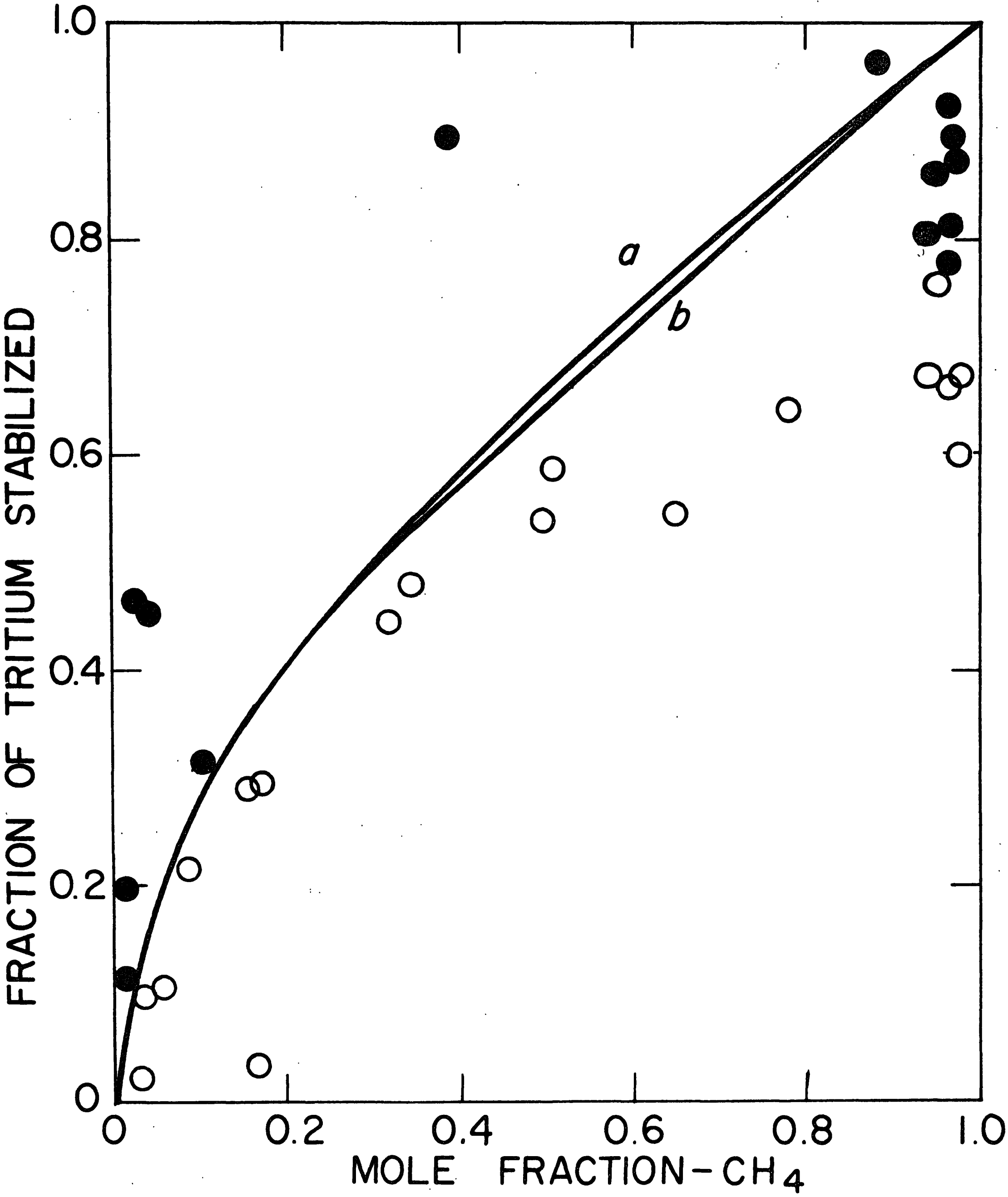

Figure 24. Fraction of tritium stabilized as a function of the mole fraction of CH_4. Curve a, r = 0.25. Curve b, $r = r_e = 0.342$. Data: ●, unscavenged, ○, I_2 scavenged.

Hence, for this curve, $r = 0.25$. If the effective energy-degradation factor, $r_e = 0.342$ is used, the calculated curve is b. Thus, the choice of r has very little effect on the calculated yields.

Also plotted in Fig. 24 are the experimental data[22,51] for the HT + CH_3T yields in scavenged systems. These data by no means extrapolate to 1.0 at unit mole-fraction of CH_4. The experimental data[22] for the HT + CH_3T yields in unscavenged systems, however, are in much better agreement with these curves. (In the scavenged systems the HT yields are much lower. The reason why the I_2 scavenger affects only the HT and not the CH_3T is not obvious.)

It should be pointed out that the lack of agreement between these scavenged data and the two curves of Fig. 24 is not a result of an improper choice of r. It is probably due to the fact that additional reactions with the scavenger were not included in the calculations. For example, it was assumed that between 2.73 and 0.91 ev only $T + CH_4 \rightarrow CH_3 + HT$ occurs. However, between 3.1 and 0.0 ev the reaction $T + I_2 \rightarrow TI + I$ can occur. If, in the range 3.1 to 0.91 only $T + I_2$ reactions occur, which is by no means possible in the experimental systems studied since the pressure of CH_4 far exceeded that of I_2, then the calculated yields of HT are given by curve b in Fig. 25.

Another, perhaps more realistic reaction, which could lead to the depletion of HT is the thermal reaction : $HT + I_2 \rightarrow HI + TI$.

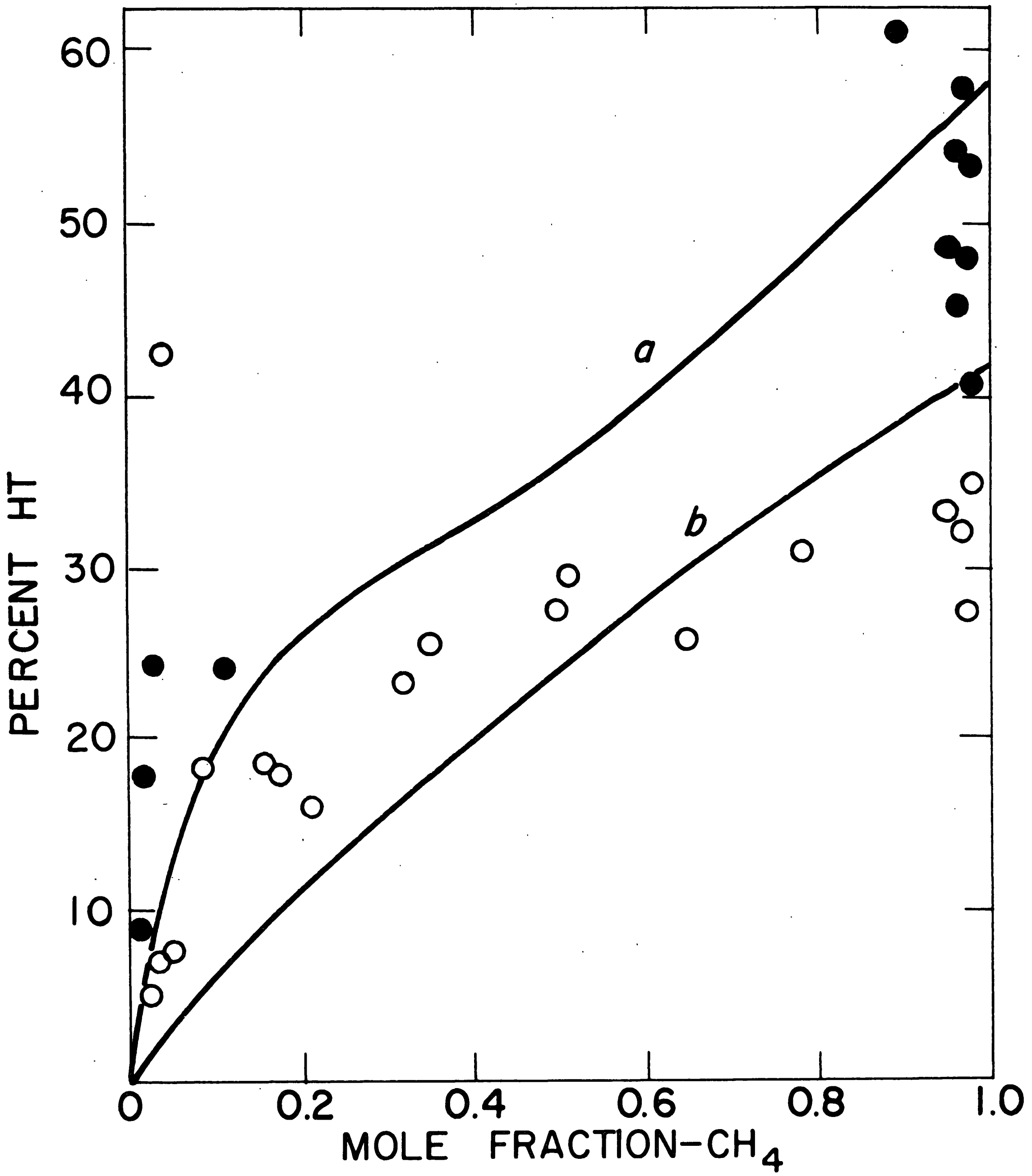

Figure 25. Percent HT as a function of the mole fraction of CH_4. Curve a, unscavenged. Curve b, a scavenger totally effective in the range 3.1-0.91 ev. Data: ●, unscavenged, ○, scavenged.

c. The HT/CH_3T Yield - The ratio of yields of HT/CH_3T was discussed above in relation to the calculation of the steric factor. One other point bears comment. Estrup and Wolfgang[22] noted that the ratio HT/CH_3T increased in highly moderated systems and stated that this is probably due to the reaction of T with HI. Calculations indicate that such a variation in this yield ratio should occur and would be a direct consequence of the fact that the reactive-energy range for the production of HT is greater than that for the production of CH_3T. These data are depicted in Fig. 26.

2. T - CD_4 + He^4

The discussion for this system exactly parallels that given for the T - CH_4 + He^4 system. The value of s_{CD_3T} calculated from the ratio Y_{DT}/Y_{CD_3T} was 0.67 for scavenged and 0.44 for unscavenged systems[51]. A value of s_{CD_3T} = 0.50 was used in the calculation of the solid curve of Fig. 22.

3. Br^{80} - CH_4 + Inert Gas

At least 18% of the Br^{80} produced by (n,γ) activation is positively charged[9]. Since no information about possible excited species was available, it was assumed that only ground-state $Br(^2P_{3/2})$ atoms and $Br^+(^3P_2)$ ions took part in the reaction. A steric factor of 0.5 was assumed, although it may be slightly high. Since the bromine atom is much larger than the size of a hydrogen atom in CH_4, it was assumed that the bromine collides with the whole methane molecule. Thus, $r = 0.445$.

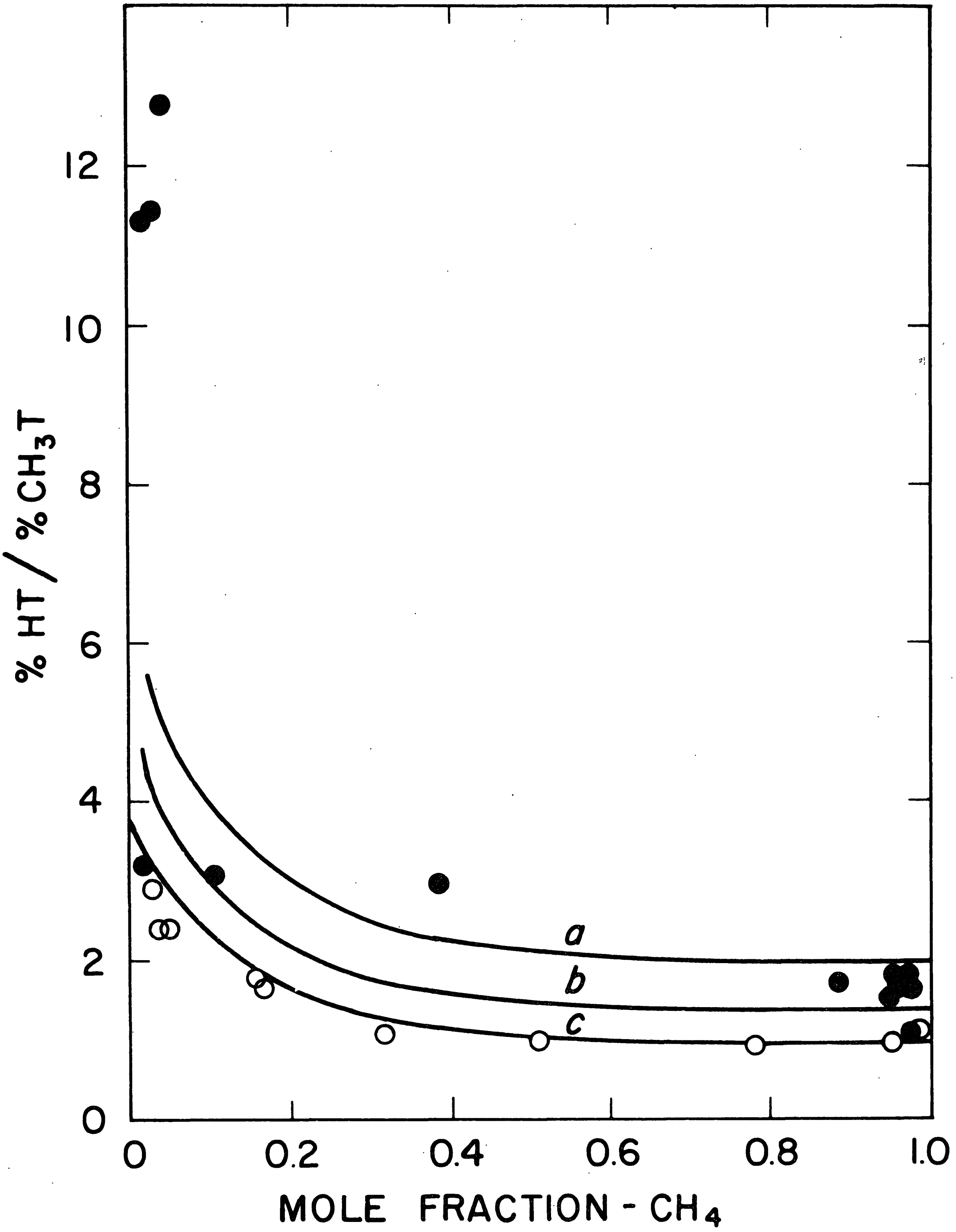

Figure 26. %HT/%CH$_3$T vs the mole fraction of CH$_4$ for various steric factors. Curve a, s = 0.40; b, s = 0.50; c, s = 0.60.

The ionization potentials of CH_4, Ne, Ar, and Kr are greater than that of Br and charge-transfer between Br^+ and CH_4, Ne, Ar, and Kr would not occur. In Br^{80} - CH_4 systems containing these inert gases both Br^+ and Br species will exist.

For pure CH_4 + $Br^+(^3P_2)$, a yield of 45.0% is calculated. The effect of Ne, Ar, and Kr on this reaction is indicated by curves a in Figs. 27, 28, and 29. For pure CH_4 + $Br(^2P_{3/2})$, a yield of 6.2% is calculated. The effect of Ne, Ar, and Kr on this reaction is indicated by curves d in Figs. 27, 28, and 29. In these figures, curve b corresponds to a mixture of 80% Br and 20% Br^+; curve c corresponds to a mixture of 85% Br and 15% Br^+. Thus, curves b and c define a region corresponding to 15-20% positively charged Br^{80}. These calculated curves agree surprisingly well with the experimental data[17].

The xenon-moderated reaction can involve the charge-transfer reaction of $Br^+(^3P_1)$ with Xe to yield $Br(^2P_{3/2})$ + $Xe^+(^2P_{3/2})$. If the $Br^+(^3P_1)$, while in the reaction energy range, encounters a CH_4 before meeting a xenon atom, it will react with the CH_4. If the $Br^+(^3P_1)$ meets a xenon first, it will be neutralized to $(^2P_{3/2})$ which, if it possessed enough kinetic energy, can still react with CH_4. The fate of the $Br^+(^3P_1)$ will be a function of the probability that it collides with CH_4, g_A. Curve a of Fig. 30 indicates the fraction of bromine originally as $Br^+(^3P_1)$ which reacts with CH_4. Curve d is the reaction of Br + CH_4. Curves b and c cor-

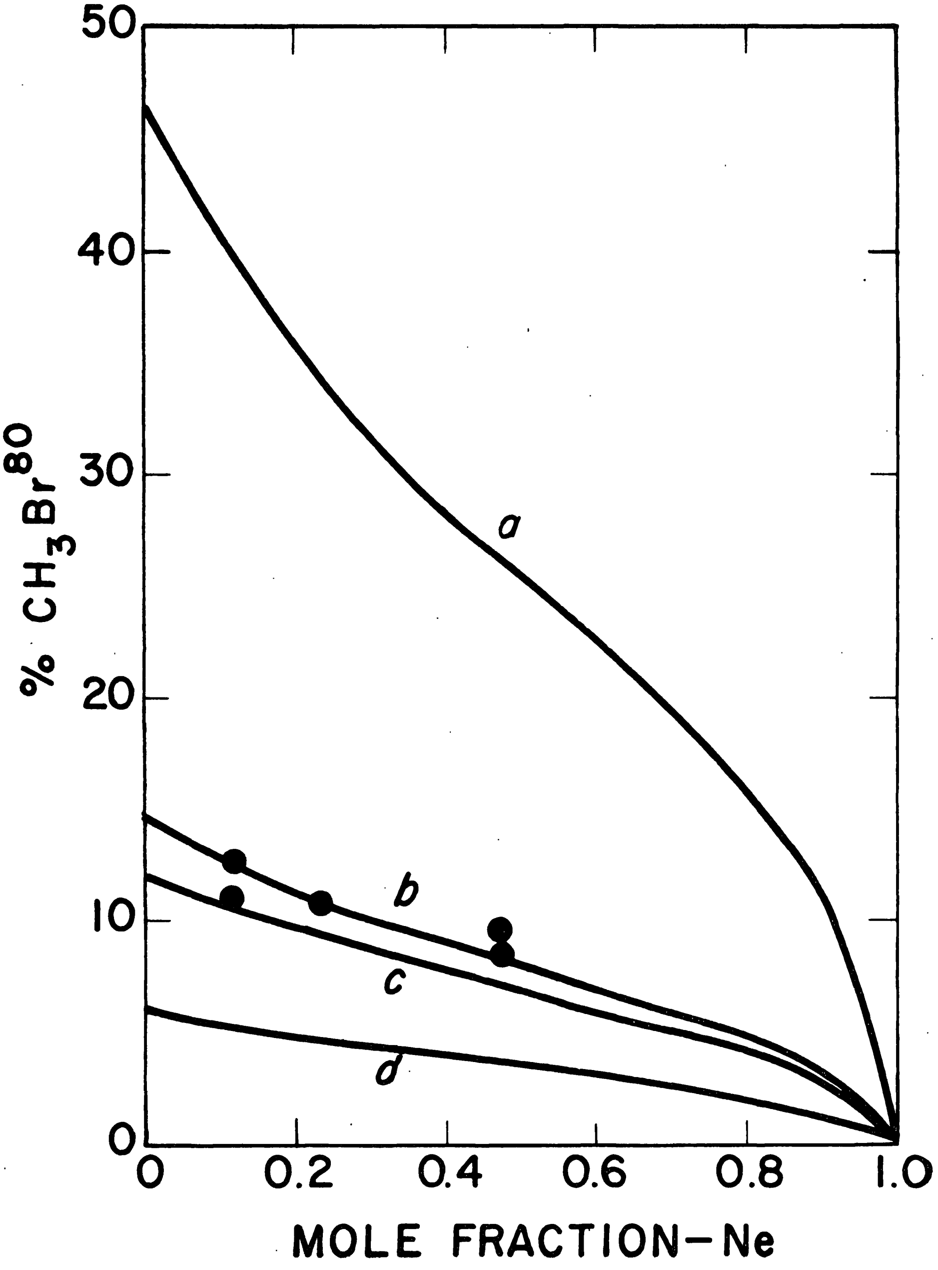

Figure 27. Effect of Neon on the yield of CH_3Br^{80}. Curve a, $Br^+ + CH_4$; b, 80% Br, 20% $Br^+ + CH_4$; c, 85% Br, 15% $Br^+ + CH_4$, d, $Br + CH_4$.

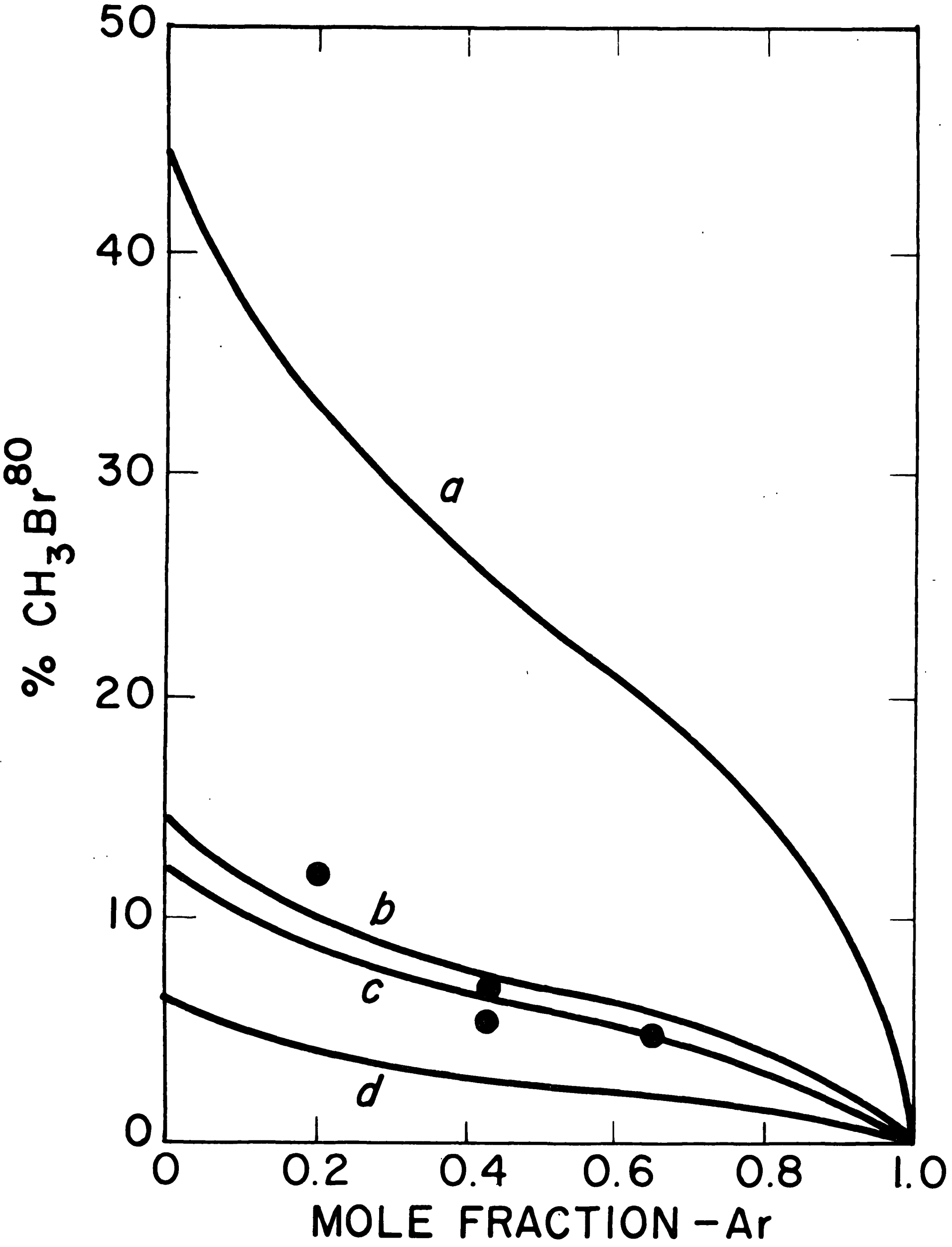

Figure 28. Effect of Argon on the yield of CH_3Br^{80}. Refer to Fig. 27.

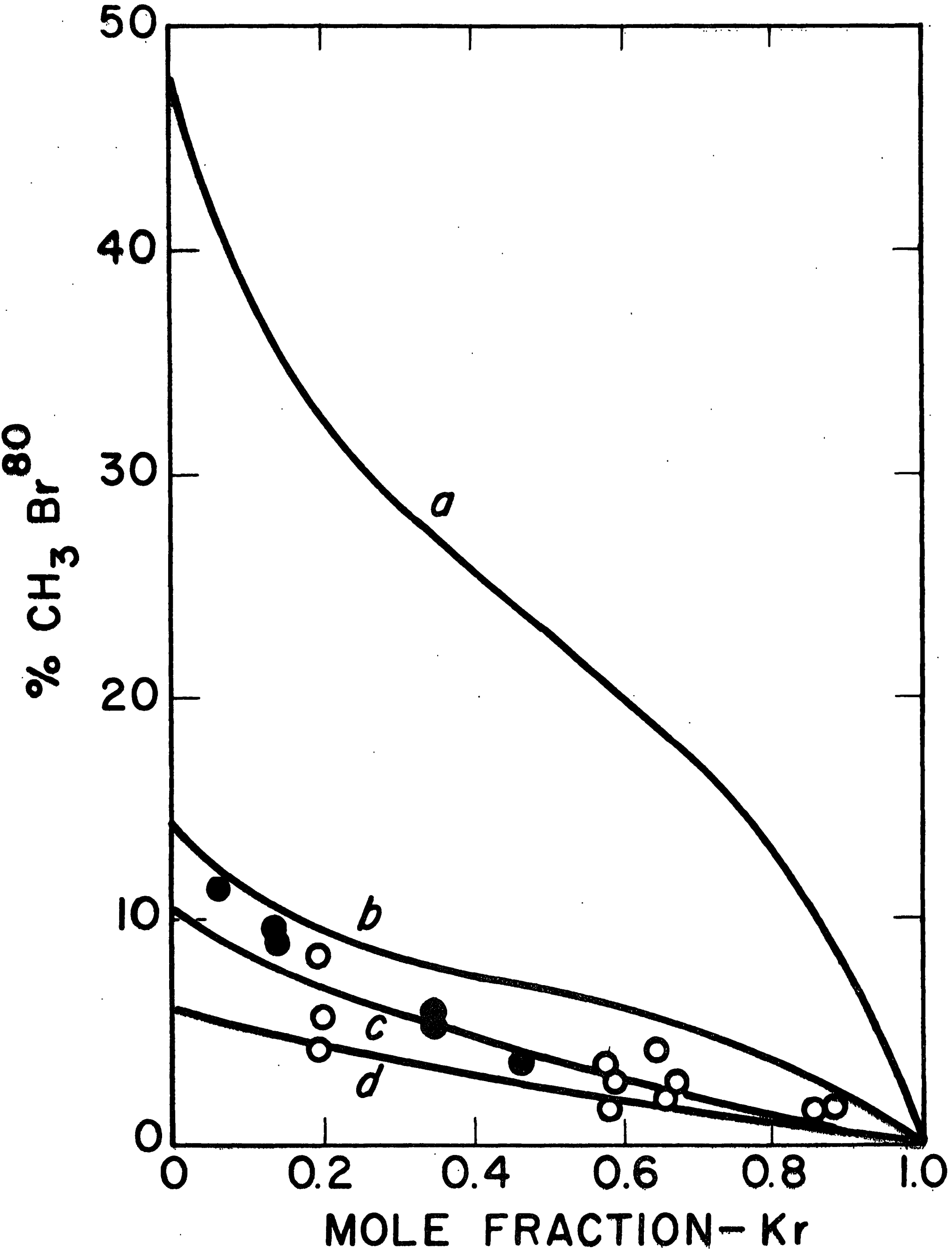

Figure 29. Effect of Krypton on the yield of CH_3Br^{80}. Refer to Fig. 27. Data: ●, Rack and Gordus [17]; ○, Gordus, unpublished.

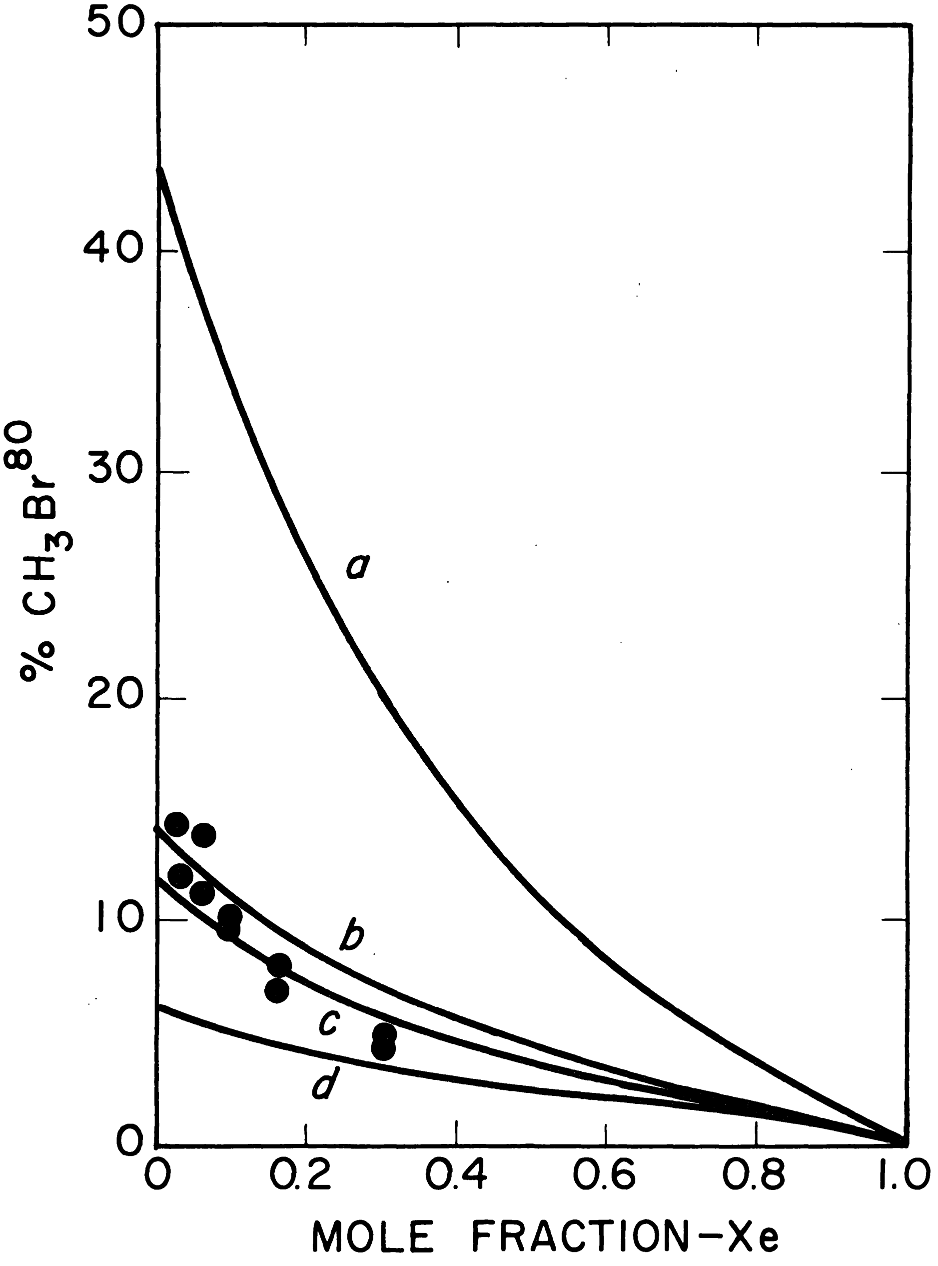

Figure 30. Effect of Xenon of the yield of CH_3Br^{80}. Curve a, $CH_4 + Br^+ (^3P_1)$ or $Br(^2P_{3/2})$ formed from $Br^+(^3P_1)$; b, 80% Br, 20% $Br^+(^3P_1) + CH_4$; c, 85% Br, 15% $Br^+(^3P_1) + CH_4$; d, Br + CH_4.

respond to 80% and 85% Br, respectively. The calculated curves, b and c encompass most of the data points[17].

4. I^{128} - CH_4 + Inert Gas

These reaction systems are very similar to those involving the inert-gas moderation of Br^{80} + CH_4. In the case of I^{128}, however, at least 50% of the atoms are positively charged[9] and at least 25% are $I^{+}(^{1}D_{2})$[14,55]. A steric factor of 0.5 was assumed and the value of $r = 0.605$, which corresponds to collisions between I and CH_4 molecules was chosen.

With xenon moderator, $I^{+}(^{1}D_{2}) + Xe \rightarrow I(^{2}P_{3/2}) + Xe^{+}(^{2}P_{3/2})$ can occur. Experimental data[14] and various calculated curves are given in Figs. 31 and 32.

$I^{+}(^{1}D_{2})$ cannot undergo charge-transfer with krypton. The effects of this gas on various processes which yield CH_3I^{128} are given in Fig. 33 and compared with experimental data[14].

Since the I^{128} ionic abundances are not known, the net CH_3I^{128} yields cannot be calculated. These curves serve only to indicate the general trends in moderating the various reactions.

D. Non-Moderated Systems

Presented in this section are the calculated yields for various non-moderated reaction systems where the target molecule is in great excess. The agreement between the calculated and experimental values is fairly good. It should be emphasized that, in these calculations, unlike those of the isotope yield ratio; the choice of the effective energy-degradation factor and, particularly, the steric factor

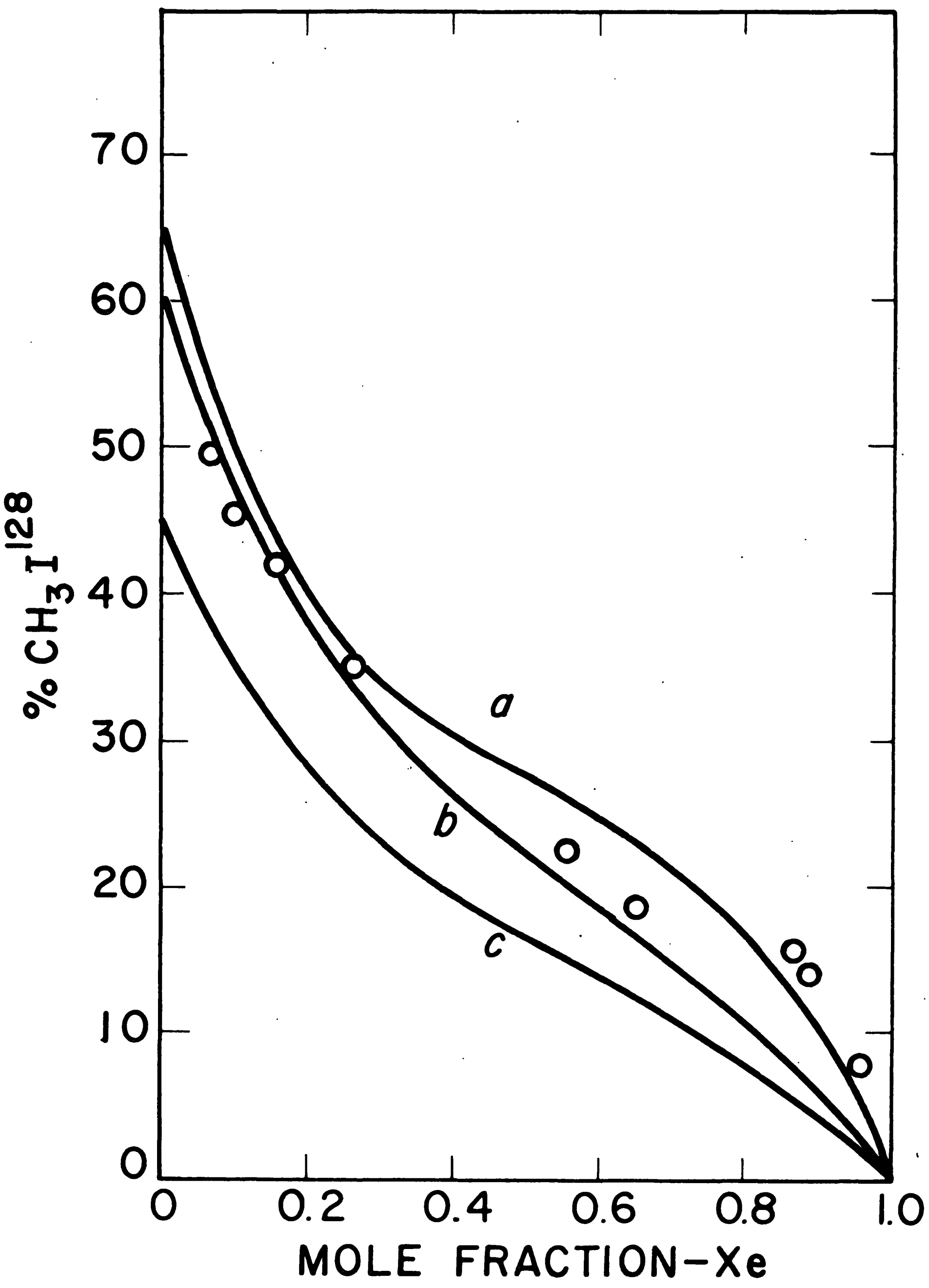

Figure 31. Effect of Xenon on the yield of CH_3I^{128}. (a) $I^+(^1D_2) + CH_4$ and $I^+(^1D_2)$ + Xe charge transfer, (b) $I + CH_4^+$, (c) $I(^2P_{3/2}) + CH_4$.

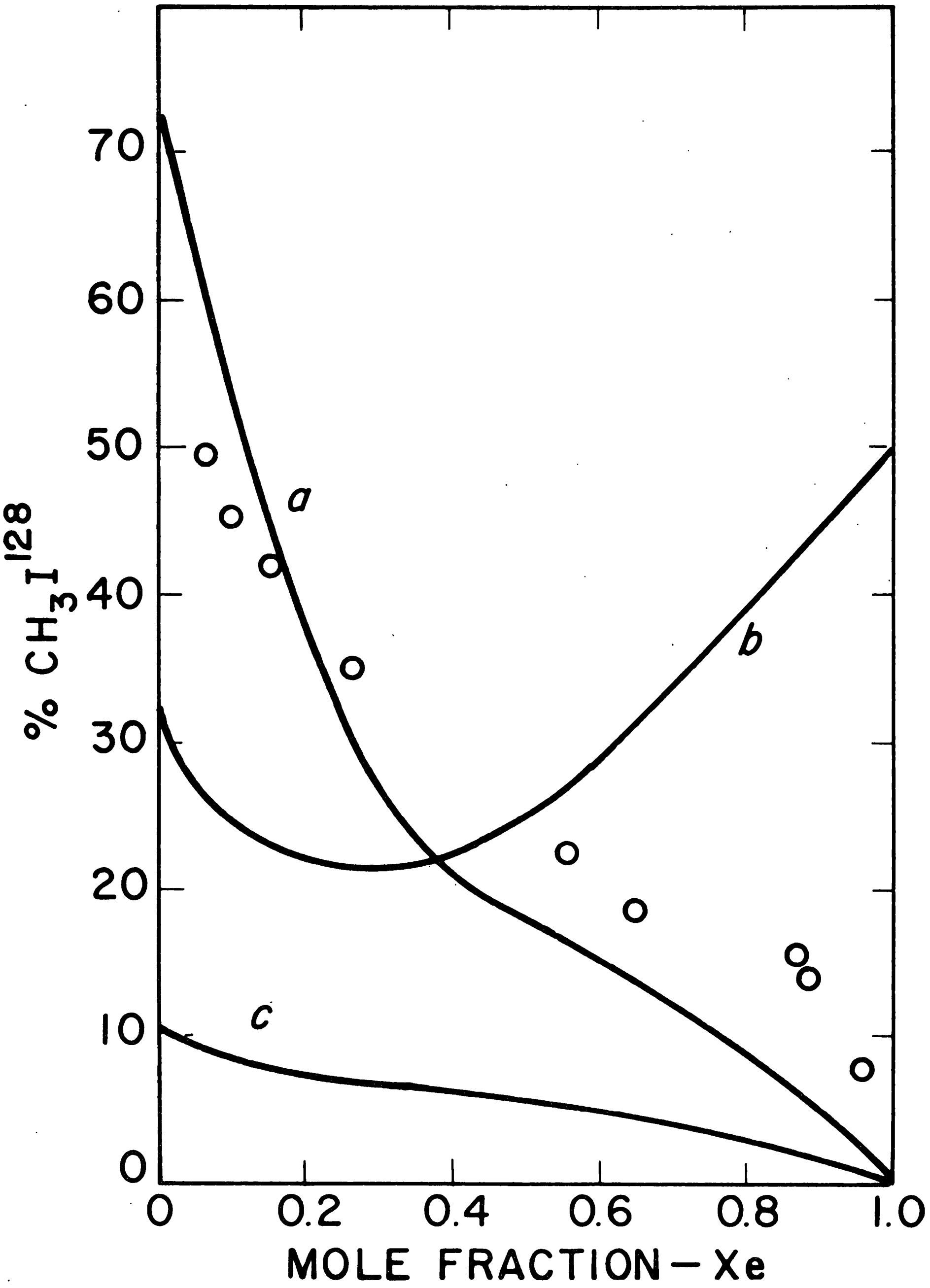

Figure 32. Effect of Xenon on the yield of CH_3I^{128}. (a) $I^+(^3P_1, ^3P_0) + CH_4$, (b) $I(^1S_{1/2})$ and $I^+(^3P_2) + CH_4$, (c) $I(^4P_{5/2}, ^4P_{3/2}, ^4P_{1/2}) + CH_4$.

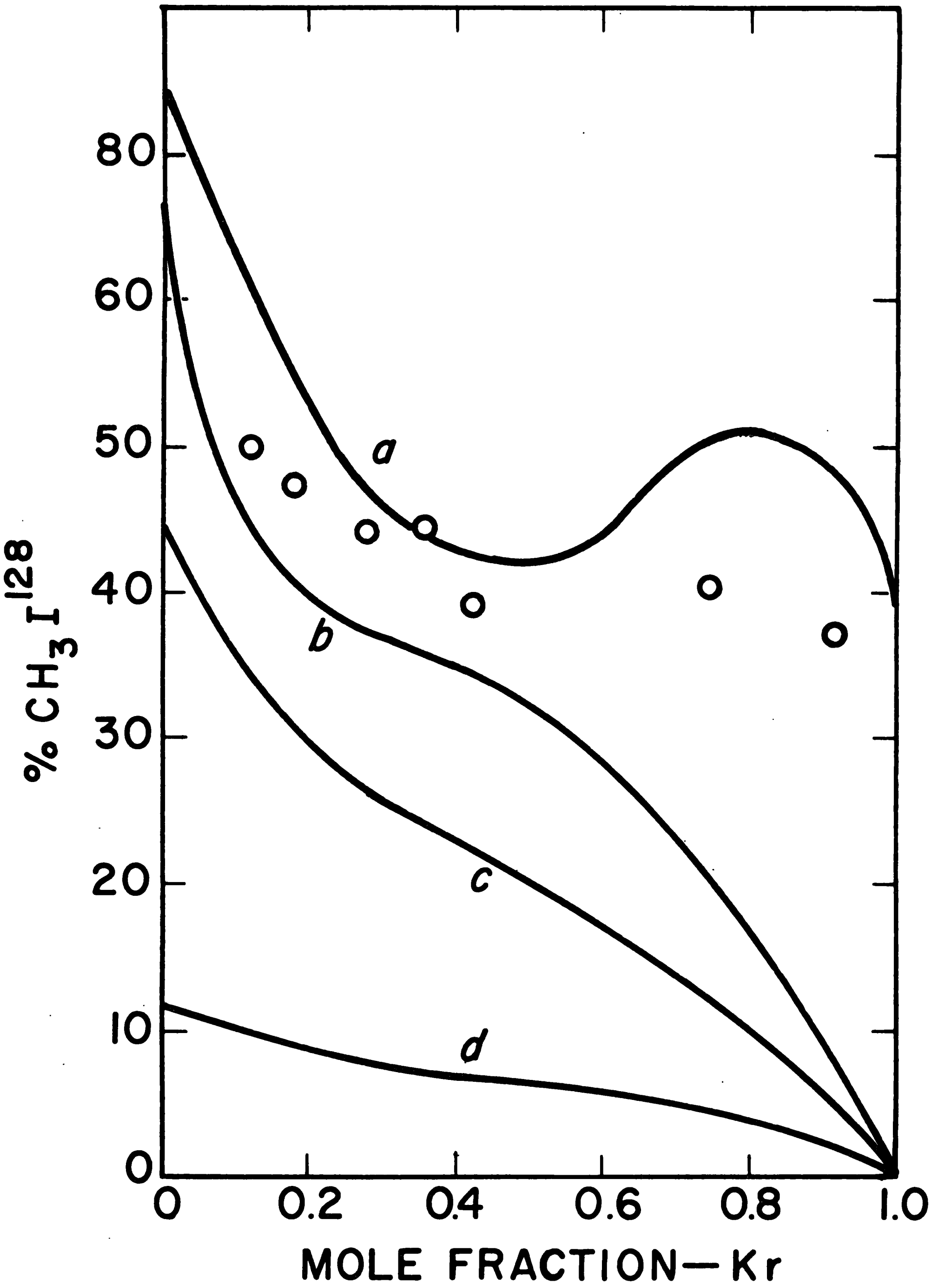

Figure 33. Effect of Krypton on the yield of CH_3I^{128}. (a) $I^+(^3P_1, ^3P_0) + CH_4$, (b) $I(^1S_{1/2})$ or $I^+(^3P_2) + CH_4$, (c) $I(^4P_{5/2}, ^4P_{3/2}, ^4P_{1/2}) + CH_4$, (d) $I(^2P_{3/2}) + CH_4$.

can strongly affect the calculated yield.

1. T + Hydrocarbons

These yields were calculated using the energy-degradation factors, steric factors, and reaction-energy limits listed in Table VIII. The steric factors were based on values derived from experimental data by Urch and Wolfgang[43]. The values were calculated according to the methods outlined in Chapter VI-H. These yields are listed in Table X.

2. Br^{80} + Hydrocarbons

For ground-state $Br(^2P_{3/2})$ atoms a CH_3Br yield of 6.2% is calculated. For ground-ionic state $Br^+(^3P_2)$ ions a yield of 45.0% is calculated. Excited ionic states of $^1D_2$ or greater should undergo charge-transfer with CH_4. The CH_3Br calculated yield is therefore (0.82)(6.2) + (0.18)(45.0) = 13.7%. The agreement with the experimental value[17], 13.3±0.5%, is remarkably good, although fortuitous.

Charge transfer can occur between ground-state Br^+ ions and C_2H_6. The calculated yields, therefore, were based on the reaction of ground-state Br atoms. The disagreement between experimental and calculated data in Table X could be due to an improper choice of the steric factor which was the same as that used in the tritium-ethane system.

3. I^{128} + Hydrocarbons

At least 50% of the I^{128} produced by (n,γ) activation is positively charged[9] and some of these I^{128} ions are in

Table X. Calculated and Experimental Yields in Non-Moderated Systems.

System	Product	Yield %		Reference
		Calc.	Exp.	
T + CH_4	CH_3T	41.6	36.0	22, 51, 53
	HT	58.4	$34^a, 56^b$	22
T + CD_4	CD_3T	33.0	30.6	51, 53
	DT	66.6	25-30	51
T + C_2H_6	C_2H_5T	30.3	27.5	54
	CH_3T	4.0	3.8	54
	HT	51.8	43.4	54
$Br(^2P_{3/2})+CH_4$	CH_3Br	6.2	13.3	17
$Br^+(^3P_2)+CH_4$	CH_3Br^+	45.0		
$Br(^2P_{3/2})+CH_4$	C_2H_5Br	12.3	4.0	11
	CH_3Br	1.9	5.6	11
$I(^2P_{3/2})+CH_4$	CH_3I	11.7	54.4	14
$I(^4P_{5/2})$, $I(^4P_{3/2})$, $I(^4P_{1/2})+CH_4$	CH_3I	45.7		
$I(^2S_{1/2})+CH_4$	CH_3I	60.5		
$I^+(^3P_2)+CH_4$	CH_3I^+	60.5		
$I^+(^3P_1)$, $I^+(^3P_0)$ $+CH_4$	CH_3I^+	64.8		
$I(^2P_{3/2})+CD_4$	CD_3I	12.7	52.3	52
$I^+(^3P_2)+CD_4$	CD_3I^+	59.7		
$I(^2P_{3/2})+C_2H_6$	C_2H_5I	4.4	1.0	11, 55
$I^+(^3P_2)+C_2H_6$	$C_2H_5I^+$	0.0		
$I(^2P_{3/2})+C_2H_6$	CH_3I	0.8	0.4	11, 55
$I^+(^3P_2)+C_2H_6$	CH_3I^+	1.3		
$I(^2P_{3/2})+C_3H_8$	$n-C_3H_7I$	0.3	0.3	11
	$i-C_3H_7I$	0.0	0.5	11
	C_2H_5I	0.4	0.4	11
	CH_3I	0.5	0.5	11

[a] With I_2 scavenger

[b] Without scavenger

excited electronic states[14,55]. CH_3I^{128} yields were calculated for ground-state ($^2P_{3/2}$) iodine atoms, slightly excited ($^4P_{5/2}$), ($^4P_{3/2}$), and ($^4P_{1/2}$) iodine atoms, highly excited ($^2S_{1/2}$) iodine atoms, ground-state ($^3P_2$) iodine ions, and slightly excited ($^3P_1$) and ($^3P_0$) iodine ions. Because the relative abundance of these various species as well as $I^+(^1D_2)$ ions is not known, it is impossible to calculate an average or overall expected CH_3I yield.

In the case of the $I^{128} + C_2H_6$ reaction, I^+ ions in the $^1D_2$, or higher, state will undergo charge transfer with C_2H_6. Yields of C_2H_5I and CH_3I were calculated for ground-state iodine atoms and ions. Although it is not possible to calculate the individual yields, it is interesting to note that the orders-of-magnitude of the various calculated yields are in reasonable agreement with experiment. Similar order-of-magnitude agreement exists for the one $I + C_3H_8$ reaction calculated.

4. T + Fluoromethanes

The steric factors used in the calculations of the tritium + fluoromethane yields was based on the geometry of the interacting pairs and is given in Table VIII. An effective energy-degradation factor, r_e, was used. The lower energy limit was based on activation energies of 1.6 ev for replacement and 0.56 ev for abstraction reactions. The calculated yields, Table XI, do not agree in all cases precisely with the experimental data of Odum and Wolfgang[45]. The discrepancy could be due partially, if not completely,

Table XI. Calculated and Experimental Yields in Tritium-Fluorocarbon Systems.

Reactant	Product	Percent Yield		Corrected Values	
		Exp.	Calc.	s	%yield
CH_3F	CH_2FT	12.7	8.5	0.29	12.8
	CH_3T	5.3	2.1		
CH_2F_2	CHF_2T	5.3	3.0	0.17	5.8
	CH_2FT	1.6	2.0		
CHF_3	CF_3T	2.9	1.6	0.08	2.7
	CHF_2T	0.7	1.4		
CF_4	CF_3T	0.3	0.4		

to an improper choice of the steric factor. It may be that, in some cases, the inertial effect proposed by Odum and Wolfgang[45] contributes markedly to the effective steric factor. In the case of tritium replacement and abstraction of fluorine in fluoromethanes such an inertial effect may not be important in the calculation of s since the mass of fluorine and the radical attached to the fluorine are both much greater than the mass of the tritum atom. This would not be the case when the tritium atom abstracts or replaces a hydrogen atom in a fluoromethane.

Experiments[22] indicate that the tritium shows very little bias in the abstraction or replacement of hydrogen in CH_4 although the calculated steric factors, Table VIII, indicate $s_{CH_3T}/s_{HT} = 0.59$. To correct partially for such inertial effect, the average value of the geometric steric factors for hydrogen displacement and abstraction reactions was used as the steric factor for hydrogen replacement and is listed in Table XI. These corrected data agree remarkably well with the experimental data. The agreement is undoubtedly fortuitous.

E. Simplification of the Model

1. Estrup and Wolfgang Model[22]

Estrup and Wolfgang[22] derived an expression which can be used to describe the inert-gas moderation of hot-atom reactions. By neglecting higher-order terms, they have reduced their expression to a usable form. Using the same notation as in this dissertation, their equation is:

$$Y_{Ai} = \frac{g_A}{\alpha} I_i - \left[\frac{g_A}{\alpha}\right]^2 K_i \, , \tag{130}$$

where

$$\alpha = \sum_i g_i \alpha_i \, , \tag{131}$$

$$\alpha_i = 1 + \left[\frac{M_i - m_N}{M_i m_N}\right] \ln r_i \, , \tag{132}$$

$$I_i = s_i \int_{E^y}^{\frac{E^b}{r}} \frac{F_i(E)}{E} \, dE \, , \tag{133}$$

$$K_i = s_i^2 \int_{E^y}^{\frac{E^b}{r}} \frac{F_i(E)}{E} \left\{ \int_{E}^{\frac{E^b}{r}} \frac{F_i(E)}{E} \, dE \right\} dE \, . \tag{134}$$

2. The Proposed Model

An expression similar to Eq. (130) can be obtained by expanding the distribution function, Eq. (96), in the form of a Taylor's series. For $E^\circ > E$

$$\frac{n(E^\circ,E)}{\ell} = \frac{a+b}{E}\left[1 + (a+b-1)\left(\frac{E^\circ-E}{E}\right) + \frac{(a+b-1)(a+b-2)}{2!}\left(\frac{E^\circ-E}{E}\right)^2 + \ldots\right]. \quad (135)$$

According to the definition of R, Eq. (101), where only A is reactive,

$$\langle R_i\rangle_{Av} = g_A\,(a+b)\left[J_{1i} + (a+b-1)(J_{2i} - J_{1i}) + \frac{(a+b-1)(a+b-2)}{2!}(J_{3i} - 2J_{2i} + J_{1i}) + \ldots\ldots\right], \quad (136)$$

where

$$J_{ni} = \frac{\displaystyle\int_{E^y}^{\frac{E^a}{r}} (E^\circ)^{n-1}\,\frac{dP(E^\circ)}{dE^\circ}\,dE^\circ \int_{E^y}^{\frac{E^b}{r}} \frac{F_i(E)}{E^n}\,dE}{\displaystyle\int_{E^y}^{\frac{E^a}{r}} \frac{dP(E^\circ)}{dE^\circ}\,dE^\circ}. \quad (137)$$

If dP(E°)/dE° is a constant, as is the case for T produced by the $He^3(n,p)\,T$ reaction, then

$$J_{ni} = \frac{\left(\frac{E^a}{r}\right)^n - \left(E^y\right)^n}{n\left(\frac{E^a}{r} - E^y\right)} \int_{E^y}^{\frac{E^b}{r}} \frac{F_i(E)}{E^n}\,dE\,. \quad (138)$$

For $n = 1$,

$$J_{1i} = \int_{E^y}^{\frac{E^b}{r}} \frac{F_i(E)}{E}\,dE = \frac{I_i}{S_i}. \quad (139)$$

J_{2i} differs slightly from the constant, K_i, Eq. (134)

$$J_{2i} = \frac{1}{2}\left(\frac{E^a}{r} + E^y\right) \int_{E^y}^{\frac{E^b}{r}} \frac{F_i(E)}{E^2} \, dE . \tag{140}$$

Using the formulas for F(E) in Table VI, it is found that

$$J_{1i} = \ln \frac{E^b}{E^y} = \frac{I_i}{s_i} \tag{141}$$

and

$$J_{2i} = \frac{E^b - E^y}{2E^b E^y} (1 + r) \times \frac{1}{2}\left(\frac{E^a}{r} + E^y\right) . \tag{142}$$

Thus, J_{1i} values can be calculated and compared with experimental data for I_i.

3. T + CH_4 and T + CD_4

The ratio of I values for T + CH_4 and T + CD_4 reactions can be calculated unambiguously since the steric factors cancel.

$$\frac{(J_1)_{CH_3T}}{(J_1)_{CD_3T}} = \frac{I_{CH_3T}}{I_{CD_3T}} = 0.967$$

Cross and Wolfgang[51], using the Estrup-Wolfgang model, found this ratio to be 1.00 ± 0.13. The agreement between theory and experiment is excellent.

The calculated value of I_{CH_3T} is $I_{CH_3T} = s_{CH_3T} \ln\frac{5.23}{2.73} = 0.653\, s_{CH_3T}$. If $s_{CH_3T} = 0.5$, $I_{CH_3T} = 0.327$.

Similarly, $I_{CD_3T} = s_{CD_3T} \ln \frac{5.08}{2.58} = 0.677\ s_{CD_3T}$. If $s_{CD_3T} = 0.5$, $I_{CD_3T} = 0.339$.

The experimental values of I will depend on the choice of M_i in Eq. (132). Estrup and Wolfgang[22] and Cross and Wolfgang[51] use $M_{CH_4} = 16$ and $M_{CD_4} = 20$. On this basis they obtain[51] $I_{CH_3T} = I_{CD_3T} = 0.28 \pm 0.04$. If a value of r_T = 1.2Å is used rather than r_T = 0.53Å (see Appendix I-E), then [53], $I_{CH_3T} = 0.38$ and $I_{CD_3T} = 0.375$. It is suggested in this dissertation that, because of the relative sizes of T and CH_4 or CD_4, an effective energy-degradation factor, r_e, should be used. The value of r_e used in this dissertation is the same value that would be obtained for r if $M_{CH_4} = 11.5$ and $M_{CD_4} = 6.8$ were used[a]. Using these values for M_i, and plottong the experimental data[22,51] according to Eq. (130) using r_T = 1.2Å, it is found that $I_{CH_3T} = 0.38$ and $I_{CD_3T} = 0.40$.

Considering the various uncertainties in these calculations, and particularly in the choice of the steric factor, the agreement between theory and experiment is remarkably good.

4. $Br^{80} + CH_4$

Rack and Gordus[17], using the Estrup and Wolfgang[22] model, Eq. (130), determined $I_{CH_3Br} = 0.057 \pm 0.005$ for the $Br^{80} + CH_4$ reaction. If the reaction involves ground-

---

[a] It may appear surprising that the "effective mass" of CD_4 is less than that of CH_4. This results from the fact that T+H collisions are less effective for energy degradation than T+D collisions. Thus the T+D collisions contribute more to $(r_e)_{CD_3T}$ than do T+H collisions to $(r_e)_{CH_3T}$.

state Br^{80} atoms, then $I_{CH_3Br} = s_{CH_3Br}\ \ln\frac{15.2}{13.5} = 0.120\ s_{CH_3Br}$. If $s_{CH_3Br} = 0.5$, as was arbitrarily chosen (Table VIII), then $I_{CH_3Br} = 0.060$ in agreement with experiment.

5. $I^{128} + CH_4$

Only 18%/54.4% of the total 54.4% yield of CH_3I^{128}, in the reaction, $I^{128} + CH_4$, appears to involve a reaction requiring hot iodine[14,55]. For this 18% yield, it was found[14], using Eq. (130), that $I_{CH_3I} = 0.06 \pm 0.01$. If 18/54.4 of the total I^{128} produced by the (n,γ) reaction reacted by a hot reaction and if the remainder $1 - (18/54.4)$, reacted by processes which does not necessarily require excess kinetic energy, then the yields used in the determination of I_{CH_3I} are too low. The corrected value is $I_{CH_3I} = (0.06 \pm 0.01)(54.4/18) = 0.18 \pm 0.03$. For ground-state I^{128}, $I_{CH_3I} = s_{CH_3I}\ \ln\frac{21.1}{15.0} = 0.34\ s_{CH_3I}$. If $s_{CH_3I} = 0.50$ as was arbitrarily chosen (Table VIII), then $I_{CH_3I} = 0.17 = 0.17$ in excellent agreement with experiment.

6. $I^{128} + CHF_3$

For the reaction $I^{128} + CHF_3$, $E^b = 6.74$ and $E^y = 6.12$ if the products are $CF_3I + H$. The reaction will not take place by the process $I + CHF_3 \rightarrow CHF_2I + F$ since $E^b = 6.74$ is smaller than $E^y = 10.0$ ev. Thus, $I_{CF_3I} = s_{CF_3I}\ \ln\frac{6.74}{6.12} = 0.094\ s_{CF_3I}$. If $s_{CF_3I} = 0.5$, $I_{CF_3I} = 0.047$. Rack[52] determined that $I = 0.053 \pm 0.015$.

7. Inorganic Yields

It should be noted that when $\frac{E^a - E^y}{E^y} > 1.0$, the Taylor's series, Eq. (135) becomes divergent and it is not possible to approximate the series by only the first few terms. For all inorganic products given in Table VIII, $(E^a - E^y)/E^y > 1.0$. Thus, Eq. (136) and probably also Eq. (130) are not valid for describing the inorganic yield. This is undoubtedly the reason Estrup and Wolfgang[22] found that Eq. (130) does not apply to the HT yield in the T + CH_4 reaction.

F. Concluding Remarks

It has been shown that values of R for any product can be easily calculated. The calculation of the yield, Y, is much more uncertain because of the lack of knowledge of the steric factors. It was shown, however, that, in the hot tritium reactions, the geometrical steric factor, calculated using covalent bond radii, results in calculated values of Y which, surprisingly, are in reasonable agreement with experimental data.

Using experimental hot-atom data, this model could be used in a semi-empirical manner to calculate steric factors. For example, as noted in Section C of this chapter, s_{CH_3T} was found to be equal to 0.58 using the CH_3T yields of I_2 scavenged T + CH_4 systems. When atomic-beam techniques become perfected it should be possible to measure the steric factors directly and also determine the reaction-energy limits, E^b and E^y.

In Section E of this chapter experimental values of I, determined using the Estrup and Wolfgang equation[22], were compared with values of I calculated using the model presented in this dissertation. The fact that: (1) the Estrup and Wolfgang value of $I_i = s_iJ_{1_i}$ and ; (2) the calculated values of $s_iJ_{1_i}$ agree very well with experimental values of I_i, both indicate that these two models are similar. This is to be expected since both models are based on the same reaction mechanisms and are both derived in terms of the neutron cooling-down model. The present model, however, has greater applicability since there is provided a means of calculating: (1) the energy ranges, (2) the values of s_i, (3) the effective values of r, (4) the values of $I_i = s_iJ_{1_i}$, and, (5) the values of R_j and therefore Y_j for any product in (a) pure systems, (b) inert-gas moderated systems and (c) systems consisting of more than one reactive species.

Appendix I. PHYSICAL CONSTANTS USED IN THE CALCULATIONS

A. Structural Constants

In calculating the effects of momentum transfer to an atom in a molecule, Chapter II, it is necessary to use a number of molecular structural constants. These data were obtained from the book, Tables of Interatomic Distances by Sutton[56] and are listed in Table XII. In this table, the halogen, X, bonded to the carbon is listed in the column of C-X bond distances. Those data which were estimated are indicated by an asterisk.

B. Force Constants

A set of force constants for a molecule, though internally consistent, may differ appreciably from other sets of force constants for the same molecule. Since the force constants were used on a comparison basis to determine the extent of vibrational and rotational excitation energy received by a molecule, efforts were made to ensure internal consistency of data. Most of these data were from the series of articles on substituted methanes by F. F. Cleveland, et. al. and are listed in Table XIII.

The notations used in the table are defined as follows:

k with one subscript is the stretching-force constant

k with two subscripts is the bending-force constant

i refers to the C-I bond

b refers to the C-Br bond

c refers to the C-Cl bond

Table XII. Structural Constants of Molecules

Molecules	Bond Distances, Å			Bond Angles
	C-H	C-X	C-C	
CH_4	1.091			
C_2H_6	1.102		1.543	$\angle \mathrm{HCH}=109.3^\circ$
C_3H_8	1.09		1.54±0.02	$\angle \mathrm{CCC}=111.5^\circ \pm 3^\circ$
CH_3I	1.11±0.01	2.139 (I)		$\angle \mathrm{HCH}=111.4^\circ \pm 0.05^\circ$
CD_3I	1.10 (D)	2.139 (I)		$\angle \mathrm{DCD}=111.6^\circ$
CF_3I		1.332 (F) 2.126±0.024(I)		$\angle \mathrm{FCF}=107.5^\circ \pm 1.5^\circ$
CH_2I_2		2.12±0.04(I)		$\angle \mathrm{ICI}=114.7^\circ$
C_2H_5I *	1.103	2.18±0.05(I)	1.154	$\angle \mathrm{CCI}=110^\circ$ $\angle \mathrm{CCH}=109.5^\circ$ $\angle \mathrm{HCH}=109.5^\circ$
n-C_3H_7I *	1.09	2.12 (I)	1.54	all angles=109.5°
i-C_3H_7I *	1.09	2.12 (I)	1.54	all angles=110.5°
CH_3Br	1.11±0.01	1.939		$\angle \mathrm{HCH}=111.2^\circ \pm 0.5^\circ$
CD_3Br	1.10 (D)	1.939		$\angle \mathrm{HCH}=111.4^\circ$
CF_3Br		1.908±0.018(Br) 1.330±0.005(F)		$\angle \mathrm{FCF}=108^\circ \pm 1^\circ$
CCl_3Br		1.936(Br) 1.764(Cl)		$\angle \mathrm{ClCCl}=111.2^\circ$
CH_2Br_2	1.093	1.907(Br)		$\angle \mathrm{HCH}=109.5^\circ$ $\angle \mathrm{BrCBr}=112^\circ$
CF_2Br_2 *		1.91(Br) 1.35(F)		$\angle \mathrm{BrCBr}=114^\circ$ $\angle \mathrm{FCF}=108^\circ$ $\angle \mathrm{BrCF}=110^\circ$
CCl_2Br_2		1.93(Br) 1.75(Cl)		all angles=109.5°
$CHBr_3$	1.068±0.010	1.930±0.003(Br)		$\angle \mathrm{BrCBr}=110.8\pm 0.3^\circ$
CBr_4		1.942±0.003(Br)		

Table XII. (con't.)

Molecules	Bond Distances Å			Bond Angles
	C-H	C-X	C-C	
C_2H_5Br	1.09	1.91±0.02(Br)	1.54	∠HCH=109.5°
				∠CCH=109.5°
				∠CCBr=110°
1,1-$C_2H_4Br_2$	1.09	1.90(Br)	1.54	∠BrCBr=113°±1°
				∠CCBr= 114°±1.5°
				∠CCH=109.5°*
CH_3Cl	1.11±0.01	1.781±0.005(Cl)		∠HCH=110.5°±0.5°
CD_3Cl	1.10(D)	1.781(Cl)		∠DCD=110.7°
CF_3Cl		1.751±0.004(Cl)		∠FCF=108.6°±0.4°
		1.328±0.002(F)		
CH_2Cl_2	1.068±0.005	1.7724±0.0005(Cl)		∠HCH=112.0°±0.3
				∠ClCCl=111.8°
CF_2Cl_2		1.74±0.03(Cl)		∠FCF=108°±2°
		1.35±0.03(F)		∠ClCCl=113°±2°
				∠FCCl=110°±2°
$CHCl_3$	1.073	1.767(Cl)		∠ClCCl=110.4°
$CFCl_3$		1.76±0.02(Cl)		∠ClCCl=113°±3°
		1.44±0.04(F)		
CCl_4	1.766±0.003			
CHF_2Cl	1.06	1.73±0.03(Cl)		∠FCF=110.5°±1°
		1.36±0.03(F)		∠ClCF=110.5±1°

* These data are estimated.

Table XIII. Force Constants for Individual Molecules

Molecules	Force Constants, md/Å		Reference
CH_3I or CD_3I	k_i	2.24	57
	k_h	5.05	
	k_{hh}	0.442	
	k_{ih}	0.463	
CF_3I	k_f	6.246	58
	k_i	2.289	
	k_{if}	0.183	
	k_{ff}	1.213	
CH_2I_2	k_i	2.2333	59
	k_h	4.9688	
	k_{hh}	0.458	
	k_{ii}	0.222	
	k_{hi}	0.242	
CH_3Br or CD_3Br	k_b	2.8631	60
	k_h	5.1199	
	k_{hh}	0.448	
	k_{bh}	0.301	
CF_3Br	k_f	6.2460	58
	k_h	3.0352	
	k_{bf}	0.292	
	k_{ff}	1.213	
CCl_3Br	k_b	2.8976	61
	k_c	3.4580	
	k_{cc}	0.37094	
	k_{bc}	0.41617	

Table XIII (con't.)

Molecules	Force Constants, md/Å		Reference
CH_2Br_2	k_h	5.0455	62
	k_b	2.8965	
	k_{bb}	0.298	
	k_{hb}	0.285	
	k_{hh}	0.516	
CF_2Br_2	k_f	6.1400	63
	k_b	2.9132	
	k_{ff}	0.871	
	k_{bf}	0.463	
	k_{bb}	0.279	
CCl_2Br_2	k_b	2.7530	64
	k_c	3.3713	
	k_{cc}	0.371	
	k_{bb}	0.333	
	k_{bc}	0.337	
$CHBr_3$	k_b	2.8976	65
	k_h	4.8828	
	k_{bb}	0.333	
	k_{bh}	0.288	
CBr_4	k_b	2.8976	65
	k_{bb}	0.29473	
CH_3Cl or CD_3Cl	k_c	3.37	66
	k_h	5.01	
	k_{ch}	0.354	
	k_{hh}	0.448	

Table XIII. (con't.)

Molecules	Force Constants, md/Å		Reference
CF_3Cl	k_f	6.25	67
	k_c	3.46	
	k_{ff}	1.22	
	k_{cf}	0.652	
$CHCl_3$	k_h	4.8002	61
	k_c	3.4580	
	k_{cc}	0.37094	
	k_{ch}	0.29046	
$CFCl_3$	k_f	4.9447	61
	k_c	3.4580	
	k_{cc}	0.37094	
	k_{cf}	0.52922	
CCl_4	k_c	3.4580	61
	k_{cc}	0.39512	
CHF_2Cl	k_c	3.5910	68
	k_f	6.2925	
	k_h	5.0300	
	k_{cf}	0.470	
	k_{ch}	0.318	
	k_{ff}	0.745	
	k_{fh}	0.521	

h refers to the C-H bond

f refers to the C-F bond

For example, k_f is the stretching-force constant of a C-F bond and k_{bh} is the bending force constant between C-H and C-Br bonds.

Listed in Table XIV are force constants for various other bonds.

C. Bond-Dissociation Energy

The bond-dissociation energy is defined as the energy required to dissociate a molecule into two radicals. This definition differs from the definition of bond energy which is based on the total dissociation of a molecule. For the processes discussed in this thesis the bond-dissociation energy rather than the bond-energy is required. Unfortunately, bond-dissociation energy data are not as plentiful as bond-energy data and, in some cases, it was necessary to estimate the data. Given in Table XV are the bond-dissociation energies used in the calculations.

The bond-dissociation energy for an ionized molecule was calculated according to the following thermodynamic cycle:

$$\begin{tikzcd} AB^+ \arrow[r, "D_{AB^+}"] \arrow[d, "-IP(AB)"] & A + B^+ \arrow[d, "IP(B)"] \\ AB \arrow[r, "D_{AB}"'] & A + B \end{tikzcd}$$

Thus,

$$D_{AB^+} = D_{AB} + IP(B) - IP(AB)$$

Table XIV. Force Constants for Group Motions

	Bond	$\frac{\text{mdynes}}{\text{Å}}$	References
Stretching Force Constants	$k(CH_3\text{-}H)$	4.8	69
	$k(CH_2\text{-}H)$	4.5	69
	$k(CH\text{-}H)$	4.2	69
	$k(C\text{-}H)$	3.9	69
	$k(C\text{-}CH_3)$	3.44	70
	$k(CH_2\text{-}CH_2)$	4.00	70,71
	$k(CH_2\text{-}Cl)$	2.90	70,71
	$k(CH_2\text{-}Br)$	2.40	70,71
Bending Force Constants	$k(CH_3\text{-}CH_2\text{-}CH_3)$	0.20	71
	$k(CH_3\text{-}C\text{-}CH_3)$	0.20	69
	$k(C\text{-}CH_2\text{-}CH_3)$	0.20	70
	$k(C\text{-}C\text{-}H)$	0.15	69,72
	$k(H\text{-}C\text{-}H)$	0.40	69,72
	$k(C\text{-}CH_2\text{-}Cl)$	0.17	70
	$k(C\text{-}CH_2\text{-}Br)$	0.10	70
	$k(Cl\text{-}CH_2\text{-}Cl)$	0.13	71
	$k(Br\text{-}CH_2\text{-}Br)$	0.10	71
	$k(Cl\text{-}C\text{-}Cl)$	0.10	69
	$k(Br\text{-}C\text{-}Br)$	0.05	69
	$k(F\text{-}C\text{-}F)$	0.15	69
	$k(H\text{-}C\text{-}F)$	0.06	72,73
	$k(H\text{-}C\text{-}Cl)$	0.05	72,73
	$k(H\text{-}C\text{-}Br)$	0.04	72,73
	$k(H\text{-}C\text{-}I)$	0.04	72,73

Table XV. Bond Dissociation Energies

Molecule	Bond Dissociation Energy, ev	Reference
CH_3-H	4.42	74
C_2H_5-H	4.16	74
CH_3-CH_3	3.60	74
p-C_3H_7-H	4.30	74
s-C_3H_7-H	4.07	74
CH_3-C_2H_5	3.62	74
CH_3-I	2.34	74
CD_3-I	2.34	est
CF_3-I	2.10±0.2	78
CH_2I-I	2.03	est
C_2H_5-I	2.26	74
n-C_3H_7-I	2.17	74
i-C_3H_7-I	2.00	74
CH_3-Br	2.92	75
CD_3-Br	2.92	est
CF_3-Br	2.80	75
CCl_3-Br	2.12	75
CH_2Br-Br	2.59±0.15	76
CF_2Br-Br	2.60	est
CCl_2Br-Br	2.12	est
$CHBr_2$-Br	2.67±0.17	76
CBr_3-Br	2.12	75
C_2H_5-Br	2.82	75
1,1-C_2H_4Br-Br	2.70	est
CH_3-Cl	3.46	74
CD_3-Cl	3.46	est
CF_3-Cl	3.60	74
CH_2Cl-Cl	3.19±0.12	76
CF_2Cl-Cl	3.36	est
$CHCl_2$-Cl	2.89±0.12	76
$CFCl_2$-Cl	3.28±0.10	77
CCl_3-Cl	2.95	74
CHF_2-Cl	3.28	est
NO-O	3.12	79

D. Ionization Potentials

Listed in Table XVI are the ionization potentials used in the calculations. Many of the data were taken from the table compiled by Kiser[80]; the most recent value was chosen.

E. Collision Cross-Sections

The collision cross-section can be calculated, in principle, from the collision radii of the interacting particles.

$$\sigma_{ij} = \pi(r_i + r_j)^2$$

where σ_{ij} is the collision cross-section for an encounter between i and j and r_i and r_j are the collision radii.

The collision cross-section of non-rigid particles is a function of energy. If the interacting potential field takes the form of the Lennard-Jones potential, the energy dependence of the collision cross-section will be[41]

$$\frac{\sigma_1}{\sigma_2} = \left[\frac{E_2}{E_1}\right]^{\frac{1}{3}}$$

where σ_1 and σ_2 are the collision cross-sections of a given pair at energies E_1 and E_2, respectively.

The collision cross-sections are used in calculating the collisional probability of N in a mixture, A + B, according to the equation

$$g_A = \frac{X_A\sigma_{AN}}{X_A\sigma_{AN} + (1-X_A)\sigma_{BN}} = \frac{1}{1 + \frac{1-X_A}{X_A}\,\frac{\sigma_{BN}}{\sigma_{AN}}}$$

Table XVI. Ionization Potentials of Molecules and Radicals

Molecules	Ionization Potential, ev	References
CH_4	12.99	80
C_2H_6	11.65	80
C_3H_8	11.88	80
CH_3I	9.54	80
CD_3I	9.54	est
CF_3I	10.0	78
C_2H_5I	9.35	80
n-C_3H_7I	9.41	80
i-C_3H_7I	9.30	est
CH_3Br	10.54	80
CD_3Br	10.54	est
CF_3Br	11.82	80
CH_2Br_2	8.34	76
$CHBr_3$	8.10	76
C_2H_5Br	10.29	81
HBr	11.62	81
HI	10.38	81
CO_2	14.4	80
CO	14.1	80
NO_2 *	9.78	79
NO	9.25	81
I	10.454	84
Br	11.84	83
T	13.60	82
$CH_3\cdot$	9.95	85
$C_2H_5\cdot$	8.78	85
p-$C_3H_7\cdot$	8.68	85
s-$C_3H_7\cdot$	7.97	85
$CF_3\cdot$	10.2	85
$CCl_3\cdot$	8.28	77
$CH_2Br\cdot$	9.30	85
$CHBr_2\cdot$	8.13	80

* for linear molecule

where X_A is the mole fraction of A in a mixture of A and B containing only a trace of N. It should be noted that only the ratio of the collision cross-section appears in this calculation. Since the energy dependence of the collision cross section will be the same for both types of interactions,

$$\frac{(\sigma_{BN})_1}{(\sigma_{AN})_1} = \frac{(\sigma_{BN})_2}{(\sigma_{AN})_2}$$

and the ratio will remain constant with respect to energy. Hence, it is necessary to ascertain this ratio at only one energy and the obvious choice is to use a thermal-energy value since the most data are tabulated at this energy.

There exists in the literature two major types of cross-section data: those derived from the second virial coefficient and those obtained from transport properties. They are use in different areas of study and serve different purposes[86]. Since the collision cross-sections were used to calculate the collision probability, it is more appropriate to use data based on transport properties. Although such data are available for most common molecules, collision radii based on transport properties were not available for the hot atoms considered in this dissertation.

Given in Table XVII are atomic and molecular radii obtained from a variety of sources. It is seen that the van der Waal radii are in good agreement with viscosity data. On the other hand, radii determined from atomic volume measurements are consistently greater than the

Table XVII. Collision Radii of Atoms and Molecules

References	Collision Radii, Å						
	I	II	III	IV	V		VI
					a	b	
Xe	2.05	2.03	2.58	2.46		1.99	2.03
Kr	1.80	1.80	2.34	2.09		1.80	1.80
Ar	1.70	1.71	2.13	1.83		1.73	1.71
Ne	1.37	1.39	1.89	1.30		1.41	1.39
He	1.28		2.82	1.09			1.28
I			2.42		2.12		2.12
Br			2.12		1.95		1.95
T			1.71		1.2		1.2
$CH_3\cdot$					2.0		2.0
CH_4	1.92	1.94					1.94
CF_4	2.35						2.35
CCl_4		2.94					2.94
H_2	1.46						1.46
D_2	1.46						1.46
C_2H_6	1.98	2.21					2.21
C_3H_8	2.82	2.53					2.53

I refers to the 2nd virial coefficient[86].

II refers to viscosity coefficient[86].

III refers to atomic volume[87].

IV refers to viscosity coefficient, before 1939[90].

V refers to van der Waal radii, a[88], b[89].

VI refers to the value used.

radii based on viscosity coefficient data. Hence, the data chosen for use in the calculations in this dissertation, as indicated in Table XVII, were based on either viscosity coefficients, the 2nd virial coefficient, or the van der Waal radius.

It should be noted that Estrup and Wolfgang[22] have used a tritium collision radius of 0.53Å whereas 1.2Å is used here. The value of 1.2Å is internally consistent with the radii chosen for the other molecules and atoms. In addition, although of only minor importance, is the fact that collision radii used by Estrup and Wolfgang for inert gases was taken from a 1939 compilation by Chapman and Cowling[90]. These data are numerically greater than the more recent tabulations.

In calculating the geometric steric factors, an internally consistent set of radii must also be used. In this case the values were based principally on structural constants and are: T - 0.53[100], H or D in H_2 or D_2 - 0.37[87], H in CH_4, etc. - 0.32[87], C in CH_4, etc. - 0.77[87], F in fluoromethanes - 0.72[87], Br - 0.90[100], Br in bromomethanes - 1.14[87], I in iodomethanes - 1.33[87], Cl in chloromethanes - 0.99 Å [87].

Appendix II. USE OF THE RANDOM-WALK MODEL IN CASCADE-GAMMA EMISSION

In Chapter III it was suggested that the observed failure to bond-rupture following (n,γ) activation was due to partial cancellation of gamma-ray recoil momenta in cascade gamma emission[10,26,91-93]. The net recoil momentum imparted to the activated atom can be described by a random-walk model and the probability that the net recoil momentum exceeds a certain value, R, could be calculated using the equation[26,27].

$$P(R) = \frac{1}{2^n (n-2)! \prod_{i=1}^{n} \ell_i} \int_0^R \sum_{j=1}^{2^{n-1}} \left(M_j^{\,n-3} \left| M_j \right| - N_j^{\,n-3} \left| N_j \right| \right) R\,dR, \tag{143}$$

where

n is the total number of momenta randomly directed

ℓ_i is the magnitude of the momentum $\underline{i}$

$P(R)$ is the probability that the net momentum is $\leqslant R$

M_j is an algebraic sum of R, ℓ_1, ℓ_2, etc., with an odd number of total negative signs

N_j is an algebraic sum of R, ℓ_1, ℓ_2, etc., with an even number of total negative signs

If more than one cascade is possible, the probability, $P_k(R)$, for each cascade, k, can be calculated. If p_k is the fractional occurrence of a cascade, k, then

$$P(R) = \sum_{k=1}^{m} p_k P_k(R). \tag{144}$$

The only complex neutron capture-gamma spectrum for a halogen for which sufficient data are available is the for the $Cl^{35}(n,\gamma)Cl^{36}$ process[28,94,95]. The spectral data could be resolved into the 17 cascades given in Table XVIII. Using these data, the probability $P(E_\gamma)$ was calculated and plotted as a function of E_γ/E_{max} where $E_{max} = 8.55$ Mev. This curve is depicted in Fig. 34.

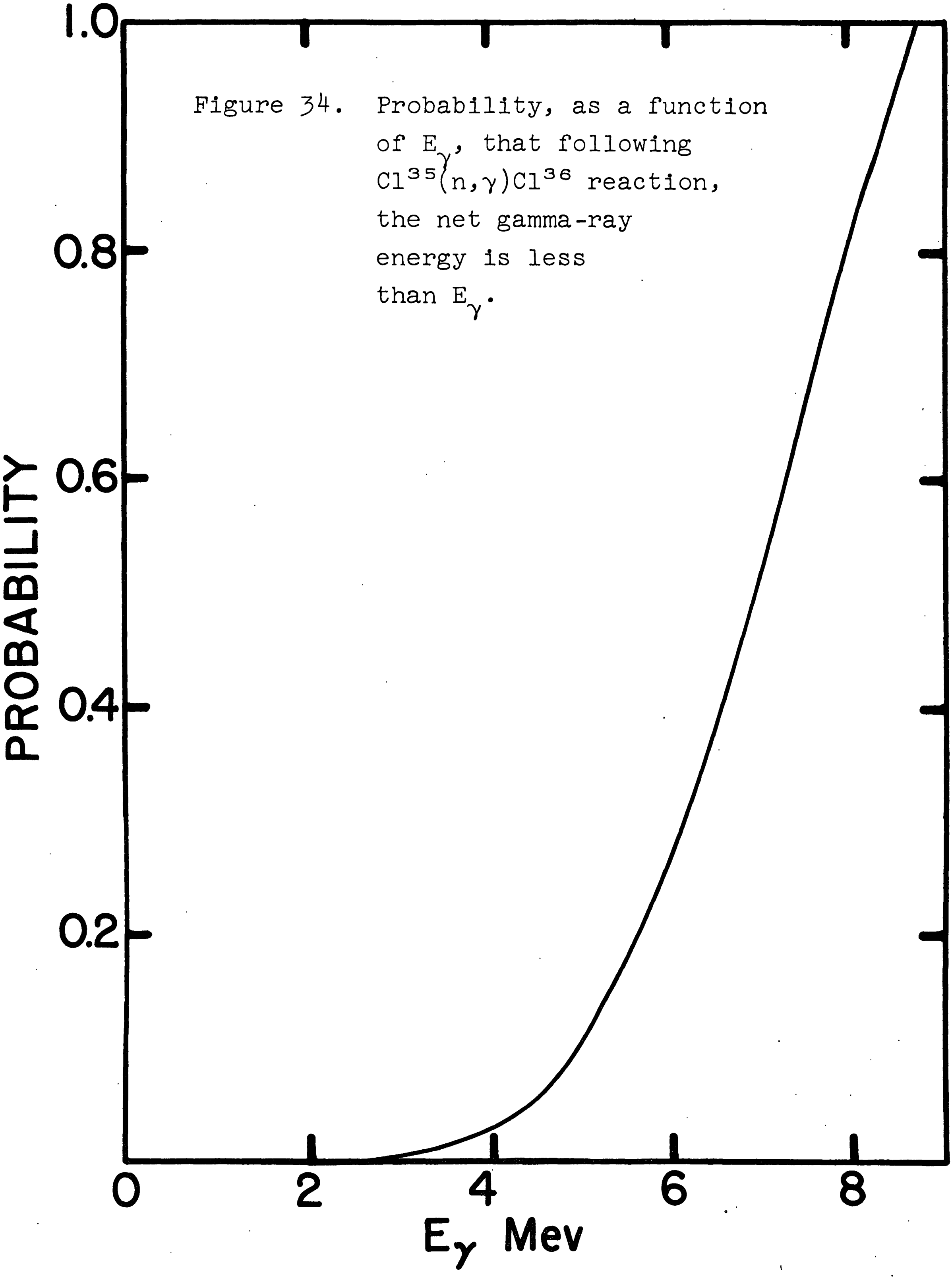

Figure 34. Probability, as a function of E_γ, that following $Cl^{35}(n,\gamma)Cl^{36}$ reaction, the net gamma-ray energy is less than E_γ.

Table XVIII. Gamma-Ray Cascades from $Cl^{35}(n,\gamma)Cl^{36}$

Energies, Mev					Occurrence, %
8.55					3.39
7.78	0.79				9.43
7.40	1.16				16.93
6.96	1.60				2.30
6.64	1.95				13.90
5.72	2.87				6.77
5.28	3.34				1.94
4.54	4.04				2.66
6.64	1.16	0.79			3.51
6.12	0.51	1.95			15.61
5.01	1.65	1.95			2.90
3.01	3.62	1.95			3.62
2.76	3.87	1.95			2.42
6.12	0.51	1.16	0.79		10.28
5.01	1.13	0.51	1.95		2.17
5.01	1.65	1.16	0.79		0.79
5.01	1.13	0.51	1.16	0.79	1.45

Appendix III. SAMPLE CALCULATIONS

A. Moments of Inertia from Structural Constants

For most molecules, the moments of inertia given in the literature are based on their principal axes. In the calculations presented in this dissertation the required moments of inertia are based on another set of coordinates where the z axis is always parallel to the bond which received most of the excitation from the recoil momentum. The calculation of the moments of inertia of C_2H_5Br is given here as an example. For simplicity, the methyl group is considered as a point with its mass concentrated at the center of mass of the methyl group.

1. Molecular Structural Data

The bond distances are: C-C = 1.54, C-H = 1.103, and C-Br = 1.938 Å. The bond angles are : ∠CCBr = 110°, ∠CCH = 109°28' for the methyl end, and ∠CCH = 110°48' for the CH_2Br end. The ∠HCH is estimated to be 109.5°.

2. Center of Mass of the Methyl Group

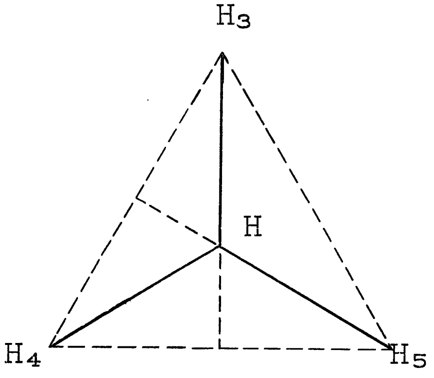

Top view of CH_3

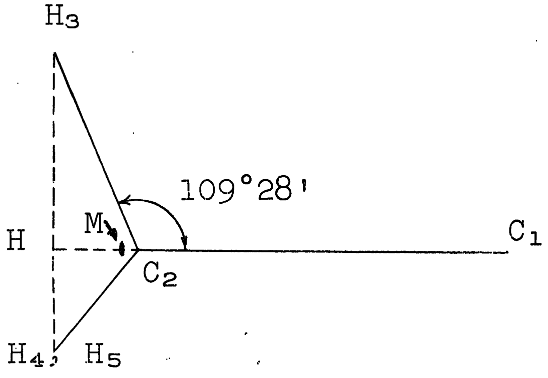

Side view of CH_3

Let M be the center of mass of the methyl group. The center of mass of the three hydrogen atoms, H_3, H_4, and H_5 is at H. The location of M can be calculated by the equation

$$3HM = 12C_2M = 12\ (C_2H - HM).$$

Thus,

$$HM = \tfrac{4}{5}C_2H.$$

But, $C_2H = C_2H_3 \cos\ (\pi - 109°28') = (1.103)(0.3333) = 0.3676 \text{Å}$

and HM = 0.2941Å.

Therefore $C_1M = 1.54 + 0.3676 - 0.2941 = 1.614\text{Å}$.

3. Coordinates of Each Atom or Group in the Molecule

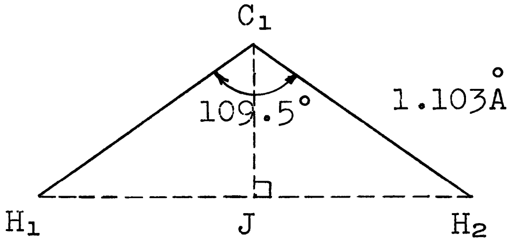

$$JH_1 = 1.103 \sin \frac{109.5°}{2} = 0.9007\text{Å}$$

$$C_1J = 1.103 \cos \frac{109.5°}{2} = 0.6366\text{Å}$$

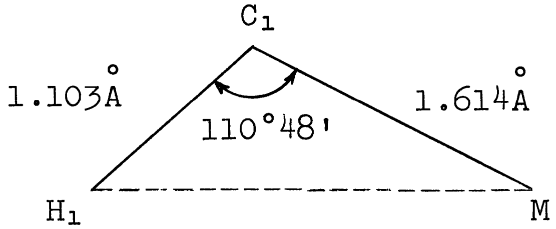

$H_1M = [1.103^2+1.614^2-(2)(1.103)(1.614)(\cos 110°48')]^{\frac{1}{2}} = 2.255\text{Å}$

The general representation of the molecule is:

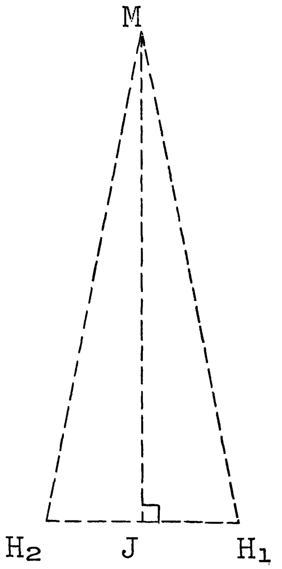

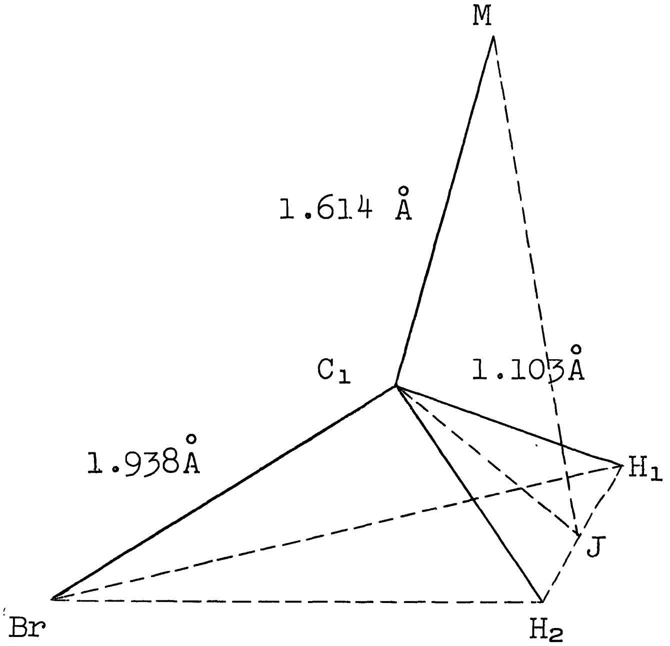

$$JM = (H_1M^2 - JH_1{}^2)^{\frac{1}{2}} = (2.255^2 - 0.9007^2)^{\frac{1}{2}} = 2.067\text{Å}$$

$$\cos\angle MC_1J = \frac{1.614^2 + 0.6366^2 - 2.067^2}{(2)(1.614)(0.6366)} = -0.6152$$

$\angle MC_1J = 127°58'$

The projected view on the x-z plane is as follows

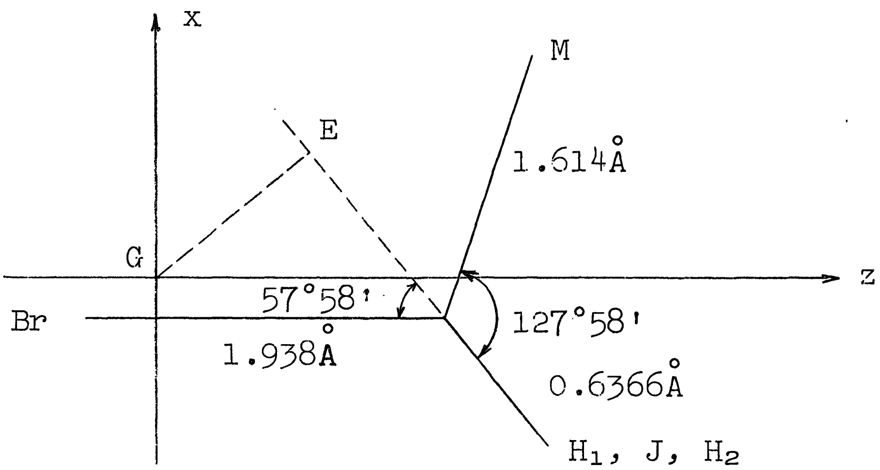

G is the center of mass of the molecule,

$$EG = \frac{(1.938)(80)(\sin 57°58') - (1.614)(15)(\sin 52°2')}{109} = 1.0307 \text{Å},$$

$$EC_1 = \frac{(1.938)(80)(\cos 57°58') + (1.614)(15)(\cos 52°2') - (2)(0.6366)}{109}$$

$$= 0.8793 \text{Å}.$$

The $\underline{z}$ coordinate of C_1 is $[+ C_1E \cos 57°58' + EG \sin 57°58']$

$$= +(0.8793)(0.5304)+(1.0307)(0.8477) = 1.3401 \text{Å}.$$

The $\underline{x}$ coordinate of C_1 is $[- C_1E \sin 57°58' + EG \cos 57°58']$

$$= -(0.8793)(0.8477) + (1.0307)(0.5304) = -0.1987 \text{Å}.$$

In a similar manner, the coordinates of the atoms are found to be:

H_1	(-0.7383, 0.9007, + 1.6778),
H_2	(-0.7383, -0.9007, + 1.6778),
C_1	(-0.1987, 0 , 1.3401),
Br	(-0.1987, 0 , -0.5979),
CH_3	(1.3175, 0 , +1.8919).

4. Moments of Inertia for C_2H_5Br

According to the definition,

$$I_{xx} = \sum_i m_i (y_i^2 + z_i^2),$$

$$I_{yy} = \sum_i m_i (x_i^2 + z_i^2),$$

$$I_{zz} = \sum_i m_i (x_i^2 + y_i^2).$$

Thus,

$$I_{xx} = (15)(1.8919^2)+(2)(1)(0.9007^2+1.6778^2)+(12)(1.3401^2) + (80)(0.5979^2) = 111.090 \text{ amu } \text{Å}^2.$$

Similarly,

$I_{yy} = 140.227$ amu Å^2,

$I_{zz} = 32.382$ amu Å^2.

The moments of inertia of other alkyl halides and alkanes are given in Table XIX.

B. Fraction of the Rotational Energy Deposited in Bond j

The calculation of f_j, the fraction of the rotational energy deposited in bond *j* can be determined using Eqs. (18) and (19). C_2H_5Br is again used as an example.

1. Vibrational Constants

The stretching vibrational constants are: C-Br=2.4×10^5, C-H=4.2×10^5, and C-CH_3=4.00×10^5 dynes/cm. The bending vibrational constants are: H-C-Br=0.04×10^5, C-C-Br=0.15×10^5, C-C-H=0.15×10^5, and H-C-H=0.40×10^5 dynes/cm.

For the C-Br bond

$k_{sj} = 2.4 \times 10^5$ dynes/cm,

$k_{bj} = \frac{1}{3}(0.04+0.04+0.15)\times10^5 = 0.077\times10^5$ dynes/cm.

The values of k_{sj} and k_{bj} for each bond is

	k_{sj}	k_{bj}
C-Br	2.4×10^5	0.077×10^5
C-H	4.2×10^5	0.197×10^5
C-CH_3	4.0×10^5	0.15×10^5

2. Distances from the Center of Gravity

The distance from the center of gravity, a_j, can be calculated from the equation: $a_j^2 = x_j^2 + y_j^2 + z_j^2$.

Table XIX. Moments of Inertia (in amu Å^2 units)

Molecule[a]	I_{xx}	I_{yy}	I_{zz}
CH_3I	67.3	67.3	3.37
CD_3I	83.7	83.7	6.73
CF_3I	336.4	336.4	88.0
CH_2I_2	585.9	836.5	253.9
C_2H_5I	152.2	182.7	33.7
i-C_3H_7I	266.0	229.5	67.7
n-C_3H_7I	252.3	371.1	122.0
CH_3Br	52.8	52.8	3.36
CD_3Br	65.6	65.6	6.70
CF_3Br	242.0	242.0	88.6
CCl_3Br	432.7	432.7	500.9
CH_2Br_2	282.0	417.8	139.0
CF_2Br_2	366.3	519.1	243.5
CCl_2Br_2	484.8	621.8	427.0
$CHBr_3$	769.0	410.4	448.4
$CHClBr_2$	383.8	540.2	295.0
CBr_4	804.5	804.5	804.5
C_2H_5Br	111.1	140.2	32.4
1,1-$C_2H_4Br_2$	320.8	480.0	194.5
CH_3Cl	38.1	38.1	3.33
CD_3Cl	47.8	47.8	6.66
CF_3Cl	157.7	157.7	88.4
CH_2Cl_2	115.1	172.6	60.5
CF_2Cl_2	176.5	236.3	201.6
$CFCl_3$	306.3	219.9	219.3
$CHCl_3$	290.9	162.4	170.4
CHF_2Cl	144.9	107.0	57.1
CCl_4	302.7	302.7	302.7
CH_3T	5.30	5.30	3.17
C_2H_5T	9.08	27.81	23.38
n-C_3H_7T	11.87	45.52	36.90
i-C_3H_7T	59.54	14.79	62.6
CH_4	3.72	3.72	3.72

---

[a] The dissociating element is the last atom listed in the formula.

Thus:

$$a_{Br} = (0.1987^2 + 0^2 + 0.5979^2)^{\frac{1}{2}} = 0.6331\text{Å}$$

Similarly, $a_H = 2.0924\text{Å}$, $a_{CH_3} = 2.3054\text{Å}$, and $a_C = 1.3547\text{Å}$.

3. Calculation of the Angle, α_j

According to the definition $\alpha_j = \angle GjC_1$ and can be calculated by the cosine law

$$\cos \alpha_j = \frac{-\overline{GC_1}^2 + \overline{C_1j}^2 + \overline{Gj}^2}{2\ \overline{Gj} \times \overline{C_1j}}$$

For α_{Br}, $\overline{GC_1} = a_C = 1.354\text{Å}$, $\overline{C_1j}$ = the C-Br bond distance = 1.938Å, and $\overline{Gj} = a_{Br} = 0.6331\text{Å}$. Thus $\cos \alpha_{Br} = 0.9460$ and $\cos^2\alpha_{Br} = 0.8949$, $\sin^2\alpha_{Br} = 0.1051$. Similarly, $\cos^2\alpha_H = 0.3783$, $\cos^2\alpha_{CH_3} = 0.6686$, $\sin^2\alpha_{CH_3} = 0.3314$.

4. Calculation of f_j

From Eqs. (18) and (19)

$$f_j = \frac{m_j^2\ a_j^2 \left(\dfrac{\sin^2\alpha_j}{k_{bj}} + \dfrac{\cos^2\alpha_j}{k_{sj}}\right)}{\sum\limits_j m_j^2\ a_j^2 \left(\dfrac{\sin^2\alpha_j}{k_{bj}} + \dfrac{\cos^2\alpha_j}{k_{sj}}\right)}$$

Using the values calculated above, $f_{Br} = 0.6092$. Other values are given in Table XX.

Table XX. The Fraction of the Rotational Energy Deposited in Bond *j*, f_j.

Molecule	f_j	Molecule	f_j
CH_3I	0.943	CH_3Br	0.914
CD_3I	0.861	CD_3Br	0.802
CF_3I	0.713	CF_3Br	0.576
CH_2I_2	0.500	CCl_3Br	0.395
C_2H_5I	0.613	CH_2Br_2	0.500
i-C_3H_7I	0.743	CF_2Br_2	0.483
n-C_3H_7I	0.712	CCl_2Br_2	0.410
CH_3Cl	0.910	$CHBr_3$	0.333
CD_3Cl	0.796	$CHClBr_2$	0.448
CF_3Cl	0.612	CBr_4	0.250
CH_2Cl_2	0.500	C_2H_5Br	0.610
CF_2Cl_2	0.431	1,1-$C_2H_4Br_2$	0.492
$CHCl_3$	0.333	CH_4	0.250
CHF_2Cl	0.546	CH_3T	0.666
$CFCl_3$	0.318	C_2H_5T	0.212
CCl_4	0.250		

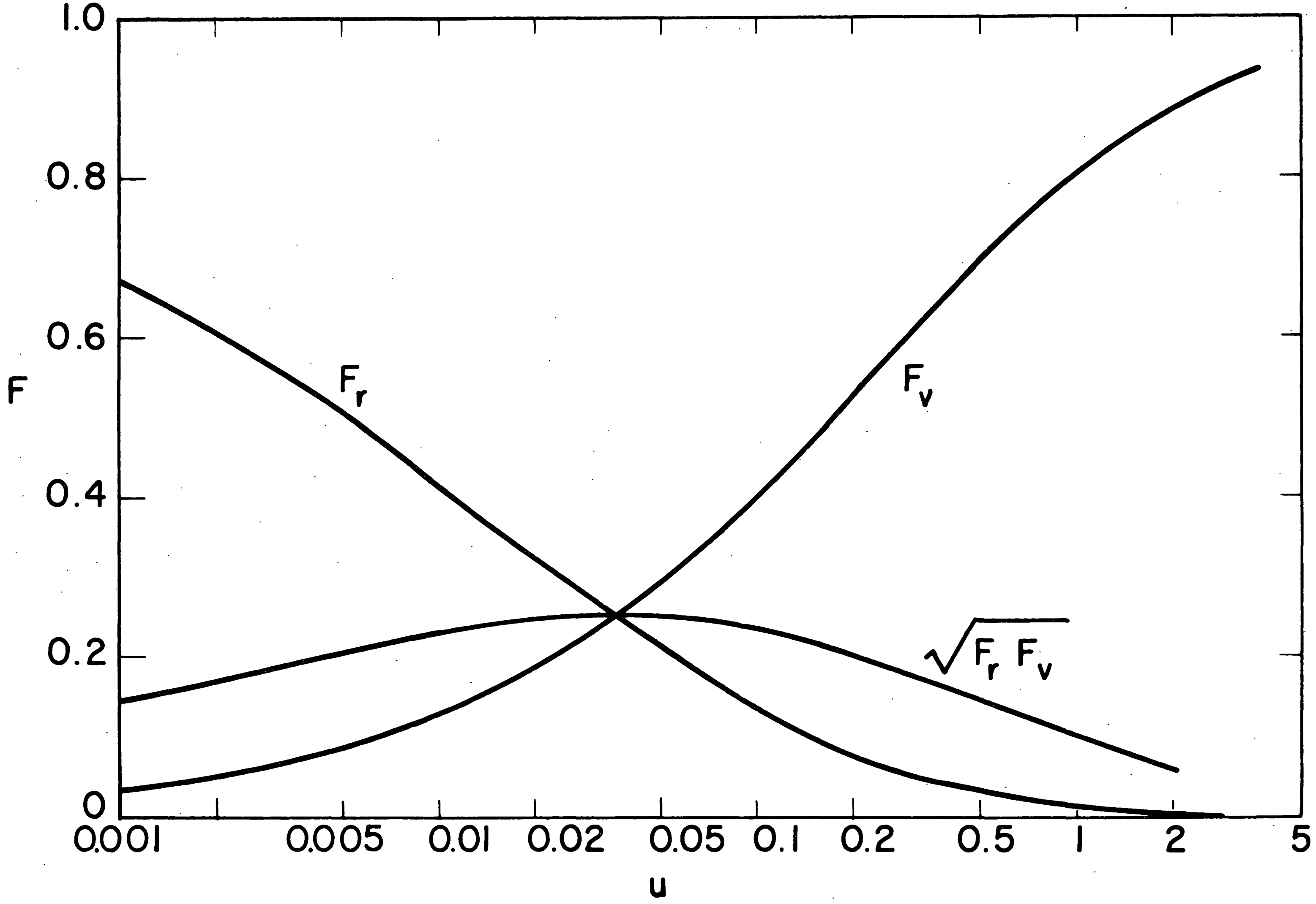

Figure 35. A generalized plot of F_v, F_r, and $\sqrt{F_v F_r}$ as a function of u.

C. Calculation of E_T^o

E_T^o can be calculated using the methods outlined in Chapter II. Two graphs were prepared to assist in the calculations.

Equations (43) and (44) indicate that $\sqrt{F_{yv}}$ and $\sqrt{F_{tv}}$ are given by the same form of equation. Since $\sqrt{F_{yr}}$ = $1 - \sqrt{F_{yv}}$ and $\sqrt{F_{tr}}$ = $1 - \sqrt{F_{tv}}$, $\sqrt{F_{yr}}$, and $\sqrt{F_{tr}}$ are also described by the same form of equation. A graph of F_{yv}, F_{yr}, and $\sqrt{F_{yv}F_{yr}}$ as a function of u_y is the same as a graph of F_{tv}, F_{tr}, and $\sqrt{F_{tv}F_{tr}}$ as a function of u_t. Hence, a generalized graph can be prepared of F_v, F_r, and $\sqrt{F_vF_r}$ as a function of u. This is given in Fig. 35.

The inelastic-stretching effect due to rotation is calculated using Eq. (48). The object in solving Eq. (48) is to obtain the quantity d_N^{*2} $(2-d_N^*)$ for a certain value of B and a particular bond of interest. Obtaining such a solution is possible but tedious since Eq. (48) is a function of d_N^* to the fourth power. Figure 36 is a graph of $d_N^{*2}(2-d_N^*)$ as a function of B for C-I, C-Br, and C-Cl bonds.

1. E_T^o for C_2H_5Br

From the equation, $\cos\gamma = (a_C^2 + a_{Br}^2 - \overline{CBr}^2)/(2a_Ca_{Br})$, it is found that $\cos\gamma = -0.8860$. The quantities u_t and u_y are defined in terms of Eqs. (43) and (44) and

$$u_t = 2.588 \times 10^{-3} \frac{\left[\dfrac{\cos^2\alpha_N}{k_{bN}} + \dfrac{\sin^2\alpha_N}{k_{sN}}\right]^{-1} I_{yy}}{E_\gamma^2}$$

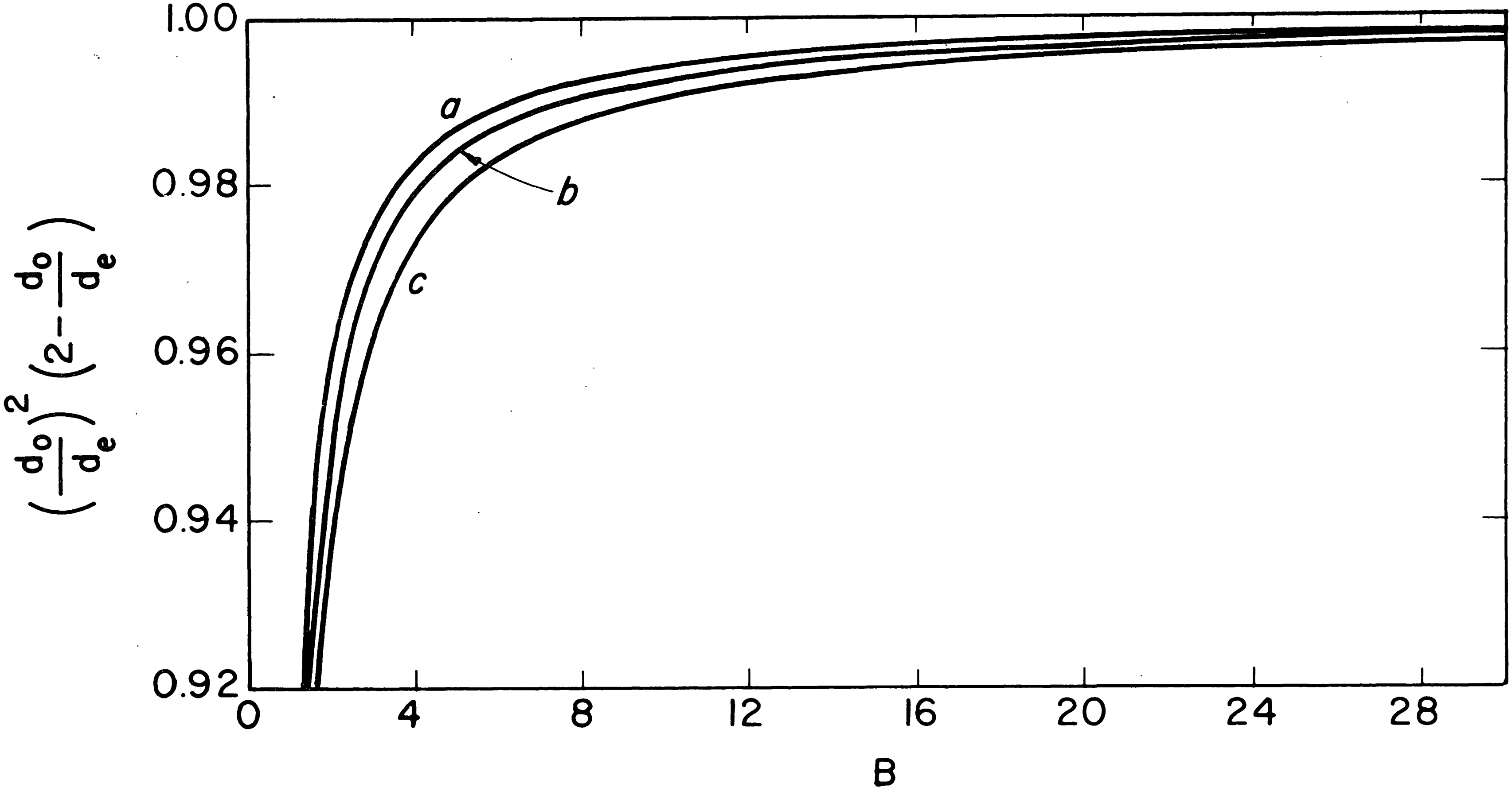

Figure 36. A graphical aid for the solution of d* in Equation (48), for bonds: C-I, curve a; C-Br, curve b; C-Cl, curve c.

$$u_y = 2.588 \times 10^{-3} \frac{(I_{xx} \cos^2\alpha_N + I_{zz} \sin^2\alpha_N)}{E_\gamma^2}$$

For C_2H_5Br, $k_{bN} = 0.077$ mdynes/Å, $k_{sN} = 2.4$ mdynes/Å $\cos^2\alpha_N = 0.8949$, $\sin^2\alpha_N = 0.1051$, $I_{xx} = 111.1$, $I_{yy} = 140.2$, $I_{zz} = 32.4$ amu Å^2. Thus, $u_t = 0.0279/E_\gamma^{\circ 2}$ and $u_y = 0.0206/E_\gamma^{\circ 2}$.

Proceeding by trial-and-error, it was first assumed that $E_\gamma^\circ = 1.50$ Mev from which $u_t = 0.0124$ and $u_y = 0.00915$. From Fig. 35,

$$F_{yr} = 0.429 \qquad F_{tr} = 0.390$$
$$F_{yv} = 0.118 \qquad F_{tv} = 0.141$$
$$\sqrt{F_{yr}\ F_{yv}} = 0.227 \qquad \sqrt{F_{tr}\ F_{tv}} = 0.235$$

Together with values of a_C and a_N, B is calculated from Eq. (47) and found to be 11.92. From Fig. 36, curve <u>b</u>, $d_N^{*2}(2-d_N^*) = 0.994$. For the C-Br bond in C_2H_5Br, E_{BN} = 2.815 ev. Using Eq. (45) and $E_\gamma^\circ = Q^\circ c$, it is calculated that $E_\gamma^\circ = 1.49$ Mev. Thus, further calculations are unnecessary.

From the equation, $E_T^\circ = 537\ E_\gamma^{\circ 2}/m_N$, it is found that $E_T^\circ = 15.14$ ev.

D. Momentum Transfer to C in $C^{14}O_2$

1. Mathematics

When momentum is transferred to a center atom in a molecule, as C in CO_2, the expressions for the calculation of E_T° will differ slightly from those given in Chapter II.

The carbon in CO_2 is located at the center of mass of the molecule and no rotational excitation is expected when the carbon receives a recoil momentum impulse. The space velocities of the atoms are

$$\vec{S}_i = \dot{\vec{R}} + \vec{v}_i .$$

Since $\Sigma m_i \vec{v}_i = 0$, and assuming $\vec{Q}$ is large compared to the thermal motion of the molecule, the total internal-energy increase can be written as

$$\Delta E_{int} = \tfrac{1}{2} \Sigma m_i v_i^2 + V(\vec{r}_i) - V(\vec{a}_i).$$

The increase of internal energy in the two bonds are:

$$\Delta E_{i1} = \tfrac{1}{2} m_1 \vec{v}_c \cdot (\vec{v}_1 - \vec{v}_c) + V(\vec{r}_1) - V(\vec{a}_1),$$

$$\Delta E_{i2} = \tfrac{1}{2} m_2 \vec{v}_c \cdot (\vec{v}_2 - v_c) + V(\vec{r}_2) - V(\vec{a}_2).$$

From momentum balance, $\dot{\vec{R}} = \vec{Q}/\Sigma m_i$. Using the assumptions: $\vec{S}_c = \vec{Q}/m_c$ and $\vec{S}_1 = \vec{S}_2 = 0$, then

$$\Delta E_{i1} = \frac{m_1}{\Sigma m_i} E_T + V(\vec{r}_i) - V(\vec{a}_1),$$

$$\Delta E_{i2} = \frac{m_2}{\Sigma m_i} E_T + V(\vec{v}_2) - V(\vec{a}_2).$$

When the carbon atom is at its equilibrium position, the internal energy is distributed evenly between the two C-O bonds. When the carbon receives a momentum impulse, Q, an asymetric stretching vibration results. One of the bonds will receive somewhere between $\frac{1}{2}$ and all of the internal energy increase. On the average, it will receive $\frac{3}{4}$ of ΔE_{int}. Thus, $\Delta E_{i1} = \frac{3}{4} \Delta E_{int} = \frac{3}{2} \frac{m_1}{\Sigma m_i} E_T$. Dissociation will result when $E_T > \frac{2}{3} \frac{\Sigma m_i}{m_1} E_{BN}$.

2. Evaluation of E_{BN}

The beta-decay product of $C^{14}O_2$ is NO_2^+. Since CO_2 is a linear molecule, the NO_2^+ product should be linear[96-98]. The dissociation energy for $NO_2 \rightarrow NO + O$ is 3.12 ev (Table XV). The ionization potential of NO_2 to yield linear NO_2^+ is 9.78 ev (Table XVI) and that of NO is 9.25 ev (Table XVI). Thus from a thermodynamic cycle, the bond-dissociation energy of an electronic ground state, linear NO_2^+ is $-9.78 + 3.12 + 9.25 = 2.59$ ev.

Using a Morse potential function, the potential-energy curves for the C-O bond in CO_2 and the N^+-O bond in N^+O_2 were calculated. Hence, $V(\xi) = E_{BN}(1-e^{-2\beta\xi})^2$ where $\xi = (r-a)/a$ and $\beta = \omega_e/4(E_{BN}B_e)^{\frac{1}{2}}$. For CO_2, $a = 1.1615\text{Å}$[99], $\omega_e = (1351.2\ \text{cm}^{-1})$[99], $B_e = (0.3906\ \text{cm}^{-1})$[99], and $E_{BN} = 5.51$ ev (Table XV). For NO_2^+, $a = 1.197\text{Å}$[97], $\omega_e = (1400\ \text{cm}^{-1})$[98], $B_e = (0.3678\ \text{cm}^{-1})$[99], and $E_{BN} = 2.59$ ev. The zero-point energy, $\frac{1}{2}hc\omega_e$, is 0.082 ev for CO_2 and 0.087 for NO_2^+. From potential curves, it was estimated that the average electronic excitation energy is 0.6 - 1.0 ev.

3. Calculation of E_T°

For the reaction:

$$C^{14}O_2 \xrightarrow{\beta} NO_2^+ \rightarrow NO^+ + O$$

$$E_T^\circ = \frac{2}{3}\frac{\Sigma m_i}{m_i}E_{BN} = (\tfrac{2}{3})(\tfrac{46}{16})(2.59-E_e)$$

where E_e is the electronic excitation energy. Thus, E_T° = 3.05 - 3.82 ev.

E. Upper and Lower Energy Limits

Consider the reaction of T with CH_4. Two reactions are $T + CH_4 \rightarrow CH_3T + H$ and $T + CH_4 \rightarrow CH_3 + HT$. For the replacement reaction, the activation energy is 1.6 ev[47]. Thus, $1.6 \text{ ev} = \gamma m_{CH_4} E^y/(m_T + m_{CH_4})$. Since $\gamma = 0.696$ (Table I), $E^y = 2.73$ ev. The C-T bond energy is 4.42 ev (Table XV). Thus $4.42 \text{ ev} = m_{CH_4} E^b/(m_T + m_{CH_4})$ and $E^b = 5.25$ ev. In a similar manner, using 0.56 ev as the activation energy for the abstraction process, $E^y = 0.91$ ev; the HT bond energy is 4.52 ev and $E^b = 5.37$ ev.

F. Effective Energy Degradation Factor

If $s_{CH_3T} = 0.5$ then, for the $T + CH_4$ reaction, $r_e = \sqrt{r_{T\text{-}H}\, r_{T\text{-}CH_4}}$. But $r_{T\text{-}H} = [(m_T - m_H)/(m_T + m_H)]^2 = 0.25$. For the T-C contact collisions, the total mass of the molecule will probably partake in a momentum transfer. Hence, $r_{T\text{-}CH_4} = [(m_T - m_{CH_4})/(m_T + m_{CH_4})]^2 = 169/289$. Therefore $r_e = 0.342$.

G. The Reaction Probability, F(E)

The reaction probability, F(E), is zero for $E > E^b/r$ or $E < E^y$. For $E^b/r > E > E^y$, F(E) is given in Table VI as a function of E. For the reaction, $T + CH_4 \rightarrow CH_3T + H$, $r = 0.342$ (refer to the preceding Section, F,) $E^b = 5.25$ ev, and $E^y = 2.73$ ev (Section E).

For $E^b/r > E > E^y/r$, that is, $15.35 \text{ ev} > E > 7.98$ ev,

$$F(E) = \frac{E^b - rE}{(1-r)E} = \frac{7.98}{E} - 0.520$$

For $E^y/r > E > E^b$, that is, 7.98 ev > E > 5.25 ev,

$$F(E) = \frac{E^b - E^y}{(1-r)E} = \frac{3.83}{E}.$$

For $E^b > E > E^y$, that is 5.25 ev > E > 2.73 ev,

$$F(E) = \frac{E - E^y}{(1-r)\,E} = 1.52 - \frac{4.15}{E}.$$

Presented in Fig. 37 is the reaction probability, F(E) plotted as a function of E for the reactions $T + CH_4 \rightarrow CH_3T + H$ (curve a) and $T + CD_4 \rightarrow CD_3T + D$ (curve b). The overall probability that the reaction occurs is $s_i F(E)$. It should be noted that

$$R = \frac{1}{\ell} \int_{E^y}^{\frac{E^b}{r}} n(E^\circ,E)F(E)dE.$$

H. Calculation of R

Consider the reaction of $T + CH_4$. For the product, CH_3T, $E^b = 5.25$ and $E^y = 2.73$ ev; for the product, HT, $E^b = 5.37$ and $E^y = 0.91$ ev. Thus, $E^a = 5.37$ and $E^z = 2.73$ ev.

For CH_3T, $rE^a = (0.342)(5.37) = 1.83 < E^y$ and $rE^b = (0.342)(5.25) = 1.79 < E^y$. The condition $E^a > E^b > E^y > rE^a > rE^b$ applies to the reaction $T + CH_4 \rightarrow CH_3T + H$ and Eq. (110) is used to calculate R_{CH_3T}. $Y_{CH_3T} = s_{CH_3T}R_{CH_3T}$.

For HT, $E^b = E^a = 5.37$ ev and $E^y = E^z = 0.91$ ev. Thus, $E^a = E^b > rE^a = rE^b > E^y = E^z$ and Eq. (112) is used to calculate R_{HT}. $Y_{HT} = R_{HT} - Y_{CH_3T}$.

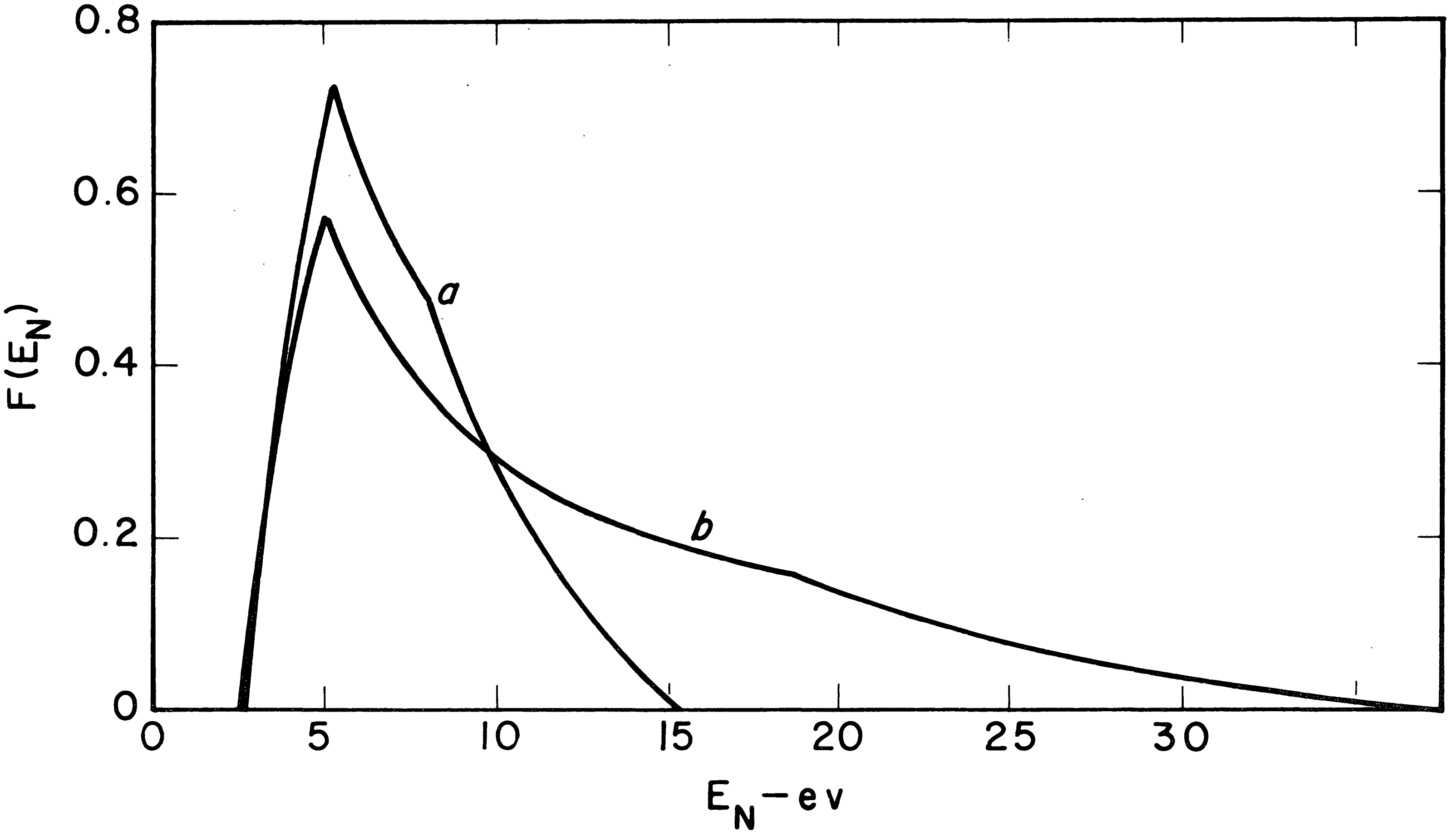

Figure 37. Reaction probability F(E) as a function of E. Curve a: T + CH_4 to form CH_3T; T + CD_4 to form CD_3T.

I. Calculation of the Steric Factor

If gas-phase collisions are considered, radii based on viscosity, second virial coefficient, or the van der Waal equation are appropriate. For the reaction of a hot atom with a gaseous molecule, it is more appropriate to use radii based on covalent bond-length measurements since the hot atom must interact with the valence bonds of the molecule.

Consider the reaction of T with CH_2F_2. For this reaction, $r_H = 0.32$, $r_F = 0.72$, $r_C = 0.77$, and $r_T = 0.53$ Å (Appendix I-E). The areas of the two hydrogen atoms or the two fluorine atoms which are exposed to the tritium can be calculated according to Eq. (126). Hence, $A_j = 4\pi(r_j + r_T)^2 (1 + \cos\theta_j)$, where j = H or F. From Fig. 19, $\cos\theta_H = (r_H + r_T)/2\overline{HC}$, where $\overline{HC}$ is the C-H bond distance and equals 1.091Å. Thus, $A_H = 12.6\text{Å}^2$ and, using a C-F bond distance of 1.32Å, A_F = 29.1Å.

Two types of triangles are considered in calculating the surface of carbon exposed to the tritium.

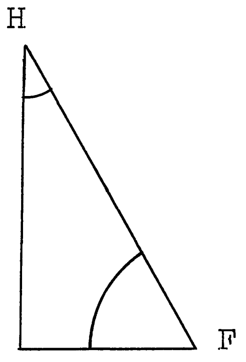

Type I

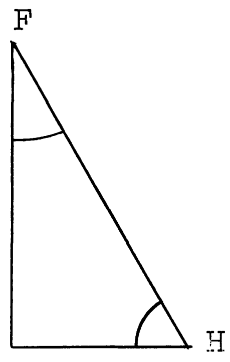

Type II

For the four triangles of type I, the total carbon surface area is $(A_C)_I = 4\pi(r_C + r_T)^2(\frac{1}{3}\cos\theta_{CH} + \frac{2}{3}\cos\theta_{CF} - \frac{1}{2})$. From Fig. 19, $\cos\theta_{CH} = [\overline{HC}^2 + (r_C + r_T)^2 - (r_H + r_T)^2] \div 2\overline{HC}\,(r_C + r_T)^2 = 0.79$. Similarly, $\cos\theta_{CF} = 0.56$. Hence, $(A_C)_I = 2.92\text{Å}$. For the type I spherical triangles, two-thirds of $(A_C)_I$ is in proximity to the fluorine atom and it is assumed that collisions of T with this portion of the carbon surface will lead to F displacement. Similarly, collisions of T with the remaining one-third of the surface which is close to the hydrogen is assumed to result in H displacement.

For the four triangles of type II, the total carbon area, $(A_C)_{II} = 4\pi(r_C + r_T)^2(\frac{1}{3}\cos\theta_{CF} + \frac{2}{3}\cos\theta_{CH} - \frac{1}{2}) = 4.54\text{Å}^2$. For these triangles, one-third of the area is assumed to correspond to F displacement and two-thirds to H displacement.

Hence, for F replacement:

$$(A_C)_F = \frac{2}{3}(A_C)_I + \frac{1}{3}(A_C)_{II} = 3.46\ \text{Å}^2.$$

For H replacement:

$$(A_C)_H = \frac{1}{3}(A_C)_I + \frac{2}{3}(A_C)_{II} = 4.00\text{Å}^2.$$

Thus, $s_{HT} = 12.6/(12.6 + 29.1 + 3.46 + 4.00) = 0.25$. Similarly, $s_{TF} = 0.59$, $s_{CH_2FT} = 0.08$, $s_{CHF_2T} = 0.08$.

REFERENCES

1. Szilard, L. and Chalmers, T. A., Nature, 134, 462 (1934).
2. Fermi, E., et.al., Proc. Roy. Soc. (London), A146, 483 (1934) and A149, 522 (1935).
3. Gluckauf, E. and Fay, J., J.Chem. Soc., 1936, 390.
4. Willard, J. E., Ann. Rev. Nuclear Sci., 3, 193 (1953).
5. Willard, J. E., Ann. Rev. Phys. Chem., 6, 141 (1955).
6. Wahl, A. C. and Bonner, N. A., Radioactivity Applied to Chemistry, John Wiley and Sons, Inc., New York, 1951, p.511.
7. Suess, H., Z. physik. Chem., B45, 312 (1940).
8. Libby, W. F., J. Am. Chem. Soc., 69, 2523 (1947).
9. Wexler, S. and Davies, T. H., J. Chem. Phys., 20, 1688 (1952).
10. Cobble, J. W. and Boyd, J. E., J. Am. Chem. Soc., 74, 1282 (1952).
11. Gordus, A. A. and Willard, J. E., J. Am. Chem. Soc., 79, 4609 (1957).
12. Gordus, A. A. and Hsiung, C. H., J. Chem. Phys., 36, 954 (1962).
13. Williams, R. R., Jr., and Hamill, W. H., J. Chem. Phys., 18, 783 (1950).
14. Rack, E. P. and Gordus, A. A., J. Chem. Phys., 34, 1855 (1961).
15. Hornig, J. F., Levey, G., and Willard, J. E., J. Chem. Phys., 20, 1556 (1952).
16. Levey, G. and Willard, J. E., J. Chem. Phys., 25, 904 (1956).
17. Rack, E. P. and Gordus, A. A., J. Phys. Chem., 65, 944 (1961).
18. Friedman, L. and Libby, W. F., J. Chem. Phys., 17, 647 (1949).
19. Fox, M. S. and Libby, W. F., J. Chem. Phys., 20, 487 (1952).
20. Miller, J. M., Gryder, J. W., and Dodson, R. W., J. Chem. Phys., 18, 579 (1950).

21. Capron, P. C. and Oshima, T., J. Chem. Phys., 20, 1403 (1952).

22. Estrup, P. J. and Wolfgang, R., J. Am. Chem. Soc., 82, 2661, 2665 (1960).

23. Steinwedel, H. and Jensen, J. H. D., Naturforsch., A2, 195 (1947).

24. Svoboda, K., Zhur. Neorg. Khim., 3, 187 (1958); U. S. Atomic Energy Comm. Nuclear Sci. Abstr., 13, 10954 (1959).

25. Wolfsberg, M., J. Chem. Phys., 24, 24 (1956).

26. Hsiung, C. H., Hsiung, H. C., and Gordus, A. A., J. Chem. Phys., 34, 535 (1960).

27. Nagai, K., J. Phys. Soc. Japan, 13, 928 (1958).

28. Groshev, L. V., et.al., Atlas of Gamma-Ray Spectra from Radiative Capture of Thermal Neutrons, Pergamon Press, London, 1959, pp. 48-49.

29. Siegbahn, K., Beta- and Gamma-Ray Spectroscopy, Interscience Publishers, Inc., New York, 1955, p. 815.

30. American Institute of Physics Handbook, McGraw-Hill Book Company, Inc., New York, 1957, p. 8-96.

31. Reference 29, p. 329.

32. Moljk, A. and Curran, S. C., Phys. Rev., 96, 395 (1954).

33. Cooper, E. P. and Rodgers, F. T., Jr., Phys. Rev., 77, 402 (1950).

34. Wexler, S., J. Inorg. Nucl. Chem., 10, 8 (1959).

35. Snell, A. H. and Pleasonton, F., J. Phys. Chem., 62, 1377 (1958).

36. Wexler, S. and Hess, D. C., J. Phys. Chem., 62, 1382 (1958).

37. Wexler, S., Anderson, G. R., and Singer, L. A., J. Chem. Phys., 32, 417 (1960).

38. Wolfgang, R., Anderson, R. C., and Dodson, R. W., J. Chem. Phys., 24, 16 (1956).

39. Amell, A. R., U. S. Atomic Energy Commission Nuclear Sci. Abstr., 15, 10968 (1961), Report No. TID-11651.

40. (a) Cantwell, M., Phys. Rev., 101, 1747 (1959), (b) Evett, A. A., J. Chem. Phys., 24, 150 (1956).

41. Landau, L. D. and Lifshitz, E. M., Mechanics, Addison-Wesley Pub. Co., Inc., Cambridge, Mass., 1960.

42. Benson, S. W., The Foundations of Chemical Kinetics, McGraw-Hill Book Co., Inc., New York, 1960, p. 162.

43. Urch, D. and Wolfgang, R., J. Am. Chem. Soc., 83, 2982 (1961).

44. Henchman, M. and Wolfgang, R., J. Am. Chem. Soc., 83, 2991 (1961).

45. Odum, R. and Wolfgang, R., J. Am. Chem. Soc., 83, 4668 (1961).

46. Lee, J. K., Musgrave, B., and Rowland, F. S., J. Chem. Phys., 32, 1266 (1960).

47. Glasstone, S., Laidler, K. J., and Eyring, H., The Theory of Rate Processes, McGraw-Hill Book Co., Inc., New York, 1941, p. 210.

48. Weston, R. E., Jr., J. Chem. Phys., 31, 892 (1959).

49. Rowland, F. S., private communication.

50. Lee, J. K., Musgrave, B., and Rowland, F. S., J. Phys. Chem., 64, 1950 (1960).

51. Cross, R. J., Jr., and Wolfgang, R., J. Chem. Phys., 35, 2002 (1961).

52. Rack, E. P., PhD. Dissertation, The University of Michigan, 1961.

53. Gordus, A. A., Progress Report No. 2, U. S. Atomic Energy Comm. Contract No. AT (11-1)-912, February, 1962.

54. El-Sayed, M. A., Estrup. P. J., and Wolfgang, R., J. Phys. Chem., 62, 1356 (1958).

55. Rack, E. P. and Gordus, A. A., J. Chem. Phys., 36, 287 (1962).

56. Sutton, L. E., et.al., Tables of Interatomic Distances, Special Publication No. 11, The Chemical Society (London), 1958.

57. Fenlon, P. F., Cleveland, F. F., and Meister, A. G., J. Chem. Phys., 19, 1561 (1951).

58. McGee, P. R., Cleveland, F. F., Meister, A. G., Decker, C. E., and Miller, S. I., J. Chem. Phys., 21, 242 (1953).

59. Voelz, F. L., Cleveland, F. F., Meister, A. G., and Bernstein, R. B., J. Opt. Soc. Amer., 43, 1061 (1953).

60. Weissman, H. B., Bernstein, R. B., Rosser, S. E., Meister, A. G., and Cleveland, F. F., J. Chem. Phys., 23, 544 (1955).

61. Zeitlow, J. P., Cleveland, F. F., and Meister, A. G., J. Chem. Phys., 18, 1076 (1950).

62. Dowling, J. M., and Meister, A. G., J. Chem. Phys., 22, 1042 (1954).

63. Decker, C. E., Meister, A. G., Cleveland, F. F., and Bernstein, R. B., J. Chem. Phys., 21, 1781 (1953).

64. Davis, A., Cleveland, F. F., and Meister, A. G., J. Chem. Phys., 20, 454 (1952).

65. Meister, A. G., Rosser, S. E., and Cleveland, F. F., J. Chem. Phys., 18, 346 (1950).

66. Barrow, G. M., and McKean, D. C., Proc. Roy. Soc. (London), A213, 27 (1952).

67. Decker, C. E., Meister, A. G., and Cleveland, F. F., J. Chem. Phys., 19, 784 (1951).

68. Weissman, H. B., Meister, A. G., and Cleveland, F. F., J. Chem. Phys., 29, 72 (1958).

69. Simanouti, T., J. Chem. Phys., 17, 848 (1949).

70. Hayashi, M., J. Chem. Soc. (Japan), 78, 1743 (1957).

71. Mizushima, S. I., Shimanouchi, T., Nakagawa, I., and Miyake, A., J. Chem. Phys., 21, 215 (1953).

72. Nakagawa, I., J. Chem. Soc. (Japan), 77, 603 (1956).

73. Nakagawa, I., J. Chem. Soc. (Japan), Pure Chem. Sect., 76, 540 (1950).

74. Cottrell, T. L., The Strength of Chemical Bonds, 2nd Ed., Butterworths Scientific Publications, London, 1958.

75. (a) Sehon, A. H., and Szwarc, M., Proc. Roy. Soc. (London), A209, 110 (1951); (b) Szwarc, M., and Sehon, A. H., J. Chem. Phys., 19, 656 (1951).

76. Reed, R. I., and Snedden, W., Trans. Farad. Soc., 55, 876 (1959).

77. Curran, R. K., J. Chem. Phys., 34, 2007 (1961).

78. Dibeler, V. H., Reese, R. M., and Mohler, F. L., J. Res. Nat. Bur. Stand., 57, 113 (1956).

79. Collins, J., and Lossing, F. P., J. Chem. Phys., 28, 900 (1958).

80. Kiser, R. W., Tables of Ionization Potentials, U. S. Atomic Energy Comm. Report, TID-6142 (1960).

81. Watanabe, K., J Chem. Phys., 26, 542 (1957).

82. Moore, C. E., Atomic Energy Levels, Nat. Bur. of Stand., Circ. No. 467, Vol. I, 1949, p. 3.

83. Ibid., Vol. II, 1952, p. 159.

84. Ibid., Vol. III, 1958, p. 105.

85. Lossing, F. P., Kebarle, P., and DeSousa, J. B., Advances in Mass Spectrometry, edited by J. D. Waldron, Pergamon Press, Ltd., London, 1959, p. 431.

86. Hirschfelder, J. O., Curtiss, C. F., and Bird, R. B., Molecular Theory of Gases and Liquids, John Wiley and Sons,Inc., New York, 1954, pp. 1110-1112.

87. Moeller, T., Inorganic Chemistry, John Wiley and Sons,Inc., New York, 1952, pp. 130-131.

88. Pauling, L., The Nature of the Chemical Bond, 3rd Ed., Cornell University Press, Ithaca, New York, 1960, p. 260.

89. Present, R. D., Kinetic Theory of Gases, McGraw-Hill Book Co., Inc., New York, 1958, p. 253.

90. Chapman, S., and Cowling, T. G., The Mathematical Theory of Non-Uniform Gases, Cambridge University Press, Cambridge, 1939, p. 229.

91. Campbell, I., Nucleonika, 2, 605 (1957).

92. O'Connor, D., Polish Acad. Sci., Inst. Nuclear Research, Report No. 12/I-B, Warsaw, 1958.

93. Zvara, I., Vestnik, Moskov Univ., Ser. Mat., Mekhan., Astron., Fiz., i Khim., 13, No. 6, p. 127 (1958).

94. Segel, R. E., Phys. Rev., 113, 844 (1959).

95. Draper, J. E., and Fleischer, A. A., Phys. Rev., 122, 1585 (1961).

96. Collins, J., J. Chem. Phys., 30, 1621 (1959).

97. Grison, E., Eviks, K., and de Vries, J. L., acta. cryst., 3, 290 (1950).

98. Gillespie, R. J., and Miller, D. J., Quart. Rev., Chem. Soc. (London), 2, 277 (1948).

99. Herzberg, G., Infrared and Raman Spectra, D. Von Nostrand Co., Inc., New York, 1945, pp. 21, 276.

100. Slater, J. C., Quantum Theory of Atomic Structure, Vol. I, McGraw-Hill Book Co., Inc., New York, 1960, p. 210.

Page Missing
in Original Volume

DEFINITION OF SYMBOLS

a	$g_A/(1 - r_A)$.
$\vec{a}_i$	equilibrium position of *i*th atom in a molecule .
A_i	exposed area of *i*th atom in a molecule.
b	$(1 - g_A)/(1 - r_B)$.
$\vec{b}_i$	equilibrium position of *i*th atom in molecule after rotational inelastic stretching.
B	a quantity defined in Eq. (47), p. 23.
c	velocity of light.
d_j	*j*th bond distance.
d_{oj}	equilibrium *j*th bond distance.
d_{ej}	equilibrium *j*th bond distance after rotational inelastic stretching.
d*	d_{oj}/d_{ej}.
D_{a-b}	dissociation energy of molecule *ab* into *a* and *b*.
E_{ab}	kinetic energy of *ab*.
E_{BN}	bond dissociation energy of bond joining N to the remainder of the molecule.
E_h	kinetic energy of h .
E_i	internal energy of a molecule.
E_{max}	neutron binding energy.
E_N	kinetic energy of atom N.
E_{N_o}	minimum hot-atom energy required to dissociate a thermal molecule.
E_R	kinetic energy of the radical.
E_{Ri}	internal energy of the radical.
E_{sj}	energy deposited in bond *j* due to stretching.

E_T	recoil energy.
E_γ	gamma-ray energy.
ΔE_{AB}	kinetic energy change of molecule AB.
ΔE_i	internal energy change.
ΔE_{ij}	internal energy change in bond *j*.
ΔE_N	kinetic energy change of atom *N* in a collision.
ΔE_r	rotational energy change.
ΔE_{rj}	rotational energy change in bond *j*.
ΔE_v	vibrational energy change.
ΔE_v	vibrational energy change in a collision.
ΔE_{vj}	vibrational energy change in bond *j*.
E^a	the maximum energy the hot atom may have in forming any product.
E^b	the maximum energy the hot atom may have in forming a particular product.
E^y	the minimum energy the hot atom must have to form a particular product.
E^z	the minimum energy the hot atom must have to form a particular product.
E°	initial energy of a hot atom.
E°_N	minimum kinetic energy, after bond rupture, associated with hot atom, *N*.
E°_N	initial energy of the hot atom, *N*.
E°_r	minimum rotational energy received by the bond.
E°_R	minimum kinetic energy of the radical after bond rupture.
E°_{Ri}	minimum internal energy received by the radical after bond rupture.

E_T°	minimum recoil energy required for a bond rupture.
E_v°	minimum vibrational energy received by a bond.
E_γ°	minimum gamma-ray energy required for a bond rupture.
f_j	fraction of rotational energy deposited in bond *j*.
$F_j(E)$	reaction probability in the energy zone to form product *j*.
F_{tr}	$(Q_{tr}/Q_t)^2$.
F_{tv}	$(Q_{tv}/Q_t)^2$.
F_{yr}	$(Q_{yr}/Q_y)^2$.
F_{yv}	$(Q_{yv}/Q_y)^2$.
$\mathfrak{F}$	a quantity defined in Eq. (40b), p. 20.
$\mathfrak{F}^\circ$	value of $\mathfrak{F}$ when $E_T = E_T^\circ$.
$\vec{F}_j$	centrifugal force associated with atom *j* in a rotation.
$\vec{F}_{bj}$	bending component of $\vec{F}_j$.
$\vec{F}_{sj}$	stretching component of $\vec{F}_j$.
g_i	probability that the hot atom collides with the *i*th species in a mixture.
I_i	a constant, Eq. (133), p. 140.
I_{xx}	moment of inertia about x-axis.
I_{yy}	moment of inertia about y-axis.
I_{zz}	moment of inertia about z-axis.
J_{ni}	constant defined in Eq. (137), p. 141.
k_i	average number of thermal molecules *i* dissociated.
k_{bj}	bending force constant of bond *j*.
k_{sj}	stretching force constant of bond *j*.
K	a constant, Eq. (85a), p. 67.
K_i	a constant, Eq. (134), p. 140.

ℓ	total number of hot atoms.
ℓ_i	*i*th gamma-ray momentum in a gamma cascade.
L	a constant, Eq. (85b), p. 67.
m_i	atomic weight of atom *i*.
m_{ij}	$m_i + m_j$.
Σm_i or M_i	molecular weight.
M_j	an algebraic sum defined on p. 161.
n	number of gamma rays in a gamma cascade.
n(E°,E)	number of hot atoms of inital energy, E°, having energy E.
N_j	an algebraic sum defined on p. 161.
p_k	fractional occurrence of *k*th gamma ray in a gamma cascade.
P(X)	probability that the hot atom energy is less or equal to X, where $X = E_N$, E°_N, E_γ, E°_γ, etc.
q_i	average energy degradation in a collision between a hot atom and the *i*th molecule.
$\vec{Q}$	momentum transferred to a molecule.
$\vec{Q}_R$	a component of $\vec{Q}$ resulting in rotation of a molecule.
$\vec{Q}_V$	a component of $\vec{Q}$ resulting in vibration of a molecule.
Q_r	a component of $\vec{Q}$ in the direction of $\vec{r}_N$.
Q_t	a component of $\vec{Q}$ perpendicular to $\vec{r}_N$.
Q_y	a component of $\vec{Q}$ parallel to the y-axis.
Q_{tr}	a component of Q_t effecting the rotation of bond N.
Q_{tv}	a component of Q_t effecting the vibration of bond N.
Q_{yr}	a component of Q_y effecting the rotation of bond N.
Q_{yv}	a component of Q_y effecting the vibration of bond N.
Q°	minimum momentum required for a bond rupture.

$\vec{r}$	molecular coordinates.
r_i	energy degradation factor of a hot atom colliding with molecule *i*.
r_e	effective energy degradation factor of a hot atom.
r_i	collision radius of molecule *i*.
r_N	collision radius of hot atom *N*.
$\vec{R}$	space coordinates of the frame work $\vec{r}$.
$\dot{\vec{R}}$	translational velocity of the frame work $\vec{r}$.
R	net recoil momentum.
R_j	yield of product *j* if $s_j = 1.0$.
s_{exp}	experimental steric factor.
s_g	geometrical steric factor.
s_j	steric factor for the formation of product *j*.
$\vec{S}_i$	space velocity of atom *i*.
${}_o\vec{S}_i$	initial space velocity of atom *i*.
u_t	a quantity defined on p. 22.
u_y	a quantity defined on p. 23.
v_i	velocity of particle *i* before a collision.
v_i'	velocity of particle *i* after a collision.
$\vec{v}$	vibrational velocity of atom *i* in a molecule.
$\vec{v}o_i$	vibrational velocity of atom *i* in a molecule at its equilibrium position, $\vec{b}_i$.
$V(\vec{r}_j)$	potential energy of a molecule.
V_{rj}	potential-energy change of bond *j* due to rotational inelastic stretching.
W	beta-ray energy in units of electron rest-mass energy.
W_m	maximum beta-ray energy in units of electron rest-mass energy.

X_i	mole fraction of *i*th species in a mixture,
Y_i	yield of product *j*.
α_i	a quantity defined in Eqs. (131) and (132), p. 140.
α_j	an angle defined in Fig. 1, p. 15.
γ	an angle between $\vec{r}_C$ and $\vec{r}_N$.
$\delta(x-x')$	Dirac δ-function.
δ_{bj}	bending elongation of bond *j*.
δ_{sj}	stretching elongation of bond *j*.
θ_i	interacting angle of particle *i* before a collision, Fig. 11, p. 58, Fig. 12, p. 61.
θ_i'	interacting angle of particle *i* after a collision, Fig. 11, p. 58, Fig. 12, p. 61.
$\vec{\theta}$	orientation of the frame work $\vec{r}$ in space.
$\dot{\vec{\theta}}$ or $\vec{\omega}$	angular velocity of the frame work $\vec{r}$ in space.
ξ	a probability function of collision.
ρ_i	$r_i - a_i$.
σ_i	collision cross section of hot atom and species *i* in a mixture.